



Universidad  
Politécnica  
de Cartagena



Norwegian University of  
Science and Technology

# Nonlinear Pulse Propagation in Optical Fibers

Alvaro Fructuoso Garcia

May 2012

# Contents

<b>1</b>	<b>Resumen en español</b>	<b>1</b>
<b>2</b>	<b>Introduction</b>	<b>3</b>
2.1	Fiber Characteristics . . . . .	3
2.1.1	Single-mode Condition . . . . .	3
2.1.2	Refractive Index . . . . .	4
2.1.3	Propagation Constant . . . . .	4
2.2	Helmholtz Equation . . . . .	5
2.3	Fourier Transform . . . . .	6
2.3.1	Windowed Fourier Transform . . . . .	6
2.4	Time-Frequency Analysis . . . . .	7
<b>3</b>	<b>Pulse Propagation</b>	<b>9</b>
3.1	Maxwell's Equations . . . . .	9
3.2	Linear Pulse Propagation . . . . .	12
3.3	Dispersion . . . . .	13
3.3.1	Group Velocity . . . . .	14
3.3.2	Group Velocity Dispersion . . . . .	15
3.3.3	Third Order Dispersion . . . . .	15
<b>4</b>	<b>Nonlinear Effects</b>	<b>17</b>
4.1	Nonlinear Pulse Propagation . . . . .	17
4.2	Numerical Methods . . . . .	22
4.2.1	Split-Step Fourier Method . . . . .	23
4.2.2	FDTD . . . . .	26
<b>5</b>	<b>Time-Frequency Representations</b>	<b>29</b>
5.1	Spectrogram . . . . .	29
5.1.1	Spectrogram properties . . . . .	30
5.1.2	Spectrogram drawbacks and conclusions . . . . .	31
5.2	Wigner-Ville Distribution (WVD) . . . . .	31

5.2.1	WVD properties . . . . .	32
5.2.2	WVD drawbacks and conclusions . . . . .	33
<b>6</b>	<b>Results</b>	<b>35</b>
6.1	Linear Propagation . . . . .	35
6.1.1	Propagating 100 meters changing the amplitude . . . .	36
6.1.2	Propagating 100 meters changing the phase value . . .	39
6.1.3	Propagating in other fibers . . . . .	43
6.2	Nonlinear Propagation . . . . .	45
6.2.1	Propagating 100 meters changing the amplitude . . . .	45
6.2.2	Propagating 100 meters changing the phase value . . .	55
6.2.3	Propagating 100 meters changing the phase function .	69
<b>7</b>	<b>Conclusion</b>	<b>83</b>
<b>8</b>	<b>References</b>	<b>85</b>
<b>9</b>	<b>Appendices</b>	<b>87</b>
9.1	Material parameters table . . . . .	88
9.2	Linear Propagation code . . . . .	89
9.3	Nonlinear Propagation code . . . . .	91
9.4	Others . . . . .	94

# Chapter 1

## Resumen en español

La motivación para que este proyecto eche a rodar es la confirmación, o no, de que las fibras ópticas pueden ser tratadas y evaluadas como fibras totalmente lineales, despreciando el efecto de las no linealidades existentes en el "mundo real". Además, se verá como afectan los diferentes parámetros que un pulso lleva implícitos para propagarse en el tiempo y a lo largo de una fibra óptica.

Para ello se comienza, tras una breve introducción teórica, con la realización de un estudio teórico para el caso de fibras ópticas lineales, para conocer con detalle cuales son los parámetros, fórmulas y simplificaciones a tener en cuenta. Se continúa con el estudio de las no linealidades que hay presentes en la fibra, su naturaleza y los diferentes métodos existentes para calcularlas.

Por último, con la ayuda de un programa Matlab creado íntegramente para este fin, se analiza la propagación de una señal Gaussiana de la forma  $E = Ae^{-\frac{(t-t_0)^2}{\sigma^2}} e^{jb\frac{t^2}{\sigma^2}} e^{j\omega_0 t}$ , tanto en fibras lineales (sin tener en cuenta las no linealidades), como en fibras no lineales mediante el método Split-Step Fourier.

Como parte complementaria a este proyecto, el grupo de investigación de ópticas de la universidad NTNU de Trondheim (Noruega), va a realizar las mismas medidas de manera práctica en laboratorio. En el momento de finalización de este estudio teórico aún no se había llevado a cabo su homólogo práctico, por lo que en el momento de redactar el mismo, no fue posible incluir la comparación con el caso práctico.



# Chapter 2

## Introduction

This little introduction will serve to know some parameters and theorems that allow us to understand how a pulse propagates through an optical fiber. These parameters and theorems are essentials to have an overview of the fiber characteristics that are important for understanding the linear and nonlinear effects.

### 2.1 Fiber Characteristics

An optical fiber is essentially composed of a glass core surrounded by a cladding layer with different refractive index. These fibers are typically made from pure silica glass synthesized by fusing  $\text{SiO}_2$  molecules to get low-loss optical fibers. To get different refractive indexes are used dopants such as  $\text{GeO}_2$  and  $\text{P}_2\text{O}_5$  during the fabrication process.

#### 2.1.1 Single-mode Condition

An interesting parameter that characterizes the fiber is  $V$

$$V = k_0 a \sqrt{(n_1^2 - n_2^2)} \quad (2.1)$$

which determines the number of modes supported by the fiber, also called normalized frequency. Where  $k_0$  is the wavenumber,  $a$  is the core radius,  $n_1$  is the refractive index of the core and  $n_2$  is the refractive index of the cladding, that is slightly lower than  $n_1$ . Fibers with a  $V < 2.405$ , less than the first zero of the Bessel function  $J_0$ , only supports the fundamental mode. That fibers are called single-mode fibers and in his study will focus. For this case, the core radius is usually  $a < 5\mu\text{m}$  [1].

### 2.1.2 Refractive Index

The refractive index is defined as the difference between the speed of light in vacuum  $c$  and in the medium

$$n = \frac{c}{v} = \sqrt{\varepsilon_r \mu_r} \quad (2.2)$$

For non-magnetic media  $\mu_r \simeq \sqrt{\varepsilon_r}$  and the refractive index can be directly related to the relative permittivity  $\varepsilon_r$  as

$$n \simeq \varepsilon_r \quad (2.3)$$

### 2.1.3 Propagation Constant

It is a complex number denoted by  $\gamma$ , and is used to describe the behavior of an electromagnetic wave along a transmission line

$$\gamma = jk = j\omega\sqrt{\mu\varepsilon} \quad (2.4)$$

where the permittivity  $\varepsilon$  is in general complex with both real and imaginary part, so may be written as

$$\varepsilon = \varepsilon' - j\varepsilon'' \quad (2.5)$$

Substituting the complex permittivity from equation (2.5) into equation (2.4)

$$\gamma = j\omega\sqrt{\mu\varepsilon'}\sqrt{1 - j\frac{\varepsilon''}{\varepsilon'}} \quad (2.6)$$

This expression has a real and imaginary part, for example denoted as

$$\gamma = \alpha + j\beta \quad (2.7)$$

Equation for the electric field of a plane propagating in the positive  $z$ -direction can be written with these new quantities as

$$E = E_0 e^{j(\omega t - kz)} = E_0 e^{j\omega t} e^{-\gamma z} = E_0 e^{-\alpha z} e^{j(\omega t - \beta z)} \quad (2.8)$$

where  $\alpha$ , measured in Np/m, is known as the attenuation constant and determines the absorption of the wave. The parameter  $\beta$ , measured in rad/m determines the phase of the field as the wave propagates and is known as the phase constant.

## 2.2 Helmholtz Equation

The Helmholtz equation, is a partial differential equation defined as

$$\nabla^2 E + k^2 E = 0 \quad (2.9)$$

where  $\nabla$  is the Laplacian,  $k$  is the wave number, and  $E$  is the amplitude.

This equation is used for solving physical problems involving partial differential equations in both space and time. The Helmholtz equation, which represents the time-independent form of the original equation, results from applying the technique of separation of variables to reduce the complexity of the analysis. Starting at the the wave equation

$$\nabla^2 - \frac{1}{c^2} \frac{\partial^2}{\partial t^2} = E(z, t) = 0 \quad (2.10)$$

Separation of variables begins by assuming that the wave function  $E(z, t)$  is in fact separable:

$$E(z, t) = A(z)B(t) \quad (2.11)$$

Substituting this form into the wave equation, and then simplifying, we obtain the following equation:

$$\frac{\nabla^2 A}{A} = \frac{1}{c^2 B} \frac{\partial^2 B}{\partial t^2} \quad (2.12)$$

The expression on the left side depends only on  $z$  and the right side expression depends only on  $t$ . As a result, this equation is valid in the general case if and only if both sides of the equation are equal to a constant value, for example  $-k^2$ . There are two equations, one for  $A(z)$ ,

$$\frac{\nabla^2 A}{A} = -k^2 \quad (2.13)$$

and other for  $B(t)$ :

$$\frac{1}{c^2 B} \frac{\partial^2 B}{\partial t^2} = -k^2 \quad (2.14)$$

Finally, is possible to rewrite equations (2.15) and (2.16) as Helmholtz equations

$$\nabla^2 A + k^2 A = (\nabla^2 + k^2)A = 0 \quad (2.15)$$

$$\frac{\partial^2 B}{\partial t^2} + k^2 c^2 B = \left(\frac{\partial^2}{\partial t^2} + k^2 c^2\right)B = 0 \quad (2.16)$$



## 2.3 Fourier Transform

The Fourier transform is a mathematical operation that expresses a mathematical function of time as a function of frequency, known as its frequency spectrum. Fourier's theorem guarantees that this can always be done. The function of time is called the time domain representation, and the frequency spectrum the frequency domain representation.

$$F(\omega) = \int_{-\infty}^{\infty} f(t)e^{-j\omega t} dt \quad (2.17)$$

The inverse Fourier transform expresses a frequency domain function in the time domain. Each value of the function is usually expressed as a complex number that can be interpreted as a magnitude and a phase component.

$$f(t) = \int_{-\infty}^{\infty} F(\omega)e^{j\omega t} d\omega \quad (2.18)$$

### 2.3.1 Windowed Fourier Transform

A window is a mathematical function that is zero-valued outside of some chosen interval. Is used in frequency analysis and signal processing. Some common windows are: rectangular, triangular, Hanning, Hamming, cosine, Bartlett, etc.

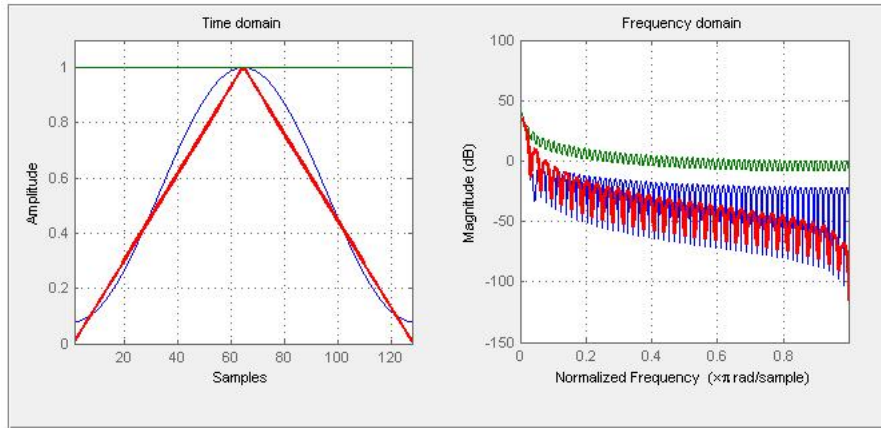


Figure 2.1: Rectangular in green, Hamming in blue and triangular in red

The Windowed Fourier Transform (WFT) replaces the Fourier transform's sinusoidal wave by the product of a sinusoid and a window which is

localized in time. It takes two arguments: time and frequency. It is defined by:

$$WFT[f(t)] \equiv F(\tau, \omega) = \int_{-\infty}^{\infty} f(t)w(t - \tau)e^{-j\omega t} dt \quad (2.19)$$

The Windowed Fourier Transform or Short-Time Fourier Transform (STFT) provides a good Time-Frequency representation of signals, has a constant time frequency resolution and, is a complete, stable, redundant representation of the signal.

But STFT has some limitations due to the nature of the joint time-frequency representation used, given that exist a inverse relationship between time domain and frequency domain, and therefore, between their respective signal resolution. This is due to a frequency (Fourier) domain property, whereby a temporal window and its spectrum cannot both be arbitrarily narrow, because if the window (time) narrows its spectrum widens and then, the signal spectrum resolution gets worse [6].

$$S_f(t, \omega) = \int_{-\infty}^{+\infty} f(t)g(t - \tau)e^{-j\omega t} dt \quad (2.20)$$

The immediate consequence of this inverse relationship between time and frequency is that, using STFT, there is just one way for improving the identification of spectral detail from a spectrogram, and this is achieved impairing the temporal resolution. Therefore, this is not good enough for pulse transmission, so is needed another kind of representation for the joint time-frequency that provides better results for this joint. Is it usually used quadratics representations because this kind of representations have a quadratic (nonlinear) relations with the signal, similar to signal-energy relation, thus showing an important signal feature, the energy distribution. Actually, these quadratic representations have to satisfy some conditions to seem a energy distribution representation[10].

## 2.4 Time-Frequency Analysis

Signal processing time-frequency analysis is a set of techniques for the characterization and manipulation of signals which statistics vary over time. Traditional time and frequency analysis are not good enough to describe what is happening. For example, with the Fourier transform is possible to know which frequencies exist for the total duration of the signal, but not when

those frequencies existed. The idea of time-frequency analysis is to describe and understand how the frequency content of a signal is changing in time. In Chapter 5, will see the techniques that provide a full description of what is happening

# Chapter 3

## Pulse Propagation

For an understanding of the nonlinear effects in optical fibers, it is necessary to consider the theory of electromagnetic wave propagation in dispersive nonlinear media. The objective of this chapter is to obtain a basic equation that governs propagation of optical fibers in single-mode fibers. Section 3.1 introduces Maxwell's equations and important concepts such as the linear and nonlinear parts of the induced polarization and the frequency-dependent dielectric constant. In section 3.3 is introduced the theory of pulse propagation in nonlinear dispersive media in the slowly varying envelope approximation considering that the spectral width of the pulse is much smaller than the frequency of the incident radiation.

### 3.1 Maxwell's Equations

The propagation of optical fields in fiber is determined by Maxwell's equations. That is

$$\nabla \times \vec{E} = -\frac{\partial \vec{B}}{\partial t} \quad (3.1)$$

$$\nabla \times \vec{H} = \vec{J} + \frac{\partial \vec{D}}{\partial t} \quad (3.2)$$

$$\nabla \cdot \vec{D} = \rho_f \quad (3.3)$$

$$\nabla \cdot \vec{B} = 0 \quad (3.4)$$

where  $\vec{E}$  is the electric field vector and  $\vec{H}$  is the magnetic field vector.  $\vec{D}$  is the electric flux density and  $\vec{B}$  is the magnetic flux density. The current density vector  $\vec{J}$  and the charge density  $\rho_f$ . In the absence of free charges in a medium such as optical fibers,  $\vec{J}=0$  and  $\rho_f=0$ .

The flux densities  $\vec{D}$  and  $\vec{B}$  appear in response to the electric and magnetic fields  $\vec{E}$  and  $\vec{H}$  propagating inside the medium and are related to them through the constitutive relations given by

$$\vec{D} = \varepsilon_0 \vec{E} + \vec{P} \quad (3.5)$$

$$\vec{B} = \mu_0 \vec{H} + \vec{M} \quad (3.6)$$

where  $\varepsilon_0 = 8.85 \times 10^{-12} \text{ F/m}$  is the vacuum permittivity,  $\mu_0 = 4\pi \times 10^{-7} \text{ N/A}^2$  is the vacuum permeability,  $\vec{P}$  is the induced electric polarization and  $\vec{M}$  is the induced magnetic polarization. For a nonmagnetic medium such as optical fibers,  $\vec{M}=0$ .

Maxwell's equations can be used to obtain the wave equation that describes light propagation in optical fibers. By taking the curl of Eq. (3.1) and using Eqs. (3.2), (3.5) and (3.6), one can eliminate  $\vec{B}$  and  $\vec{D}$  in favor of  $\vec{E}$  and  $\vec{P}$  to obtain

$$\nabla \times \nabla \times \vec{E}(t) = -\frac{1}{c^2} \frac{\partial^2 \vec{E}(t)}{\partial t^2} - \mu_0 \frac{\partial^2 \vec{P}}{\partial t^2} \quad (3.7)$$

where  $c = 3 \times 10^8 \text{ m/s}$  is the speed of light in vacuum and the relation  $\mu_0 \varepsilon_0 = 1/c^2$  was used. In the case of optical fibers with wavelength range  $0.5\text{-}2\mu\text{m}$  that is of the interest for the study of nonlinear effects governed by  $\chi^{(3)}$ , the induced polarization consists of two parts such that

$$\vec{P}(z, t) = \vec{P}_L(z, t) + \vec{P}_{NL}(z, t) \quad (3.8)$$

where the linear part  $\vec{P}_L(z, t)$  and the nonlinear part  $\vec{P}_{NL}$  (studied in next chapter) are related to the electric field

$$\vec{P}_L(z, t) = \varepsilon_0 \int_{-\infty}^t \chi^{(1)}(t-t') \cdot \vec{E}(z, t') dt' \quad (3.9)$$

$$\vec{P}_{NL}(z, t) = \varepsilon_0 \int_{-\infty}^t dt_1 \int_{-\infty}^t dt_2 \int_{-\infty}^t dt_3 \times \chi^{(3)} : \vec{E}(z, t_1) \vec{E}(z, t_2) \vec{E}(z, t_3) \quad (3.10)$$

These relations are valid in the electric-dipole approximation and assume that the medium response is local.

Equations (3.7)-(3.10) give a general idea for studying the third order nonlinear effects in optical fibers but their study is very complex, so it necessary to make several simplifying approximations. The first step consists of solving equation (3.7) with  $\vec{P}_{NL} = 0$ , that is treated as a small perturbation to the

total induced polarization. Can assume this approximation because the non-linear effects are relatively weak in optical fibers like silica fibers. Equation (3.7) is linear in  $\vec{E}$ , it is useful to write in the frequency domain as

$$\nabla \times \nabla \times \vec{E}(z, \omega) = \varepsilon(\omega) \frac{\omega^2}{c^2} \vec{E}(z, \omega) \quad (3.11)$$

where  $\vec{E}(z, \omega)$  is the Fourier transform of  $\vec{E}(z, t)$  defined as

$$\vec{E}(z, \omega) = \int_{-\infty}^{\infty} \vec{E}(z, t) e^{j(\omega t - kz)} dt \quad (3.12)$$

The frequency-dependent dielectric constant is defined as

$$\varepsilon(\omega) = 1 + \chi^{(1)}(\omega) \quad (3.13)$$

where  $\chi^{(1)}(\omega)$  is the Fourier transform of  $\chi^{(1)}(t)$  and is in general complex, so  $\varepsilon(\omega)$  is complex too and can be defined as

$$\varepsilon = (n + j \frac{\alpha c}{2\omega})^2 \quad (3.14)$$

$n(\omega)$  is the refractive index and is related to the real part of  $\chi^{(1)}(\omega)$ , and  $\alpha(\omega)$  is the absorption coefficient and is related to the imaginary part of  $\chi^{(1)}(\omega)$  by the relations

$$n(\omega) = 1 + \frac{1}{2} \text{Re}[\chi^{(1)}(\omega)] \quad (3.15)$$

$$\alpha(\omega) = \frac{\omega}{nc} \text{Im}[\chi^{(1)}(\omega)] \quad (3.16)$$

Before solving equation (3.11), two simplifications can be done. First, because of low optical losses in the wavelength region 0.5-2 $\mu\text{m}$ , the imaginary part of  $\varepsilon(\omega)$  is small in comparison to the real part, so we can replace  $\varepsilon(\omega)$  by  $n^2(\omega)$ . Second, as  $n(\omega)$  is often independent of the spatial coordinates in both the core and the cladding of step-index fibers, one can use

$$\nabla \times \nabla \times \vec{E}(t) \equiv \nabla(\nabla \cdot \vec{E}(t)) - \nabla^2 \vec{E}(t) = -\nabla^2 \vec{E}(t) \quad (3.17)$$

and applying the simplification

$$\nabla \cdot \vec{D} = \varepsilon \nabla \cdot \vec{E}(t) = 0 \quad (3.18)$$

finally equation (3.11) takes the form of the Helmholtz equation

$$\nabla^2 \vec{E}(\omega) + n^2(\omega) \frac{\omega^2}{c^2} \vec{E}(\omega) = 0 \quad (3.19)$$

### 3.2 Linear Pulse Propagation

Assuming that there is only linear polarization, so  $\vec{P} = \vec{P}_L + \vec{P}_{NL} = \vec{P}_L$  and starting at equation (3.7)

$$\frac{\partial^2}{\partial z^2} \vec{E}(z, t) - \frac{1}{c^2} \frac{\partial^2}{\partial t^2} \vec{E}(z, t) = \mu_0 \frac{\partial^2}{\partial t^2} \vec{P}(z, t) \quad (3.20)$$

This equation is in the time domain, to get the frequency domain and paying special attention to  $\frac{\partial^2}{\partial t^2} \leftrightarrow -\omega^2$  is used the Fourier transform

$$\frac{\partial^2}{\partial z^2} \vec{E}(z, \omega) + \frac{\omega^2}{c^2} \vec{E}(z, \omega) = -\mu_0 \omega^2 \vec{P}(z, \omega) \quad (3.21)$$

where  $\vec{P}(z, \omega)$  can be obtained from equation (3.9) and (3.13) as

$$\vec{P}(z, \omega) = \chi^{(2)}(\omega) \varepsilon_0 \vec{E}(z, \omega) = [\varepsilon(\omega) - 1] \varepsilon_0 \vec{E}(z, \omega) \quad (3.22)$$

To simplify, wavelength number can be expressed as  $k_n(\omega) = \frac{\omega}{c} n(\omega)$ . So the expression is

$$\frac{\partial^2}{\partial z^2} \vec{E}(z, \omega) + [k_n(\omega)]^2 \vec{E}(z, \omega) = 0 \quad (3.23)$$

That expression is a Helmholtz equation, is needed a change of variables to apply the slowly varying envelope approximation.

$$\vec{E}(z, \omega_0 + \Delta\omega) = \vec{A}(z, \Delta\omega) e^{-jk_n(\omega_0)z} \quad (3.24)$$

$$\vec{A}(z, \Delta\omega) = \int \vec{A}(z, t) e^{-j\Delta\omega t} \quad (3.25)$$

where  $\Delta\omega \equiv \omega - \omega_0$  is the pulse spectrum if is centered at  $\omega_0$ . It is developed equation (3.23) with equations (3.24) and (3.25), that is with the change of variable

$$\frac{\partial^2}{\partial z^2} \vec{A}(z, \Delta\omega) - 2jk_n(\omega_0) \frac{\partial}{\partial z} \vec{A}(z, \Delta\omega) - [k_n(\omega_0)]^2 \vec{A}(z, \Delta\omega) + [k_n(\omega_0 + \Delta\omega)]^2 \vec{A}(z, \Delta\omega) = 0 \quad (3.26)$$

In the slowly varying envelope approximation (SVEA) it is assumed that the amplitude  $\vec{A}$  only varies slowly with  $z$  and  $t$ . This implies that  $\vec{A}$  represents waves propagating forward, predominantly in the  $k_n$  direction. As a result of the slow variation of  $\vec{A}$ , when taking derivatives, the highest-order derivatives may be ignored:

$$\left| \frac{\partial A}{\partial z} \right| \ll |k_n(\omega_0) A|, \left| \frac{\partial A}{\partial t} \right| \ll |\omega_0 A| \quad (3.27)$$

So the first term in equation (3.26) can be ignored and finally it is

$$\frac{\partial}{\partial z} \vec{A}(z, \Delta\omega) + j\Delta k_n \vec{A}(z, \Delta\omega) = 0 \quad (3.28)$$

From this equation, is posible to get a simple equation of motion for the pulse envelope in the spectral domain with a easy solution, that means a phase shift  $\Delta k_n z$  for each frequency component [3].

$$\vec{A}(z, \Delta\omega) = \vec{A}(0, \Delta\omega) e^{-j\Delta k_n z} = \vec{A}(0, \Delta\omega) e^{-j[k_n(\omega_0 + \Delta\omega) - k_n(\omega_0)]z} \quad (3.29)$$

At this point, can go back to the time domain by taking the inverse Fourier transform.[1]

### 3.3 Dispersion

Dispersion arises because of frequency dependence of the refractive index. The result is that waves of different frequencies propagating through a medium will experience different amounts of delay and absorption. This delay is what is known as dispersion. The parameter that governs this is delay is  $k_n(\omega)$ .

Term  $k_n(\omega)$  is rarely known, it is useful to expand it in a Taylor series around the carrier frequency  $\omega_0$  as

$$k(\omega) = k_0 + \frac{dk}{d\omega}(\omega - \omega_0) + \frac{1}{2} \frac{d^2k}{d^2\omega}(\omega - \omega_0)^2 + \frac{1}{6} \frac{d^3k}{d^3\omega}(\omega - \omega_0)^3 + \dots + \frac{1}{n!} \frac{d^n k}{d^n \omega}(\omega - \omega_0)^n \quad (3.30)$$

$$k(\omega) = \sum_0^{\infty} \frac{1}{n!} \frac{d^n k}{d^n \omega}(\omega - \omega_0)^n \quad (3.31)$$

Where equations (3.30) and(3.31) are the general expressions for a optical glass fiber. For a non-dispersive optical glass fiber, the refractive index does not depend on the frequency so that each term is

$$k(\omega) = n \frac{\omega}{c} \quad (3.32)$$

$$\frac{dk}{d\omega} = \frac{n}{c} \quad (3.33)$$

$$\frac{d^2k}{d^2\omega} = 0 \quad (3.34)$$

$$\frac{d^3k}{d^3\omega} = 0 \quad (3.35)$$



While for a fiber dispersive optical glass fiber, the refractive index depends on the frequency, so each term is

$$k(\omega) = n(\omega) \frac{\omega}{c} \quad (3.36)$$

$$\frac{dk}{d\omega} = \frac{n(\omega)}{c} + \frac{n'(\omega)}{c} \omega \quad (3.37)$$

$$\frac{d^2k}{d^2\omega} = \frac{2n'(\omega)}{c} + \frac{n''(\omega)}{c} \omega \quad (3.38)$$

$$\frac{d^3k}{d^3\omega} = \frac{2n''(\omega)}{c} + \frac{n'''(\omega)}{c} \omega \quad (3.39)$$

First term ( $k_0$ ) adds a constant to the phase. The second term, proportional to  $\frac{1}{v_G}$ , adds delay to the pulse. Neither of these terms affects the shape of the pulse. The third term, referred to as group delay dispersion (GDD), is proportional to  $\frac{\partial}{\partial\omega}(\frac{1}{v_G})$  also known as group velocity dispersion (GVD). It introduces a frequency dependent delay of the different spectral components of the pulse, that changes the pulse with the time. The fourth term, referred to as Third Order Dispersion (TOD) applies quadratic phase across the pulse [4].

### 3.3.1 Group Velocity

The group velocity is the velocity with which the envelope of a pulse propagates in a medium, assuming a long pulse with narrow bandwidth, so that higher-order chromatic dispersion is not relevant, and the absence of non-linear effects. Is also the velocity at which the energy moves through the fiber.

$$v_G = \frac{\partial\omega}{\partial k} \quad (3.40)$$

If  $\omega$  is directly proportional to  $k$ , then the group velocity is exactly equal to the phase velocity. However, due to chromatic dispersion, the group velocity in a medium is in general different (typically smaller) from the phase velocity. Otherwise, the envelope of the wave will become distorted as it propagates. This distortion is called group velocity dispersion (GVD). The difference between group velocity and phase velocity also changes the carrier envelope offset of the pulse [5].

### 3.3.2 Group Velocity Dispersion

Group velocity dispersion is the phenomenon that the group velocity of light in a transparent medium depends on the optical frequency or wavelength. Mathematically is defined as the derivative of the inverse group velocity with respect to the angular frequency or the wavelength:

$$GVD = \frac{d^2k}{d^2\omega} = \frac{\partial}{\partial\omega}\left(\frac{1}{v_G}\right) \quad (3.41)$$

The group velocity dispersion is the group delay dispersion (GDD) per unit length. The basic units are  $s^2/m$ . For example, the group velocity dispersion of fused silica fibers is  $+36 \text{ fs}^2/\text{mm}$  at 800 nm and  $-26 \text{ fs}^2/\text{mm}$  at 1550 nm [4].

It is important to realize the different signs of GVD, resulting from the fact that a long wavelength corresponds to a smaller optical frequency. Depending on the situation, group velocity dispersion can have different important effects:

- It is responsible for dispersive temporal broadening or compression of ultrashort pulses.
- In optical fibers, the effect of nonlinearities strongly depends on the group velocity dispersion. For example, there may be spectral broadening or compression, depending on the dispersion properties.
- Dispersion is also responsible for the group velocity mismatch of different waves in parametric nonlinear interactions. For example, it can limit the interaction bandwidth in frequency doublers, optical parametric oscillators and amplifiers.

### 3.3.3 Third Order Dispersion

Third-order dispersion is defined as the chromatic dispersion related to a third-order dependence of the phase change on the frequency offset. In the Taylor expansion of the spectral phase versus angular frequency offset, it is related to the third-order term. It can be written as

$$TOD = \frac{d^3k}{d^3\omega} = \frac{d}{d\omega}(GVD) \quad (3.42)$$

The third-order dispersion of an optical element is usually specified in units of  $\text{fs}^3$ . In mode-locked lasers for pulse durations below 30 fs, it is necessary to provide dispersion compensation not only for the average group delay dispersion, but also for the third-order dispersion and possibly for even higher orders.



# Chapter 4

## Nonlinear Effects

This chapter considers the theory of pulse propagation in nonlinear dispersive media in the slowly varying envelope approximation, assuming that the spectral width of the pulse is much smaller than the frequency of the incident radiation. Later, in section 4.2, are discussed the numerical methods used to solve the resulting propagation equation.

The study of most nonlinear effects in optical fiber involves the use of short pulses with widths ranging from 10ns to 10fs. When such optical pulses propagate inside a fiber, both dispersive and nonlinear effects influence their shapes and spectrum. The starting point is the wave equation (3.7), it can be written in the form

$$\nabla^2 \vec{E} - \frac{1}{c^2} \frac{\partial^2 \vec{E}}{\partial t^2} = \mu_0 \frac{\partial^2 \vec{P}_L}{\partial t^2} + \mu_0 \frac{\partial^2 \vec{P}_{NL}}{\partial t^2} \quad (4.1)$$

where the linear and nonlinear parts of the induced polarization are related to the electric field  $\vec{E}(z, t)$ .

### 4.1 Nonlinear Pulse Propagation

Before solving equation (4.1), it is necessary to do some simplifications. First  $\vec{P}_{NL}$  is treated as a small perturbation to  $\vec{P}_L$ . This is justified because nonlinear changes in the refractive index are  $< 10^{-6}$ . Second, the optical fiber is assumed to maintain its polarization along the fiber length so it can be approximated by a scalar. Third, the pulse spectrum is centered at  $\omega_0$ , is assumed to have a spectral width  $\Delta\omega$  such that  $\Delta\omega/\omega_0 \ll 1$ . Since  $\omega_0 \sim 10^{15} s^{-1}$ , the last assumption is valid for pulses as short as 0.1ps. In the slowly varying envelope approximation (SVEA), it is useful to separate the rapidly varying

par of the electric field by writing it in the form

$$\vec{E}(z, t) = \frac{1}{2} \hat{x} [E(z, t) e^{-j\omega_0 t} + c.c.] \quad (4.2)$$

where  $\hat{x}$  is the polarization unit vector and  $\vec{E}(z, t)$  is a slowly varying function of time. The polarization components  $\vec{P}_L$  and  $\vec{P}_{NL}$  can also be expressed in a similar way by writing

$$\vec{P}_L(z, t) = \frac{1}{2} \hat{x} [P_L(z, t) e^{-j\omega_0 t} + c.c.] \quad (4.3)$$

$$\vec{P}_{NL}(z, t) = \frac{1}{2} \hat{x} [P_{NL}(z, t) e^{-j\omega_0 t} + c.c.] \quad (4.4)$$

The linear component  $P_L$  can be obtained by substituting equation (4.3) in (3.9) and is given by

$$P_L(z, t) = \varepsilon_0 \int_{-\infty}^{\infty} \chi_{xx}^{(1)}(t-t') E(z, t') e^{-j\omega_0(t-t')} dt' = \frac{\varepsilon_0}{2\pi} \int_{-\infty}^{\infty} \chi_{xx}^{(1)}(\omega) E(z, \omega - \omega_0) e^{-j(\omega - \omega_0)t} d\omega \quad (4.5)$$

The nonlinear component  $P_{NL}(z, t)$  is obtained by substituting equation (4.4) in equation (3.10). If the nonlinear response is assumed to be instantaneous so that the time dependence of  $\chi^{(3)}$  in equation (3.10) is given by the product of three delta functions of the form  $\delta(t - t_1)$ . Applying that simplification, equation (3.10) is reduced to

$$\vec{P}_{NL}(z, t) = \varepsilon_0 \chi^{(3)} : \vec{E}(z, t) \vec{E}(z, t) \vec{E}(z, t) \quad (4.6)$$

When equation (4.2) is substituted in equation (4.6),  $\vec{P}_{NL}(z, t)$  is found to have a term oscillating at  $\omega_0$  and another term oscillating at the third-harmonic frequency  $3\omega_0$ , but this term is generally negligible in optical fibers. By making use of equation (4.4),  $\vec{P}_{NL}(z, t)$  is given by

$$\vec{P}_{NL}(z, t) \approx \varepsilon_0 \varepsilon_{NL} \vec{E}(z, t) \quad (4.7)$$

where the nonlinear contribution to the dielectric constant is defined as

$$\varepsilon_{NL} = \frac{3}{4} \chi_{xxxx}^{(3)} |\vec{E}(z, t)|^2 \quad (4.8)$$

To obtain the wave equation for the slowly varying amplitude  $E(z, t)$ , it is more convenient to work in the Fourier domain. This is generally not possible as equation (3.1) is nonlinear because of the intensity dependence of  $\varepsilon_{NL}$ .

Substituting equations (4.2) through (4.4) in (4.1), the Fourier transform  $E(z, \omega - \omega_0)$

$$E(z, \omega - \omega_0) = \int_{-\infty}^{\infty} E(z, t) e^{j(\omega - \omega_0)t} dt \quad (4.9)$$

is found to satisfy the Helmholtz equation

$$\nabla^2 E + \varepsilon(\omega) k_0^2 E = 0 \quad (4.10)$$

where  $k_0 = \omega/c$  and

$$\varepsilon(\omega) = 1 + \chi_{xx}^{(1)}(\omega) + \varepsilon_{NL} \quad (4.11)$$

is the dielectric constant whose nonlinear part  $\varepsilon_{NL}$  is given by equation (4.8). As seen in the linear propagation case in the previous chapter, the dielectric constant can be used to define the refractive index  $\tilde{n}$  and absorption coefficient  $\tilde{\alpha}$ . Both of them are intensity dependent because of  $\varepsilon_{NL}$  and defined

$$\tilde{n} = n + n_2 |E|^2 \quad (4.12)$$

$$\tilde{\alpha} = \alpha + \alpha_2 |E|^2 \quad (4.13)$$

where  $n_2$  is the nonlinear index coefficient and  $\alpha_2$  is the two photon absorption coefficient. Using  $\varepsilon = (\tilde{n} + j\tilde{\alpha}/2k_0)^2$ , equation (4.8) and (4.11),  $n_2$  and  $\alpha_2$  are given by

$$n_2 = \frac{3}{8n} \text{Re}(\chi_{xxxx}^{(3)}) \quad (4.14)$$

$$\alpha_2 = \frac{3\omega_0}{4nc} \text{Im}(\chi_{xxxx}^{(3)}) \quad (4.15)$$

The linear index  $n$  and the absorption coefficient  $\alpha$  are related to the real and imaginary parts of  $\chi_{xx}^{(1)}$ .  $\alpha_2$  is ignored because in silica fibers is relatively small.

Equation (4.10) can be resolved by using the method of separation of variables, by assuming a solution of the form

$$E(z, \omega - \omega_0) = F(x, y) A(z, \omega - \omega_0) e^{j\beta_0 z} \quad (4.16)$$

where  $\beta_0$  is the wave number and  $A(z, \omega)$  is a slowly varying function of  $z$ .  $F(x, y)$  and  $A(z, \omega)$  can be obtained from:

$$\frac{\partial^2 F}{\partial x^2} + \frac{\partial^2 F}{\partial y^2} + [\varepsilon(\omega) k_0^2 - \tilde{\beta}^2] F = 0 \quad (4.17)$$

$$2j\beta_0 \frac{\partial A}{\partial z} + (\tilde{\beta}^2 - \beta_0^2) A = 0 \quad (4.18)$$

In equation (4.18), the second derivative  $\partial^2 A / \partial z^2$  is neglected because  $A(z, \omega)$  is assumed to be a slowly varying function of  $z$ . The dielectric constant  $\varepsilon(\omega)$  can be approximated by

$$\varepsilon = (n + \Delta n)^2 \approx n^2 + 2n\Delta n \quad (4.19)$$

where  $\Delta n$  is a small perturbation given by

$$\Delta n = n_2 |E|^2 + \frac{j\tilde{\alpha}}{2k_0} \quad (4.20)$$

The last unknown parameter is

$$\tilde{\beta}(\omega) = \beta(\omega) + \Delta\beta(\omega) \quad (4.21)$$

and

$$\Delta\beta(\omega) = \frac{\omega^2 n(\omega)}{c^2 \beta(\omega)} \frac{\int \int_{-\infty}^{\infty} \Delta n(\omega) |F(x, y)|^2 dx dy}{\int \int_{-\infty}^{\infty} |F(x, y)|^2 dx dy} \quad (4.22)$$

This step completes the solution of equation (4.1) to the first order in perturbation  $\vec{P}_{NL}$ . Using equations (4.2) and (4.16), the electric field  $\vec{E}(z, t)$  can be written as

$$\vec{E}(z, t) = \frac{1}{2} \hat{x} [F(x, y) A(z, t) e^{j(\beta_0 z + \omega_0 t)} + c.c.] \quad (4.23)$$

where  $A(z, t)$  is the slowly varying pulse envelope. The Fourier transform  $A(z, \omega - \omega_0)$  of  $A(z, t)$  satisfies equation (4.18), and using equation (4.21) can be written as

$$\frac{\partial A}{\partial z} = j[\beta(\omega) + \Delta\beta(\omega) - \beta_0] A \quad (4.24)$$

At this point, going back to the time domain by taking the inverse Fourier transform of equation (4.24), is obtained the equation of propagation for  $A(z, t)$ . However, like in the linear case,  $\beta(\omega)$  is rarely known, so it is useful to expand it in a Taylor series around the carrier frequency  $\omega_0$  as

$$\beta(\omega) = \beta_0 + (\omega - \omega_0)\beta_1 + \frac{1}{2}(\omega - \omega_0)^2\beta_2 + \frac{1}{6}(\omega - \omega_0)^3\beta_3 + \dots \quad (4.25)$$

where  $\beta_0 \equiv \beta(\omega_0)$  and

$$\beta_m = \left( \frac{d^m \beta}{d\omega^m} \right)_{\omega=\omega_0} \quad (m = 1, 2, \dots) \quad (4.26)$$

A similar expansion should be made for  $\Delta\beta(\omega)$

$$\Delta\beta(\omega) = \Delta\beta_0 + (\omega - \omega_0)\Delta\beta_1 + \frac{1}{2}(\omega - \omega_0)^2\Delta\beta_2 + \frac{1}{6}(\omega - \omega_0)^3\Delta\beta_3 + \dots \quad (4.27)$$

where  $\Delta\beta_m$  is defined as

$$\Delta\beta_m = \left(\frac{d^m \Delta\beta}{d\omega^m}\right)_{\omega=\omega_0} \quad (m = 1, 2, \dots) \quad (4.28)$$

The cubic and high order terms in expansion (4.25) are negligible if the spectral width of the pulse satisfies the condition  $\Delta\omega \ll \omega_0$ . After these simplifications in equation (4.24), the inverse Fourier transform is

$$A(z, t) = \frac{1}{2\pi} \int_{-\infty}^{\infty} A(z, \omega - \omega_0) e^{-j(\omega - \omega_0)t} d\omega \quad (4.29)$$

During the Fourier transform operation,  $\omega - \omega_0$  is replaced by the differential operator  $j(\partial/\partial t)$ . The resulting equation is

$$\frac{\partial A}{\partial z} + \beta_1 \frac{\partial A}{\partial t} + \frac{j\beta_2}{2} \frac{\partial^2 A}{\partial t^2} = j\Delta\beta_0 A \quad (4.30)$$

The  $\Delta\beta_0$  term on the right side includes the effects of fiber loss and non-linearity. Using  $\beta(\omega) \approx n(\omega)\omega/c$  and assuming that  $F(x, y)$  does not vary much over the pulse bandwidth, is possible to rewrite equation (4.30) as

$$\frac{\partial A}{\partial z} + \beta_1 \frac{\partial A}{\partial t} + \frac{j\beta_2}{2} \frac{\partial^2 A}{\partial t^2} + \frac{\alpha}{2} A = j\gamma(\omega_0)|A|^2 A \quad (4.31)$$

where the pulse amplitude  $A$  is assumed to be normalized such that  $|A|^2$  represents the optical power and the nonlinear parameter  $\gamma$  is defined as

$$\gamma(\omega_0) = \frac{n_2(\omega_0)\omega_0}{cA_{eff}} \quad (4.32)$$

The quantity  $\gamma|A|^2$  is measured in units of  $m^{-1}$  if  $n_2$  is expressed in units of  $m^2/W$ . The parameter  $A_{eff}$  is known as the effective mode area and is defined as

$$A_{eff} = \frac{(\int \int_{-\infty}^{\infty} |F(x, y)|^2 dx dy)^2}{\int \int_{-\infty}^{\infty} |F(x, y)|^4 dx dy} \quad (4.33)$$



$A_{eff}$  depends on fiber parameters such as the core radius and the core cladding. The transverse distribution inside the core is found to be

$$F(x, y) = J_0(p\rho) \quad \rho \leq a \quad (4.34)$$

where  $\rho = \sqrt{x^2 + y^2}$  is the radial distance. Outside the fiber core, is

$$F(x, y) = \sqrt{a/\rho} J_0(pa) e^{-q(\rho-a)} \quad \rho \geq a \quad (4.35)$$

The fundamental fiber mode is often approximated by a Gaussian distribution of the form

$$F(x, y) \approx e^{-\frac{x^2+y^2}{w^2}} \quad (4.36)$$

where the width parameter  $w$  depends on the  $\nu$  parameter and is determined by curve fitting. After this approximation,  $A_{eff} = \pi w^2$ . Typically,  $A_{eff}$  can vary in the range of 1 to  $100 \mu m^2$ . As a result,  $\gamma$  takes values in the range  $1-100 W^{-1}/km$  if  $n_2 \approx 2.6 \times 10^{-20} m^2/W$ .

Equation (4.31) describes propagation of picosecond optical pulse in single mode fibers. It is related to the nonlinear Schrodinger (NLS) equation and it can be reduced to that form under certain conditions. It includes the effects of fiber losses through  $\alpha$ , of chromatic dispersion through  $\beta_1$  and  $\beta_2$  (see chapter 3), and of fiber nonlinearity through  $\gamma$ . The term  $j\gamma(\omega_0)|A|^2 A$  governs the nonlinear effects of self-phase modulation (SPM).

## 4.2 Numerical Methods

Although the propagation equation (4.31) has been successful in explaining a large number of nonlinear effects, it may need to be modified depending on the experimental conditions. So, for pulse evolution inside a single-mode fiber, it can be rewritten as

$$\begin{aligned} \frac{\partial A}{\partial z} + \frac{1}{2}[\alpha(\omega_0) + j\alpha_1 \frac{\partial}{\partial t}]A + \beta_1 \frac{\partial A}{\partial t} + \frac{j\beta_2}{2} \frac{\partial^2 A}{\partial t^2} - \frac{\beta_3}{6} \frac{\partial^3 A}{\partial t^3} = \\ = j[\gamma(\omega_0) + j\gamma_1 \frac{\partial}{\partial t}][A(z, t) \int_0^\infty R(t') |A(z, t - t')|^2 dt'] \end{aligned} \quad (4.37)$$

where  $R(t)$  is the nonlinear response function normalized such that  $\int_{-\infty}^\infty R(t) dt = 1$ . For pulses wide enough to contain many optical cycles, it can be simplified

considerably by setting  $\alpha_1 = 0$  and  $\gamma_1 = \gamma/\omega_0$  and using the following Taylor expansion:

$$|A(z, t - t')|^2 \approx |A(z, t)|^2 - t' \frac{\partial}{\partial t} |A(z, t)|^2 \quad (4.38)$$

This approximation is reasonable if the pulse envelope evolves slowly along the fiber. Defining the first moment of the nonlinear response function as

$$T_R \equiv \int_0^\infty t R(t) dt \approx f_R \int_0^\infty t h_R(t) dt = [f_R \frac{d(Im \tilde{h}_R)}{d(\Delta\omega)}]_{\Delta\omega=0} \quad (4.39)$$

and noting that  $\int_0^\infty R(t) dt = 1$ , equation (3.37) can be approximated by

$$\frac{\partial A}{\partial z} + \frac{\alpha}{2} A + \frac{j\beta_2}{2} \frac{\partial^2 A}{\partial T^2} - \frac{\beta_3}{6} \frac{\partial^3 A}{\partial T^3} = j\gamma[|A|^2 A + \frac{j}{\omega_0} \frac{\partial}{\partial T} (|A|^2 A) - T_R A \frac{\partial |A|^2}{\partial T}] \quad (4.40)$$

where a frame of reference moving with the pulse at the group velocity  $v_G$  is used by making the transformation

$$T = t - z/v_G \equiv t - \beta_1 z \quad (4.41)$$

A second order term involving the ratio  $T_R/\omega_0$  was neglected because of its smallness.

The NLS equation (4.40) is a nonlinear partial differential equation that in general can not be solved analytically. A numerical approach is therefore necessary for an understanding of the nonlinear effects in optical fibers. A large number of numerical methods have been developed for this purpose, most of them, can be classified into two categories known as the finite-difference and pseudospectral methods. Pseudospectral methods are faster by up to an order of magnitude to achieve the same accuracy. The main method that has been used to solve the pulse propagation problem in nonlinear dispersive media is the split-step Fourier method.

### 4.2.1 Split-Step Fourier Method

The relative speed of this method compared with most finite-difference schemes is, in part, because of the use of the finite Fourier transform (FFT). To understand the split-step Fourier method, the starting point is equation (4.40), that can be written in the form

$$\frac{\partial A}{\partial z} = (\hat{D} + \hat{N})A \quad (4.42)$$

where  $\hat{D}$  is a differential operator that governs dispersion and losses within a linear medium and  $\hat{N}$  is a nonlinear operator that governs the effect of fiber nonlinearities on pulse propagation as follows

$$\hat{D} = -\frac{j\beta_2}{2} \frac{\partial^2}{\partial T^2} + \frac{\beta_3}{6} \frac{\partial^3}{\partial T^3} + \frac{\alpha}{2} \quad (4.43)$$

$$\hat{N} = j\gamma[|A|^2 + \frac{j}{\omega_0} \frac{1}{A} \frac{\partial}{\partial T} (|A|^2 A) - T_R \frac{\partial |A|^2}{\partial T}] \quad (4.44)$$

In general, dispersion and nonlinearity act together along the length of the fiber. The split-step Fourier method obtains an approximate solution by assuming as independent dispersive and nonlinear effects when propagating the optical field over a small distance  $h$ . To propagate from  $z$  to  $z + h$  are needed two steps. In the first step,  $\hat{D} = 0$  so there is only nonlinearities. In the second step,  $\hat{N} = 0$  so there is only dispersion and losses. Mathematically

$$A(z + h, T) \approx A(z, T) e^{h\hat{D}} e^{h\hat{N}} \quad (4.45)$$

The exponential operator  $e^{h\hat{D}}$  can be evaluated in the Fourier domain using

$$e^{h\hat{D}} B(z, T) = F_T^{-1} \{ e^{h\hat{D}(-j\omega)} F_T \{ B(z, T) \} \} \quad (4.46)$$

where  $F_T$  is the Fourier transform operation. As  $\hat{D}(j\omega)$  is just a number in the Fourier space, the evaluation of equation (4.46) is straight forward. The use of the FFT algorithm makes numerical evaluation of equation (4.46) relatively fast, this is the reason that makes this method even two orders of magnitude faster than finite-difference schemes.

The accuracy of the split-step Fourier method can be improved by adopting a different procedure to propagate the optical pulse over one segment from  $z$  to  $z + h$ . In this procedure, equation (4.45) is replaced by

$$A(z + h, T) \approx A(z, T) e^{h\hat{D}} e^{\int_z^{z+h} \hat{N}(z') dz'} \quad (4.47)$$

The main difference is that the effect of nonlinearity is included in the middle of the segment rather than at the segment boundary. If the step size  $h$  is small enough, the integral can be approximated by  $e^{h\hat{N}}$ , similar to equation (4.45).

The accuracy of the split-step Fourier method can be further improved by

evaluating the integral in equation (4.47) more accurately than approximating it by  $h\hat{N}(z)$ . Applying the trapezoidal rule, the integral can be approximated by

$$\int_z^{z+h} \hat{N}(z') dz' \approx \frac{h}{2} [\hat{N}(z) + \hat{N}(z+h)] \quad (4.48)$$

However, this approximation is not simple because  $\hat{N}(z+h)$  is unknown at the interval  $z + h/2$ . To solve this issue, it is possible to estimate  $\hat{N}(z+h)$  similarly to equation (4.47). Although the iteration consumes much time, it can still reduce the overall computing by increasing the step size  $h$ .

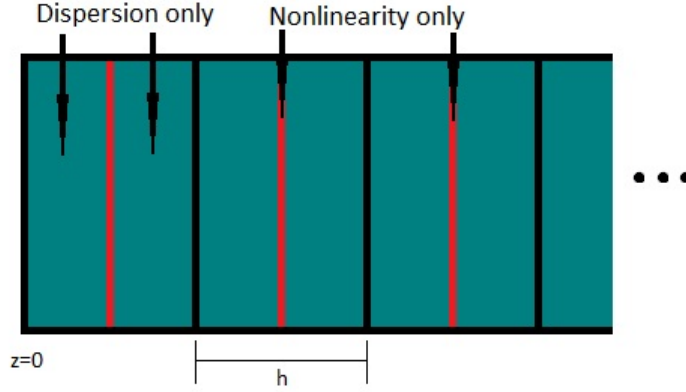


Figure 4.1: Split-Step Fourier method schematic

Figure (4.1) shows how the method works. The fiber length is divided into a large number of segments that are not necessarily equally spaced. The optical pulse is propagating from segment to segment using equation (4.47). Another way to explain it, the optical field  $A(z, t)$  is first propagated for a distance  $h/2$  with dispersion only using the FFT algorithm and equation (4.46). At the segment  $z + h/2$ , the field is multiplied by a nonlinear term that represents the effect of nonlinearity over the whole segment length  $h$ . Finally, the field propagates again for the remaining distance  $h/2$  with dispersion only to obtain  $A(z + h, T)$ .

In practice, the split-step Fourier method can be faster by applying equation

(4.47) over  $M$  successive steps

$$A(L, T) \approx e^{-\frac{1}{2}h\hat{D}} \left( \prod_{m=1}^M e^{h\hat{D}} e^{h\hat{N}} \right) e^{\frac{1}{2}h\hat{D}} A(0, T) \quad (4.49)$$

where  $L = Mh$  is the total fiber length and the integral in equation (4.48) was approximated with  $h\hat{N}$ . Thus, except for the first and last dispersive steps, all intermediate steps can be carried over the whole segment length  $h$ . This feature reduces the required number of FFTs roughly by a factor of 2 and accelerates the numerical code by the same factor.

### 4.2.2 FDTD

The Finite-Difference Time-Domain method is used to solve transient electromagnetic problems in the Time-Domain. The Time-Domain methods can also be used for the study of electromagnetic pulses propagation[7].

Time-Domain method is taken because this study is dealing with optical pulses produced by femtoseconds lasers. That means, the pulses are in a very high frequencies, thus depending of refractive index of the medium through which the pulse is propagated and being very important then the study of dispersion features of the medium.

Time-Domain methods offers a better way to handle dispersion for general medias when several dispersive models cannot do it. As well known, the electromagnetic waves propagation is described by Maxwell's Equations which describe the time and space evolution of magnetic and electric fields (See chapter 3, section 3.1, equations (3.1) to (3.4))

Kane Yee developed the Finite-Difference Time-Domain algorithm in 1966 to solve the previous equations discretizing both time and space variables and using finite differences instead the partial derivatives [8]. The FDTD algorithm employs a staggered where the distribution of electric fields and magnetic fields are given by samples at the time and spatial points on the next way:

- Electric fields

$$t = n\Delta t \quad (4.50)$$

$$z = j\Delta t \quad (4.51)$$

- Magnetic fields

$$t = (n + 1/2)\Delta t \quad (4.52)$$

$$z = (i + 1/2)\Delta z \quad (4.53)$$

For one dimensional propagation and a simple dispersion free medium there is

$$\frac{\partial \vec{H}}{\partial t} = \frac{1}{\mu} \frac{\partial \vec{E}}{\partial z} \quad (4.54)$$

$$\frac{\partial \vec{E}}{\partial t} = \frac{1}{\varepsilon} \frac{\partial \vec{H}}{\partial z} \quad (4.55)$$

Introducing  $E^n(i) = E(i\Delta z, n\Delta t)$  and  $H^{n+1/2}(j+1/2) = H((i+1/2)\Delta z, (n+1/2)\Delta t)$  and after of substituting the equations (4.41) and (4.42) by their respective finite difference formulas, finally is obtained:

$$H^{n+1/2}(i + 1/2) = H^{n-1/2}(i + 1/2) + \frac{\Delta t}{\mu \Delta z} [E^n(i + 1) - E^n(i)] \quad (4.56)$$

$$E^{n+1}(i) = E^n(i) + \frac{\Delta t}{\varepsilon \Delta z} [H^{n+1/2}(i + 1/2) - H^{n+1/2}(i - 1/2)] \quad (4.57)$$

This is a more efficient solution for Maxwell's equations by means of FDTD, is possible to do the same for a three-dimensional region example [9]. The FDTD method is a useful tool and easy to implement for solving pulse propagation problems.



# Chapter 5

## Time-Frequency Representations

A time-frequency representation (TFR) is a view of a signal represented over both time and frequency. The purpose of this chapter is see how to represent the time-frequency signals with spectrograms and Wigner-Ville distribution.

### 5.1 Spectrogram

The Fourier Transform of a signal only gives the frequency spectrum of a pulse, but provides no information about the evolution in time of different frequencies. To study the dynamics of the frequency content of a pulse, is necessary to use joint time-frequency analysis methods. The spectrogram is such a technique that allows frequency information to be obtained as a function of time. At a glance to the spectrogram, one can see when different frequencies of a signal appears or disappears as well as their duration and energy contents.



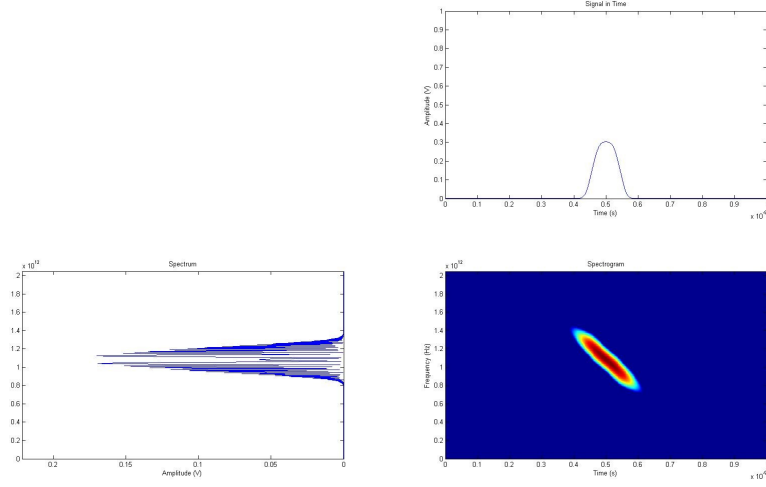


Figure 5.1: Top signal in time; Left spectrum; Right spectrogram

The spectrogram  $S(t, \omega)$  of a time signal  $f(t)$  is a quadratic distribution that is defined as the square of the magnitude of the linear short-time Fourier transform (STFT) (see chapter 2). So that

$$S(t, \omega) = |F(\tau, \omega)|^2 = \left| \int_{-\infty}^{\infty} f(t)w(t - \tau)e^{-j2\omega t} dt \right|^2 \quad (5.1)$$

where  $\tau$  set the time interval to analyze. Depending on the window function, there will be different short-time spectra, that way is possible to give more importance to the center point or to give equal weight to all points.

### 5.1.1 Spectrogram properties

The spectrogram is easy to understand and interpret, in addition to being a good time-frequency representation for many signals. But is interesting to study its properties

#### Marginal Properties

Does not satisfy marginal energies, so something is being added or subtracted. Writing the signal and window in terms of amplitude and phase

$$s(t) = A(t)e^{j\varphi(t)} \quad (5.2)$$

$$w(t) = A_w(t)e^{j\varphi_w(t)} \quad (5.3)$$

and similarly for their Fourier transforms

$$S(\omega) = B(\omega)e^{j\phi(\omega)} \quad (5.4)$$

$$W(\omega) = B_W(\omega)e^{j\phi_W(\omega)} \quad (5.5)$$

The marginals are then

$$P_1(t) = \int P_{SP}(t, \omega) d\omega = \int A^2(t') A_w^2(t' - t) dt' \quad (5.6)$$

$$P_2(\omega) = \int P_{SP}(t, \omega) d\omega = \int B^2(\omega') B_W^2(\omega - \omega') dt' \quad (5.7)$$

where  $A^2(t)$  is not equal to the instant energy and  $B^2(\omega)$  is not equal to the spectral density of energy, but they approximate that values when the window (in each domain) narrows.

### 5.1.2 Spectrogram drawbacks and conclusions

Unfortunately because of the properties of the short-time Fourier transform, is not possible to obtain both good time and frequency resolution simultaneously. This is determined by the Heisenberg-Gabor inequality that states that the time-bandwidth product

$$T \times B \geq 1 \quad (5.8)$$

where  $T$  is the standard deviation of the time-signal and  $B$  is its Fourier transform. Because of this inequality, is not possible to determinate the dynamic evolution precisely, because will always have some degree of uncertainty.

The spectrogram is just one of several energy distributions that can be used to obtain time-frequency information. Another distribution which is commonly used for studying pulse dynamics is the Wigner-Ville distribution.

## 5.2 Wigner-Ville Distribution (WVD)

The Wigner Distribution (WD) was proposed by Eugene Wigner in 1932 for application in quantum mechanics. This distribution was redefined by Ville (WVD-Wigner-Ville Distribution) in 1948 at signal context, like a time-frequency function. It has more recently been recognised as a powerful tool

for time-frequency analysis of signals, where with some care, it can be interpreted as a distribution of the signal energy in time and frequency. Claasen and Mecklenbrauker [11] show that the WVD can be evaluated from time signal  $f(t)$

$$W_f(t, \omega) = \int_{-\infty}^{+\infty} f\left(t + \frac{\tau}{2}\right) f^*\left(t - \frac{\tau}{2}\right) e^{-j\omega\tau} d\tau \quad (5.9)$$

While STFT is a linear transform, WVD is a bilinear (nonlinear) distribution. The first difference between linear and nonlinear representations is the fulfillment or not of Superposition Theorem [12]

$$T[\alpha_1 f_1 + \alpha_2 f_2] = \alpha_1 T[f_1] + \alpha_2 T[f_2] \quad (5.10)$$

Linear representations fulfill Superposition Theorem, while nonlinear representations do not, so WVD neither does it.

### 5.2.1 WVD properties

Bilinear representations have to satisfy several conditions to be a valid energy distribution interpretation. WVD is the most complete distribution, satisfying more properties or conditions than any of other distributions[13].

#### Marginal Properties

The spectral density of energy and instant energy (power) can be obtained as WVD marginal distributions

$$\int_{-\infty}^{+\infty} W_f(t, \omega) dt = |F(\omega)|^2 \quad (5.11)$$

$$\int_{-\infty}^{+\infty} W_f(t, \omega) d\omega = |f(t)|^2 \quad (5.12)$$

being  $|F(\omega)|^2$  the spectral density of energy and  $|f(t)|^2$  the instant energy (power).

#### Energy Conservation

To be considered like a energy density distribution, it must satisfy

$$\int_{-\infty}^{+\infty} \int_{-\infty}^{+\infty} W_f(t, \omega) dt d\omega = \int_{-\infty}^{+\infty} |f(t)|^2 dt = \int_{-\infty}^{+\infty} |F(\omega)|^2 d\omega \quad (5.13)$$

### Negativity or Real Property

WVD spectrum always takes real values of the signal. This means that it takes both negative and positive values, so WVD cannot be defined as density function, given that WVD spectrum should have only positive values to be a density function.

### Invariance Properties

There is

$$s(t) = f(t - t_0) \quad (5.14)$$

$$s(t) = f(t)e^{-j\omega_0 t} \quad (5.15)$$

If  $s(t)$  is equal to  $f(t)$  time-shifted or frequency-shifted function the signal is invariant to time or frequency shifts, respectively, when

$$W_s(t, \omega) = W_f(t - t_0, \omega) \quad (5.16)$$

$$W_s(t, \omega) = W_f(t, \omega - \omega_0) \quad (5.17)$$

### 5.2.2 WVD drawbacks and conclusions

The main drawback of WVD and any bilinear time-frequency distribution representation is the interference between the own terms of the distribution and its crossed terms. This crossed terms are generated due to the quadratic nature of WVD, that it has several spectral components. The crossed terms are always generated for any kind of signal or noise (each signal has their own crossed term), and it may induce to misleading representation and impair the useful signal analysis.

It can be shown that the WVD is the most basic distribution. Another important attribute is the spread of the square magnitude of any joint time-frequency distribution. It can also be shown that in the case of the WVD, the spread will be smaller and easier reduced than of the STFT[14].



# Chapter 6

## Results

This chapter will apply previously acquired knowledge to see the results in a real environment. First, section 6.1 show the results for the case of propagation considering only the linear effects in the fiber. Section 6.2 is taken into account nonlinear effects. The idea is to see how the pulse evolves when propagating along the fiber and measuring the pulse width to see the impact of the different parameters.

### 6.1 Linear Propagation

Starting function to propagate along the fiber is a Gaussian form

$$E = Ae^{-\frac{(t-t_0)^2}{\sigma^2}} e^{jb\frac{t^2}{\sigma^2}} e^{j\omega_0 t} \quad (6.1)$$

where  $A$  is the signal amplitude, the first exponential is a gaussian function, the second exponential is a chirp and  $\sigma = \frac{FWHM}{2*\sqrt{2\log 2}}$ . FWHM (full width at half maximum) is the difference between the two extreme values of the independent variable at which the dependent variable is equal to half of its maximum value.

Is selected a wavelength of 800nm, although is not the wavelength used in the laboratory, there is no literature for the same parameters at 1550nm, so that is taken 800nm to analyze the linear section (see appendix 9, figure 9.1). Could have chosen another wavelength in the range 450-900nm, but is chosen 800nm because within the possibilities offered by the table, is the most common wavelength. So its parameters for fused silica fiber are  $n = 1.453$ ,  $\frac{\partial n}{\partial \lambda} = -0.017\mu m^{-1}$ ,  $\frac{\partial^2 n}{\partial \lambda^2} = 0.040\mu m^{-2}$  and  $\frac{\partial^3 n}{\partial \lambda^3} = -0.239\mu m^{-3}$

### 6.1.1 Propagating 100 meters changing the amplitude

Will begin setting  $z$  at 100 meters,  $b$  at  $\pi/2$  and FWHM at 200fs.

#### Before Propagating

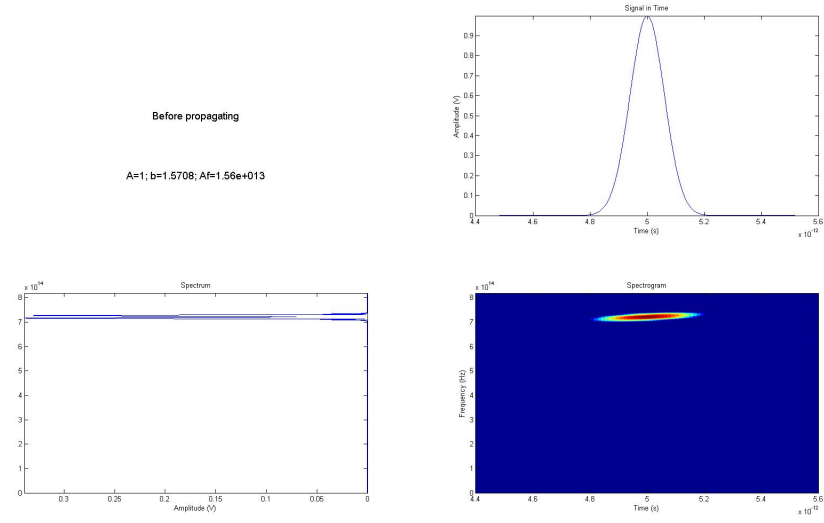


Figure 6.1:  $A=1 \Rightarrow \Delta f=15,6$  THz; Before propagating

Before crossing the fiber, both the spectrum and the signal in time does not vary (only its amplitude). Therefore, only will be represented the figures of the signal after passing through the fiber of 100 meters

After propagating

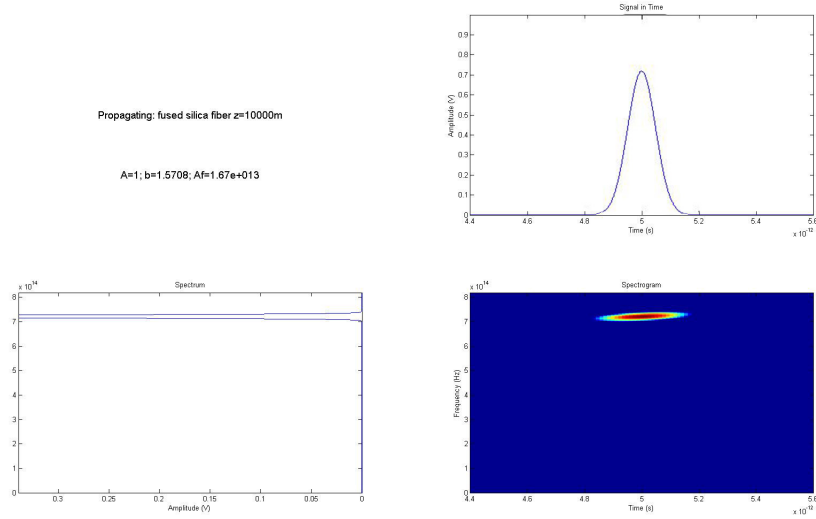


Figure 6.2:  $A=1 \Rightarrow \Delta f=16,7$  THz

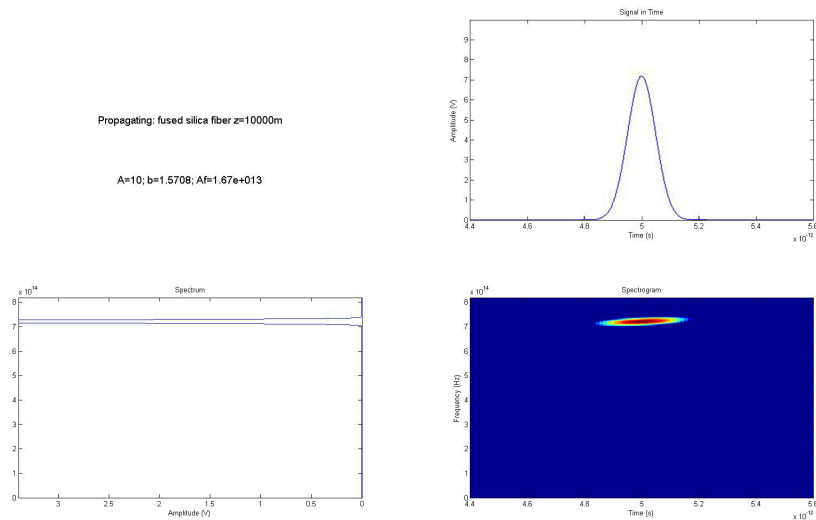
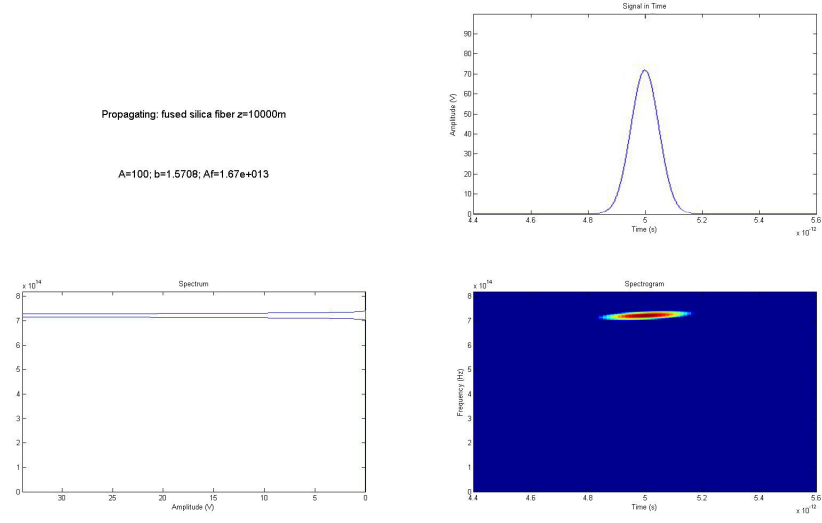
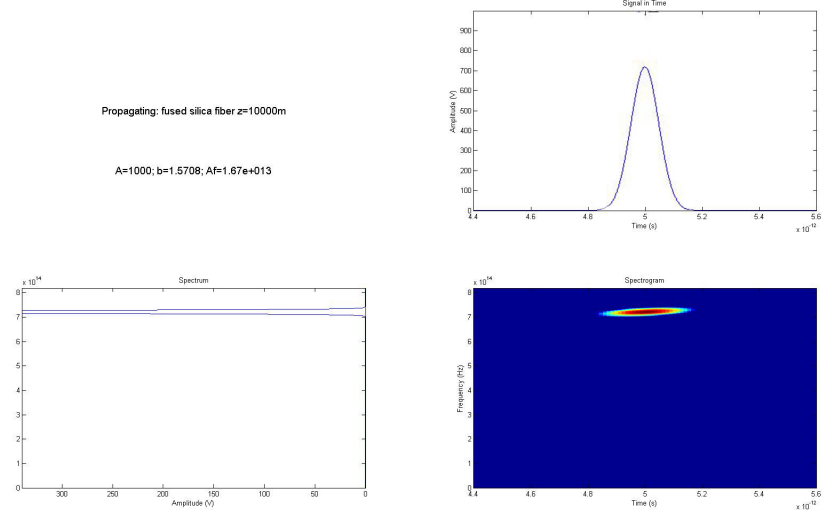


Figure 6.3:  $A=10 \Rightarrow \Delta f=16,7$  THz



Figure 6.4:  $A=100 \Rightarrow \Delta f=16,7$  THzFigure 6.5:  $A=1000 \Rightarrow \Delta f=16,7$  THz

Is observed that changing the amplitude  $A$  of the signal does not affect the pulse width in time nor frequency. In frequency, it remains in  $\Delta f = 16.7$  THz, since  $A = 1$  to  $A = 1000$ .

### 6.1.2 Propagating 100 meters changing the phase value

Will begin setting  $z$  at 100 meters,  $A$  at 1 and FWHM at 200fs. Before propagating at top and right below, propagating spectrogram

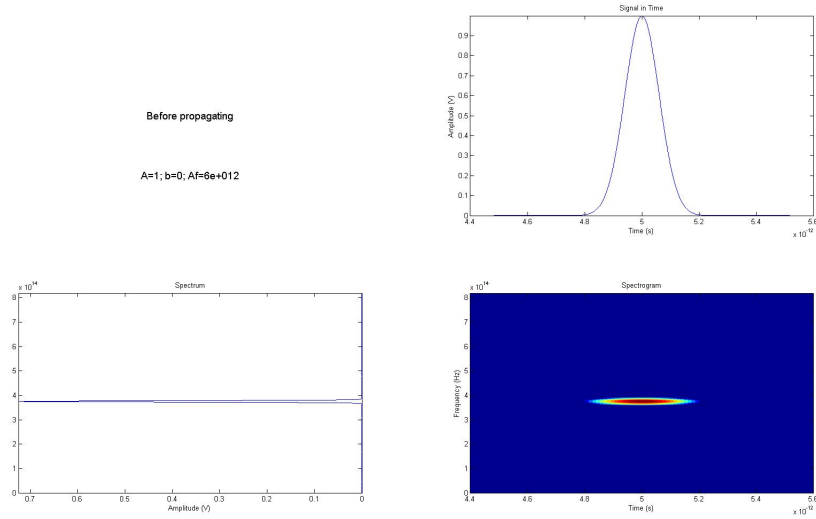


Figure 6.6:  $b=0 \Rightarrow \Delta f=6$  THz; Before propagating

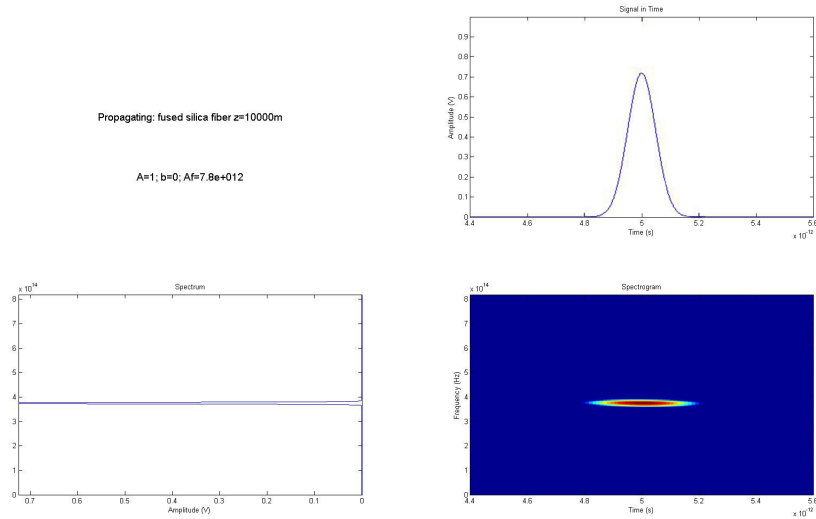
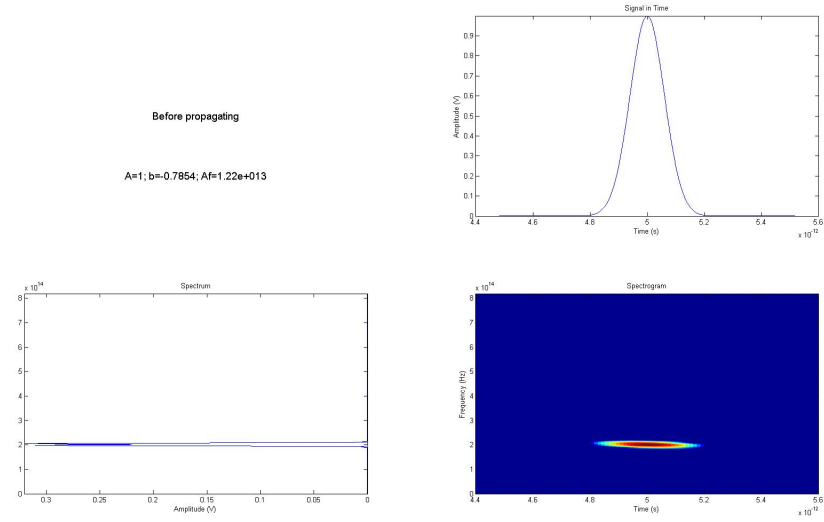
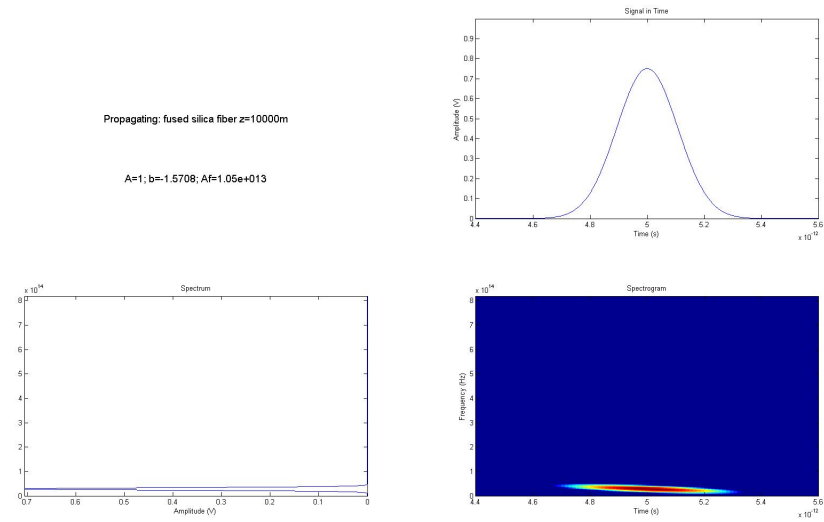
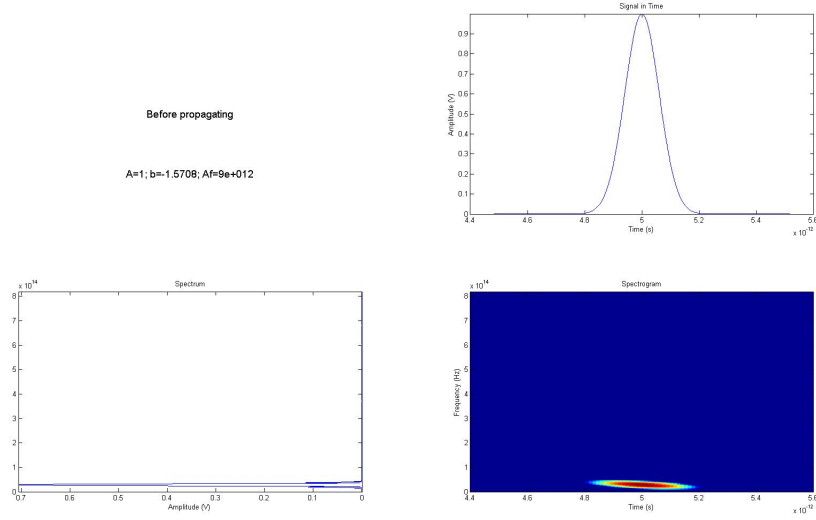
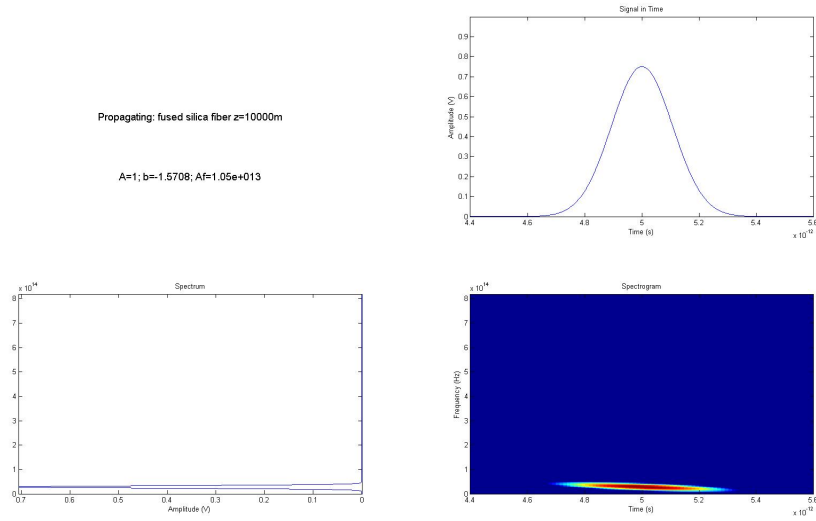


Figure 6.7:  $b=0 \Rightarrow \Delta f=5,5$  THz

Figure 6.8:  $b=-\pi/4 \Rightarrow \Delta f=12,2$  THz; Before propagatingFigure 6.9:  $b=-\pi/4 \Rightarrow \Delta f=10,2$  THz

Figure 6.10:  $b=-\pi/2 \Rightarrow \Delta f=12,2$  THz; Before propagatingFigure 6.11:  $b=-\pi/2 \Rightarrow \Delta f=10,5$  THz

To see the effect of the different values of the phase value  $b$ , will be built a table to compare numerically the results obtained.

Graphically

$b$	$\Delta f(\text{THz})$ Before Propagating	$\Delta f(\text{THz})$ After Propagating
0	6, 0	5, 5
$-\pi/4$	10, 2	7, 2
$-\pi/2$	12, 2	10, 5

Table 6.1:  $\Delta f$  for different values of  $b$

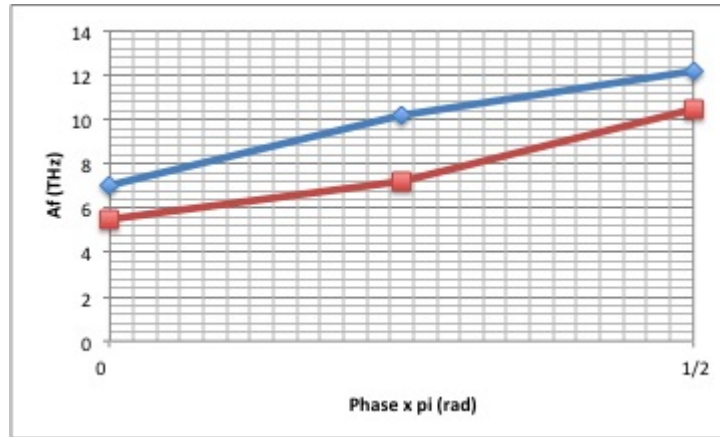


Figure 6.12: Blue  $\Rightarrow$  Before Propagating ; Red  $\Rightarrow$  After Propagating

The pulse width (in frequency) of the propagated signal gets bigger as the phase increases, exactly as happens with the signal before propagating. So it can be said that the phase value affects the signal as an offset or a frequency shift.

$b$	$f(\text{THz})$
0	$f_0 = 375$
$-\pi/4$	200
$-\pi/2$	25

Table 6.2:  $\Delta f$  for different values of  $b$

Changing the phase  $\pi/4$  means a spectral frequency shift of approximately 175THz

### 6.1.3 Propagating in other fibers

Instead of fused silica fiber, in this experiment  $A$  is fixed at 1,  $b$  is  $\pi/2$ . First fiber LAKL21, that works with the next characteristics:  $n = 1.632$ ,  $\frac{\partial n}{\partial \lambda} = -0.026 \mu m^{-1}$ ,  $\frac{\partial^2 n}{\partial \lambda^2} = 0.066 \mu m^{-2}$  and  $\frac{\partial^3 n}{\partial \lambda^3} = -0.386 \mu m^{-3}$

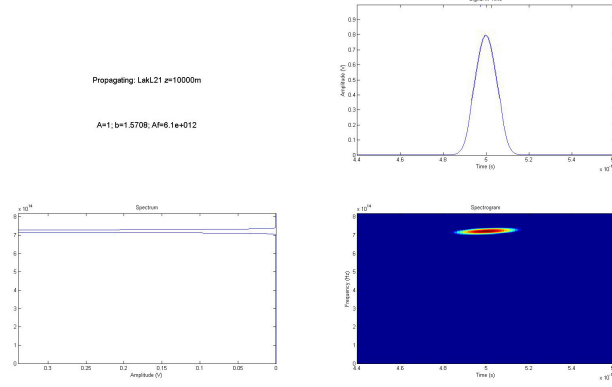


Figure 6.13: LAKL21 fiber  $\Rightarrow \Delta f=6,1$  THz

Next fiber is SF10, that works with the next characteristics:  $n = 1.711$ ,  $\frac{\partial n}{\partial \lambda} = -0.050 \mu m^{-1}$ ,  $\frac{\partial^2 n}{\partial \lambda^2} = 0.176 \mu m^{-2}$  and  $\frac{\partial^3 n}{\partial \lambda^3} = -0.988 \mu m^{-3}$

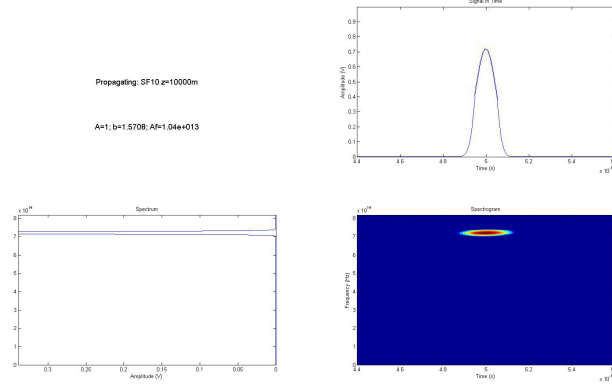


Figure 6.14: SF10 fiber  $\Rightarrow \Delta f=10,4$  THz

Last fiber is BK7, that works with the next characteristics:  $n = 1.511$ ,  $\frac{\partial n}{\partial \lambda} = -0.015 \mu m^{-1}$ ,  $\frac{\partial^2 n}{\partial \lambda^2} = 0.056 \mu m^{-2}$  and  $\frac{\partial^3 n}{\partial \lambda^3} = -0.288 \mu m^{-3}$

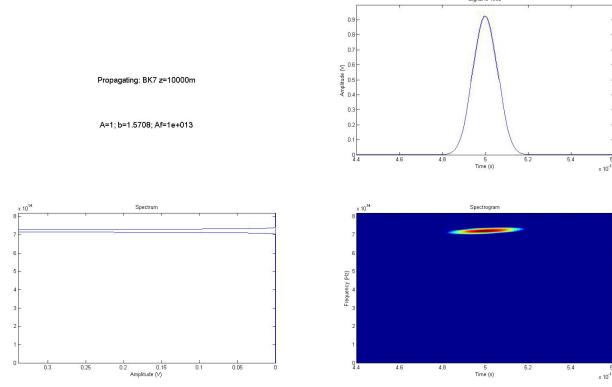


Figure 6.15: BK7 fiber  $\Rightarrow \Delta f = 10$  THz

Putting together the results in a table is obtained

Fiber	$\Delta f$ (THz)
Fused Silica	10, 7
LAKL21	6, 2
SF10	6, 0
BK7	12, 2

Table 6.3:  $\Delta f$  for different values of  $b$

SF10 is the fiber that shows less dispersion (of the tested) while the typical fiber, fused silica, has a dispersion within the average.

## 6.2 Nonlinear Propagation

For the nonlinear propagation case, the function to propagate is the same as for the linear case, see equation (6.1). It has been decided to use the split-step Fourier method.

Is selected a wavelength of 1550nm, because is the wavelength used by the laboratory's laser. Also is selected a fused silica fiber, the most common fiber in the laboratory, with measured parameters:  $\beta_2 = 5.1 \cdot 10^{-27} (s^2/km)$ ,  $\gamma = 2.2 \cdot 10^{-3} (1/Wkm)$  and  $\alpha = 0.051 \cdot 10^{-3} (1/km)$ , see equations (3.42) to (3.49).

### 6.2.1 Propagating 100 meters changing the amplitude

For this experiment,  $z$  is fixed at 100 meters,  $b$  is  $\pi/2$  and the pulse FWHM is 2ps. Let see how the pulse evolves for different values of the amplitude  $A$ , by changing it from 1 to 50, first in steps of 1 until 10 and then in steps of 10 until 50.

#### Before Propagating

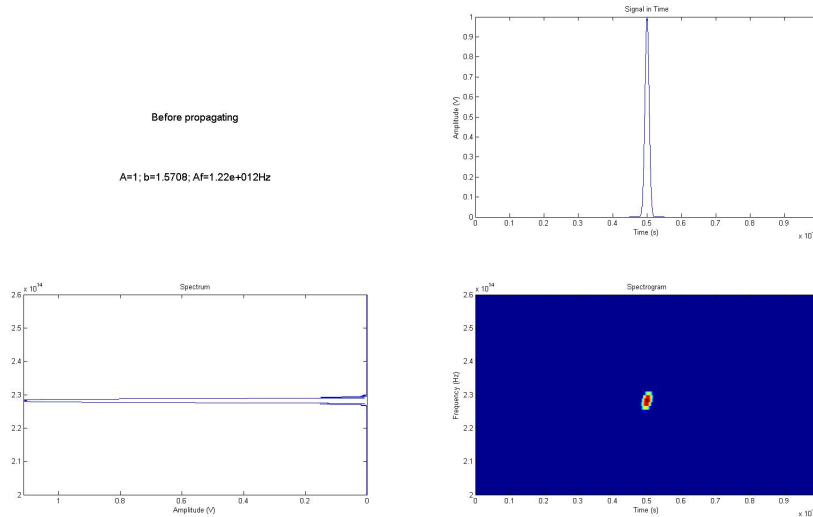
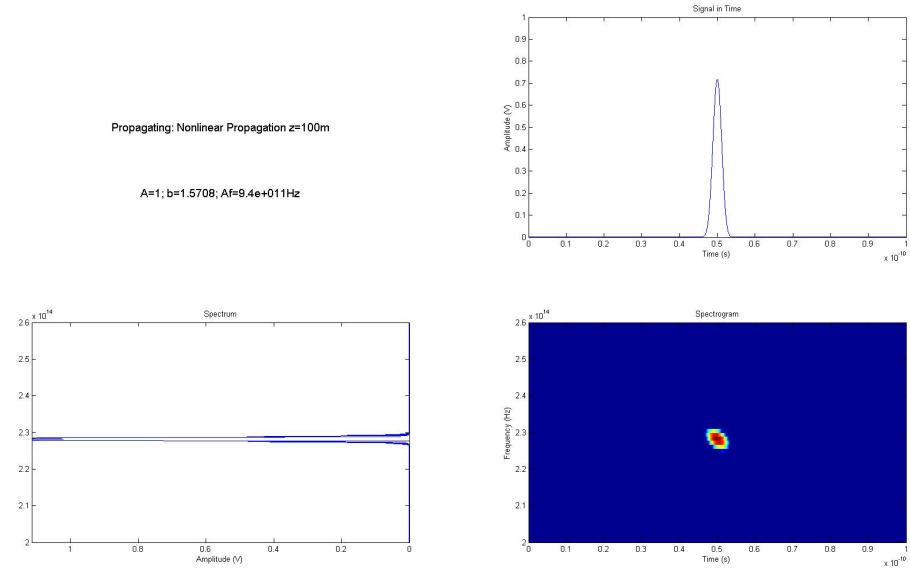
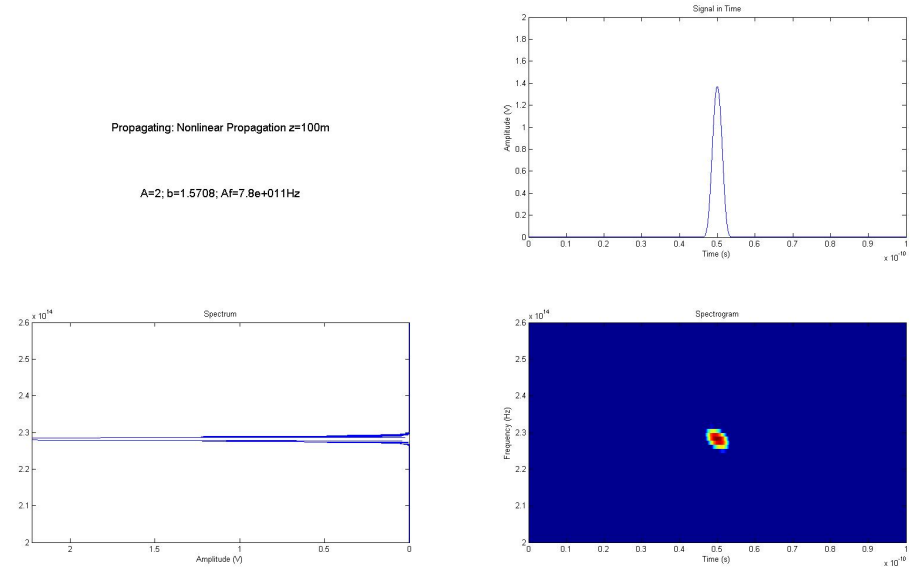
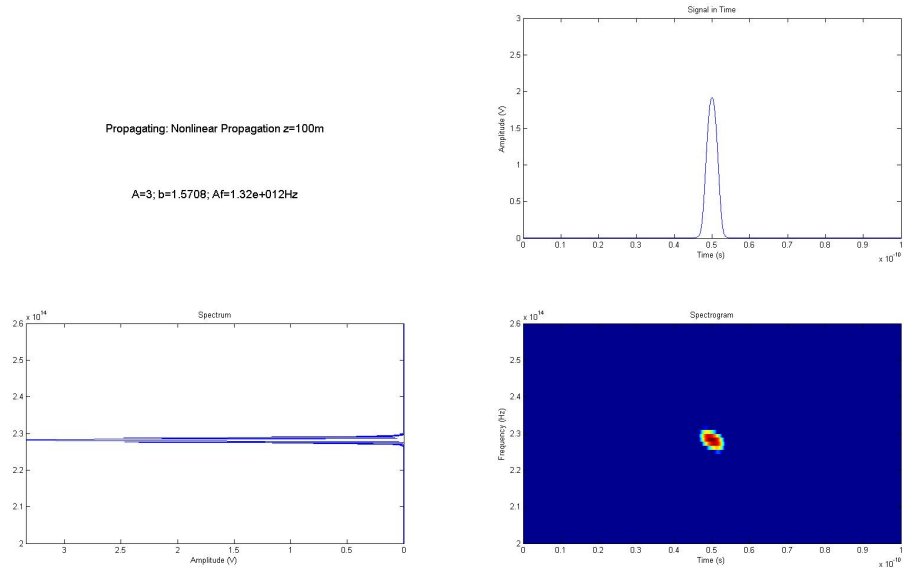
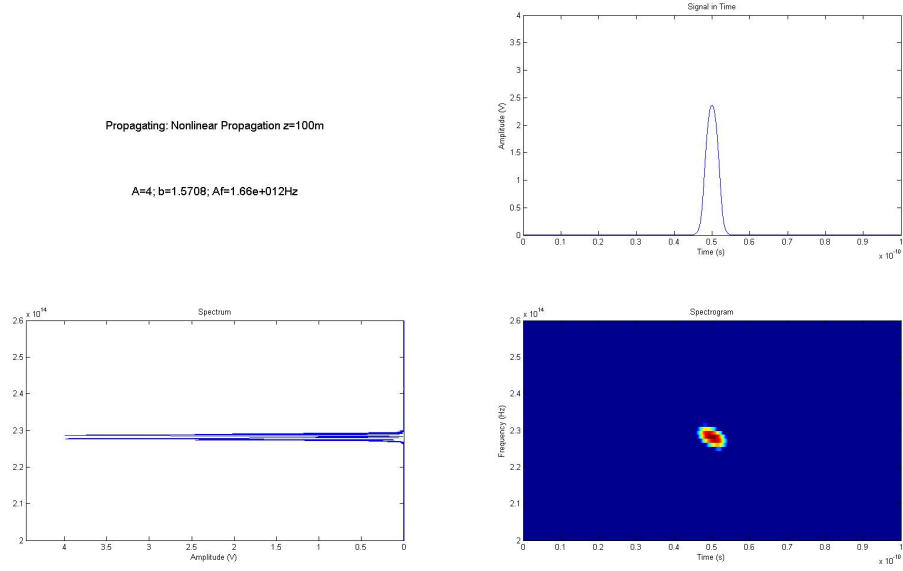


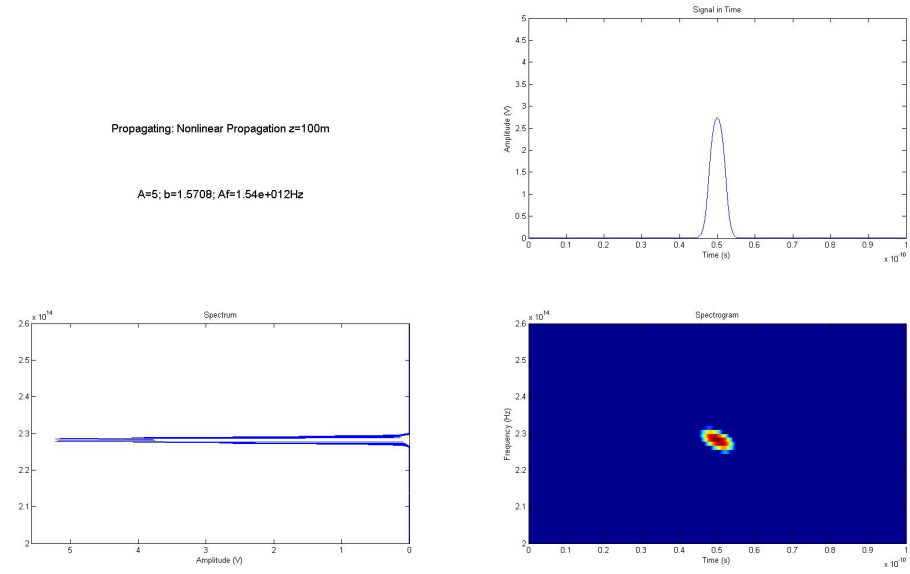
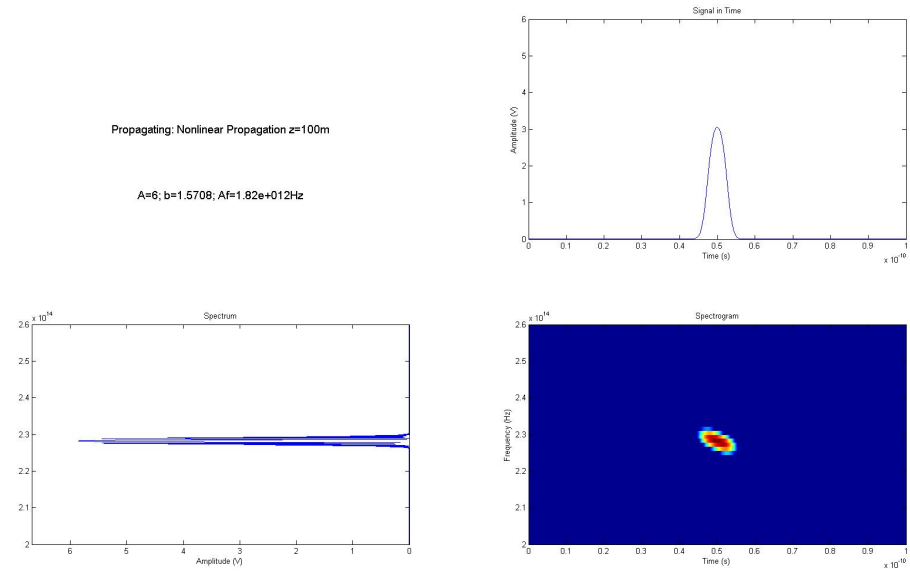
Figure 6.16:  $A=1 \Rightarrow \Delta f=1,22$  THz; Before propagating

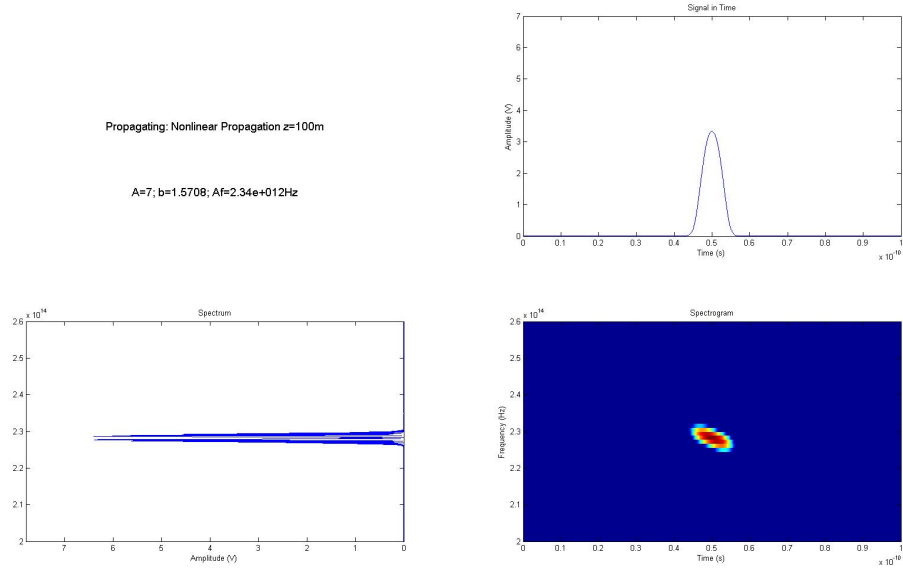
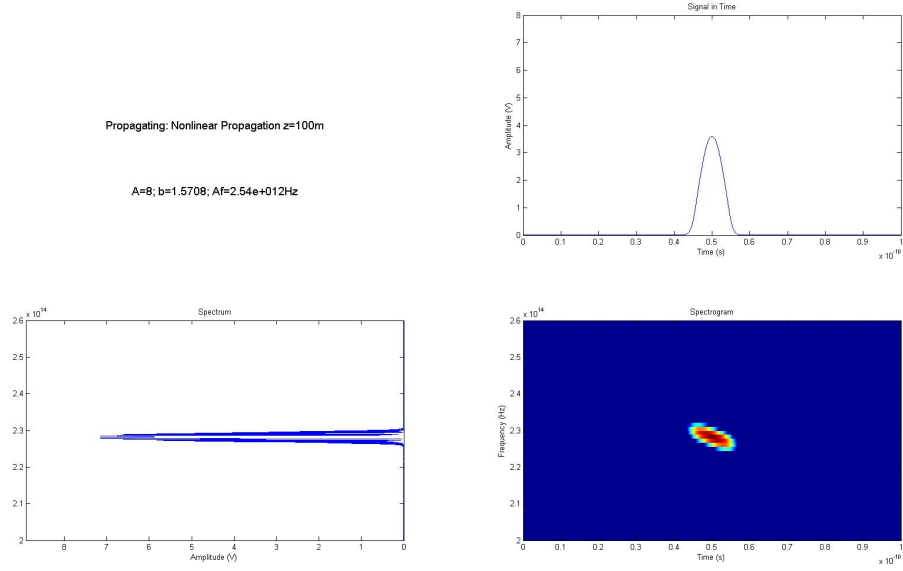


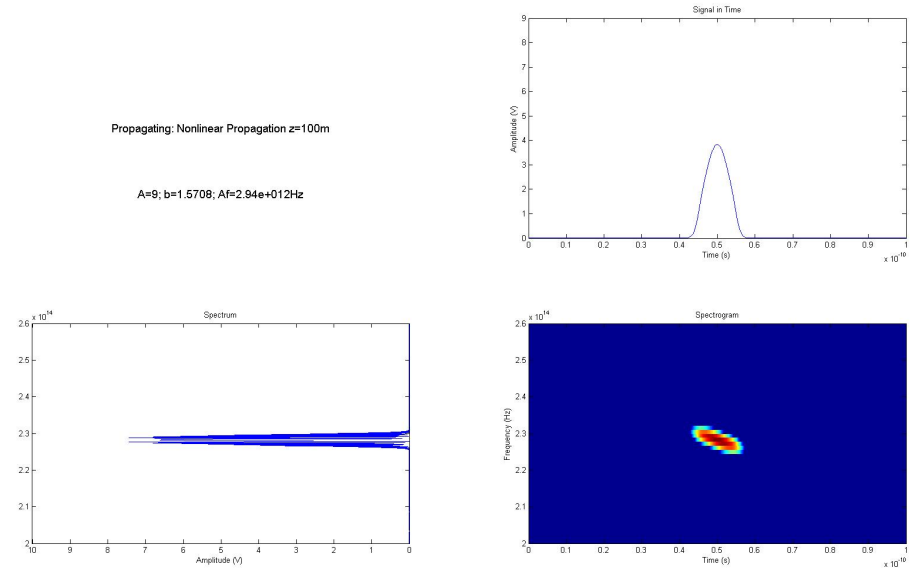
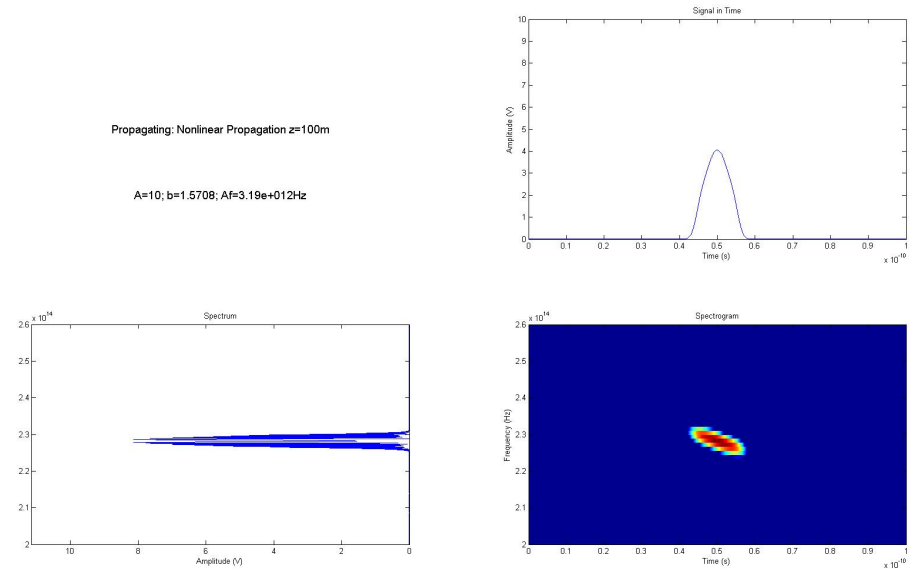
## After Propagating

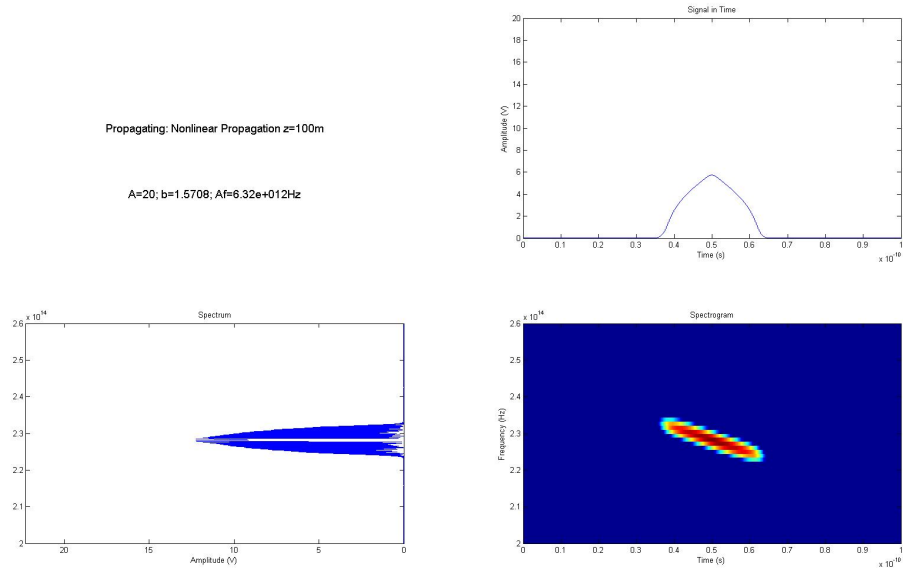
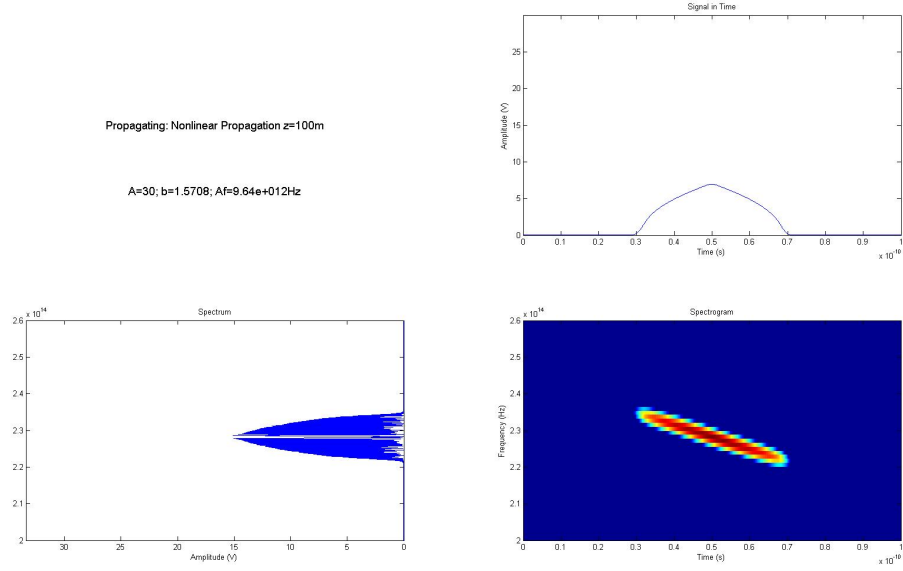
Figure 6.17:  $A=1 \Rightarrow \Delta f=0,94$  THzFigure 6.18:  $A=2 \Rightarrow \Delta f=0,78$  THz

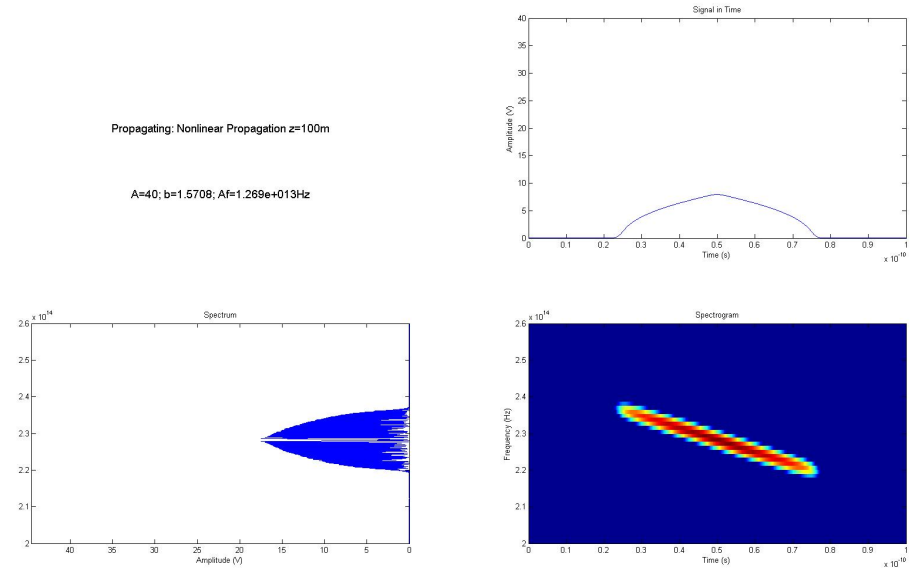
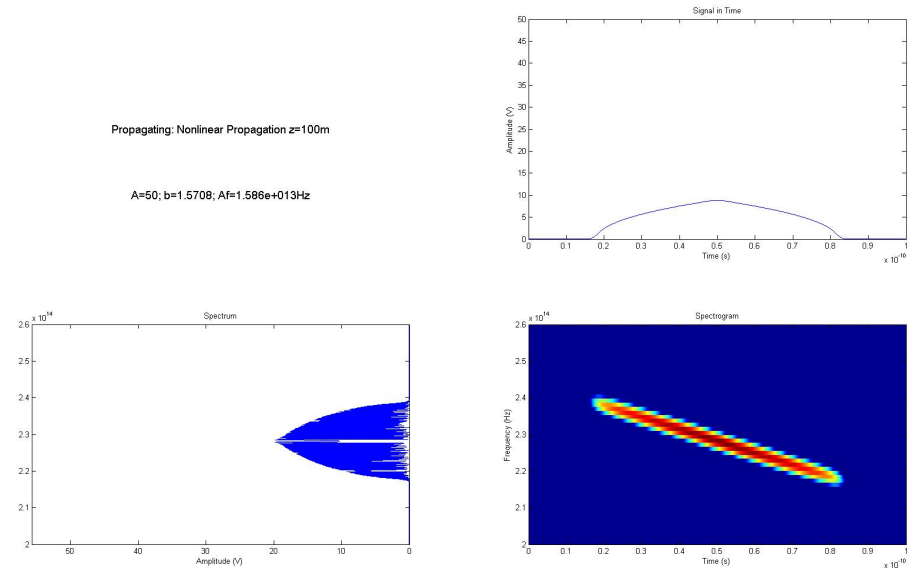
Figure 6.19:  $A=3 \Rightarrow \Delta f=1,32$  THzFigure 6.20:  $A=4 \Rightarrow \Delta f=1,66$  THz

Figure 6.21:  $A=5 \Rightarrow \Delta f=1,54 \text{ THz}$ Figure 6.22:  $A=6 \Rightarrow \Delta f=1,82 \text{ THz}$

Figure 6.23:  $A=7 \Rightarrow \Delta f=2,34$  THzFigure 6.24:  $A=8 \Rightarrow \Delta f=2,54$  THz

Figure 6.25:  $A=9 \Rightarrow \Delta f=2,94\text{ THz}$ Figure 6.26:  $A=10 \Rightarrow \Delta f=3,19\text{ THz}$

Figure 6.27:  $A=20 \Rightarrow \Delta f=6,32 \text{ THz}$ Figure 6.28:  $A=30 \Rightarrow \Delta f=9,64 \text{ THz}$

Figure 6.29:  $A=40 \Rightarrow \Delta f=12,69 \text{ THz}$ Figure 6.30:  $A=50 \Rightarrow \Delta f=15,86 \text{ THz}$

Initially, the pulse has a width (in frequency) of  $\Delta f = 1,22$  THz. So the effect of changing the amplitude  $A$ , while propagating 100 meters is

A	$\Delta f(\text{THz})$
1	0,94
2	0,78
3	1,32
4	1,66
5	1,54
6	1,82
7	2,34
8	2,54
9	2,94
10	3,19
20	6,32
30	9,64
40	12,69
50	15,86

Table 6.4:  $\Delta f$  for different values of *Amplitude*

Graphically

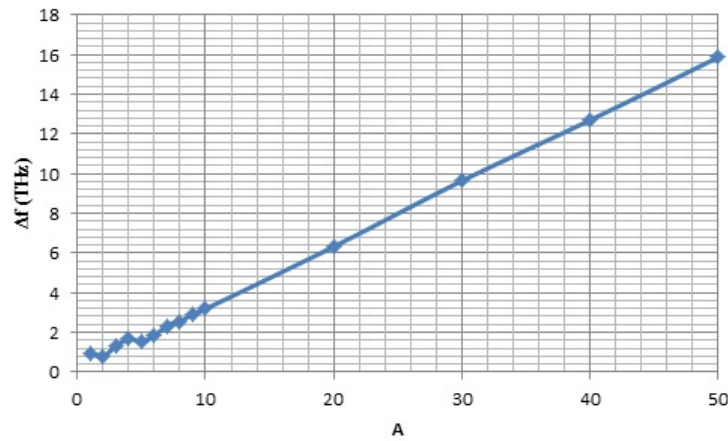


Figure 6.31: Evolution of the pulse width with the amplitude  $A$

Results offer no doubt, pulse gets wider in frequency linearly by increasing the amplitude  $A$ .



Also is possible to measure the signal attenuation and dispersion in time. First, a plot where can be observed the signal in time for several values of amplitude, where is seen how the signal attenuates and widens

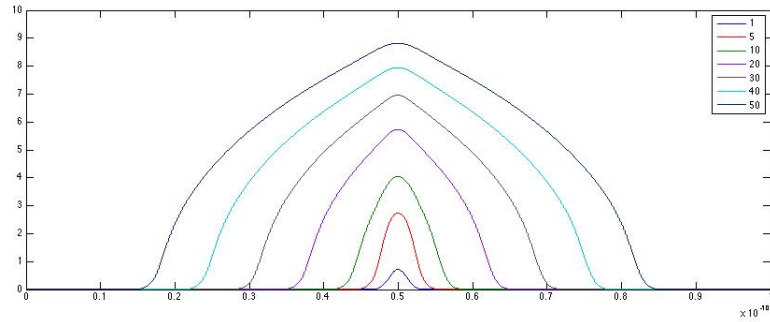


Figure 6.32: Signal in time after propagating for several amplitudes

Numerically Graphically

A	Attenuation(%)
1	27,4
2	29,8
3	36,1
4	39,5
5	44,4
6	46,5
7	50,4
8	52,7
9	56,2
10	58,1
20	69,8
30	77,3
40	81,5
50	82,9

Table 6.5: Attenuation for different values of *Amplitude*

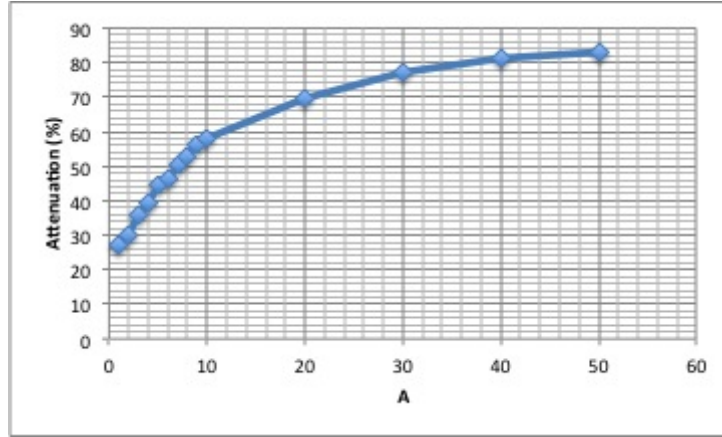
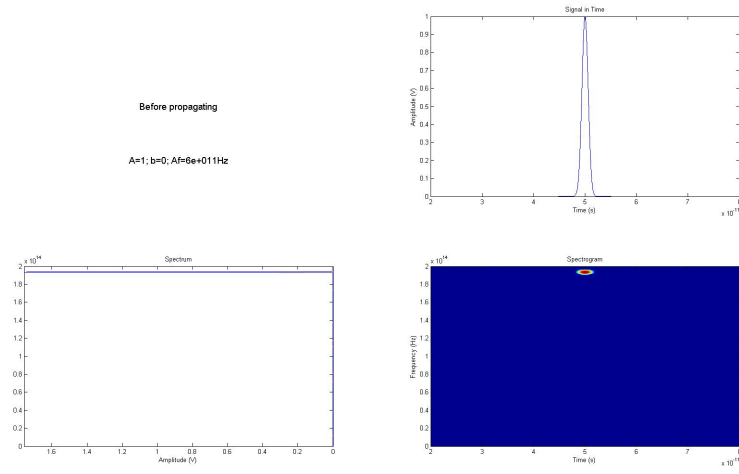
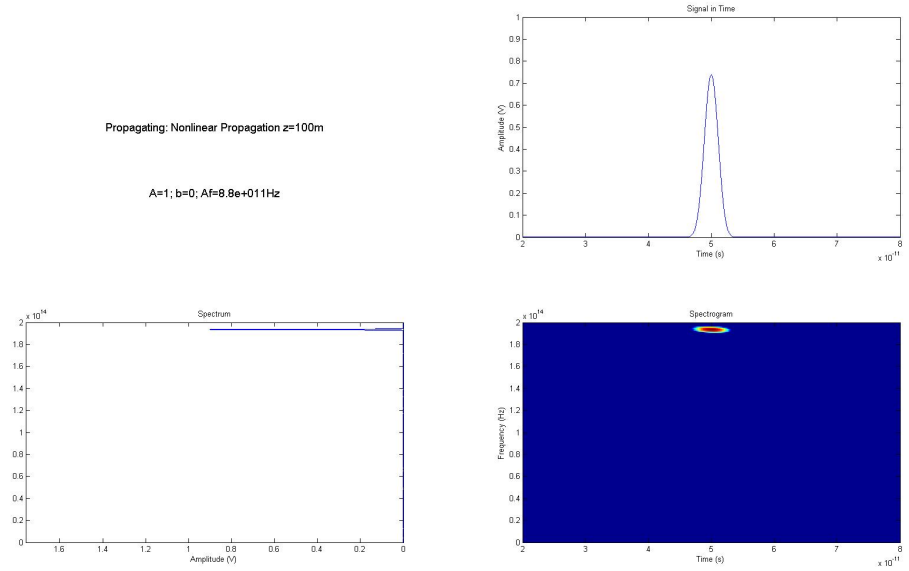


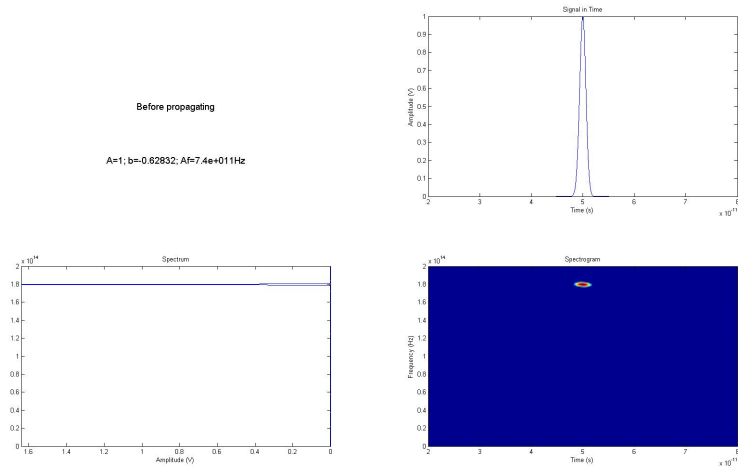
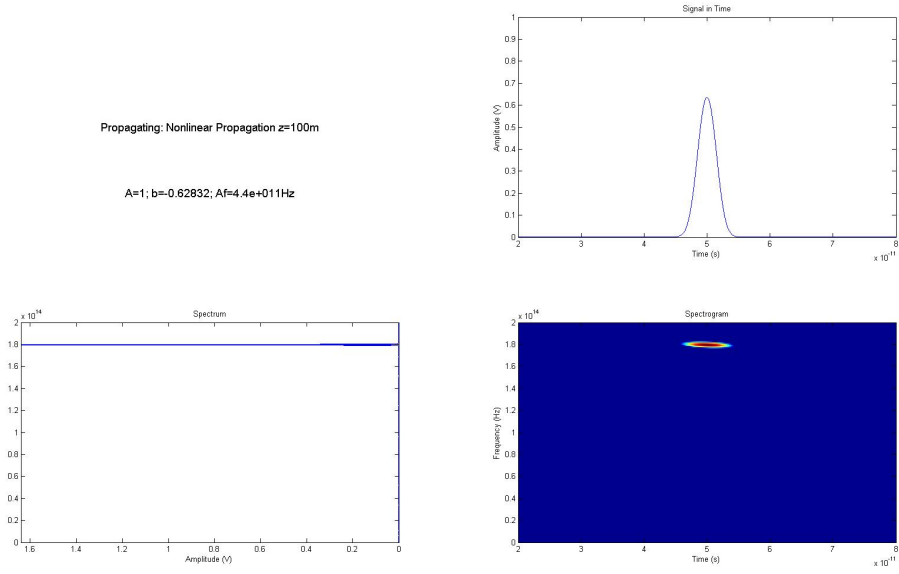
Figure 6.33: Evolution of the pulse attenuation with the amplitude  $A$

Attenuation increases exponentially by increasing input pulse amplitude. Therefore, it is seen as increasing the pulse amplitude has two significant impact on nonlinear propagation. More amplitude, means more chirp and more attenuation in the received signal.

### 6.2.2 Propagating 100 meters changing the phase value

For this experiment,  $z$  is fixed at 100 meters,  $A$  is 1 and the pulse FWHM is 2ps. Let see how the pulse evolves for different values of the  $b$ , the variable that governs the phase. Changing it from 0 to  $-2\pi$  in steps of  $-2\pi/10$ . Before propagating at top and right below, propagating spectrogram

Figure 6.34:  $b = 0 \Rightarrow \Delta f = 0,88 \text{ THz}$ Figure 6.35:  $b = 0 \Rightarrow \Delta f = 0,6 \text{ THz}$

Figure 6.36:  $b = -2\pi \frac{1}{10} \Rightarrow \Delta f = 0.74 \text{ THz}$ Figure 6.37:  $b = -2\pi \frac{1}{10} \Rightarrow \Delta f = 0.44 \text{ THz}$

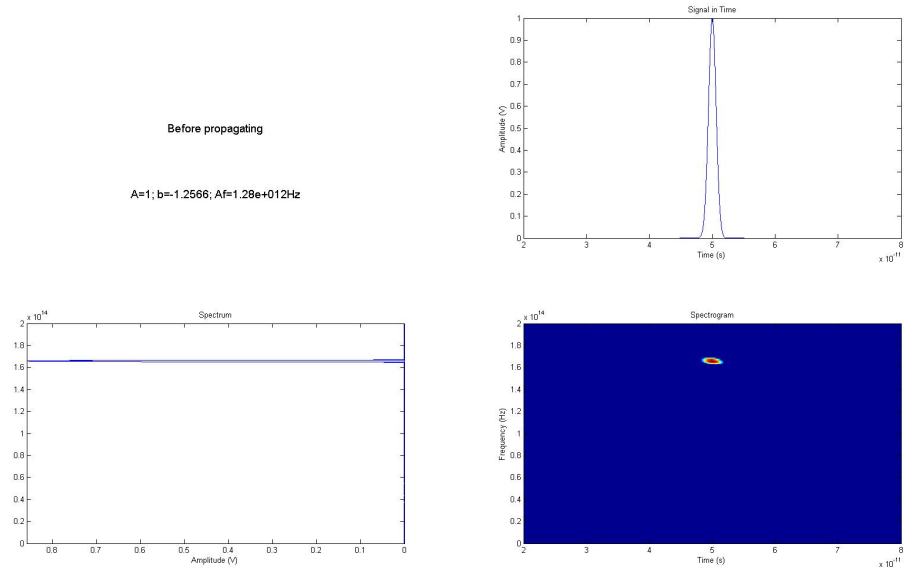


Figure 6.38:  $b = -2\pi \frac{2}{10} \Rightarrow \Delta f = 1,28 \text{ THz}$

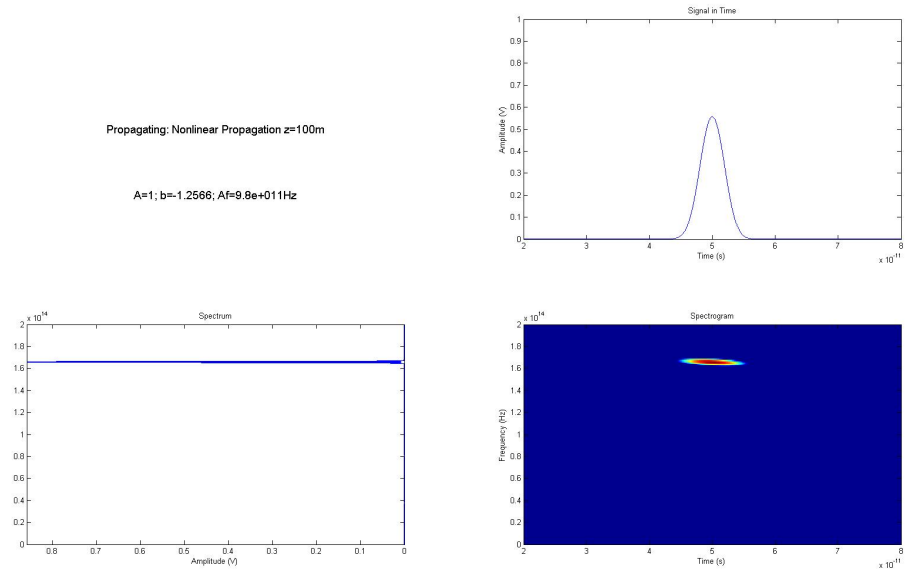
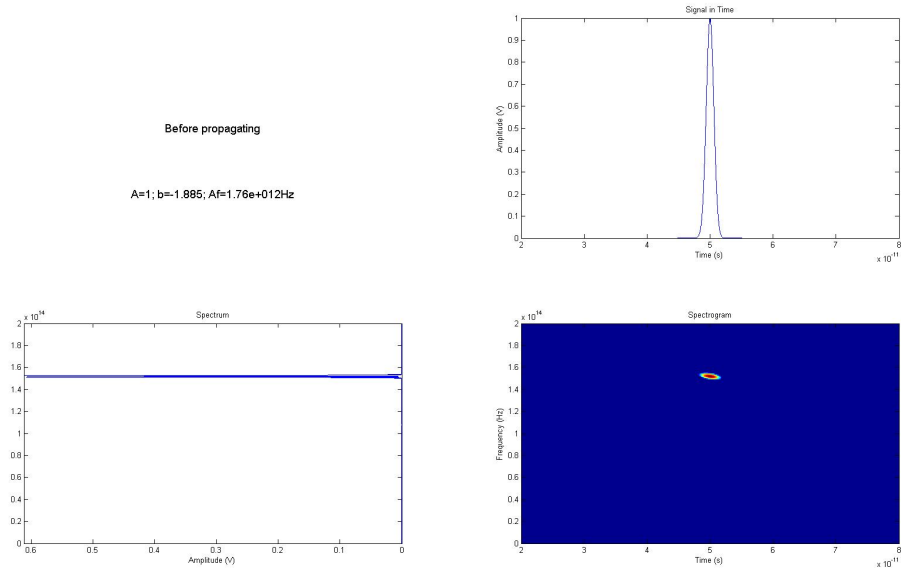
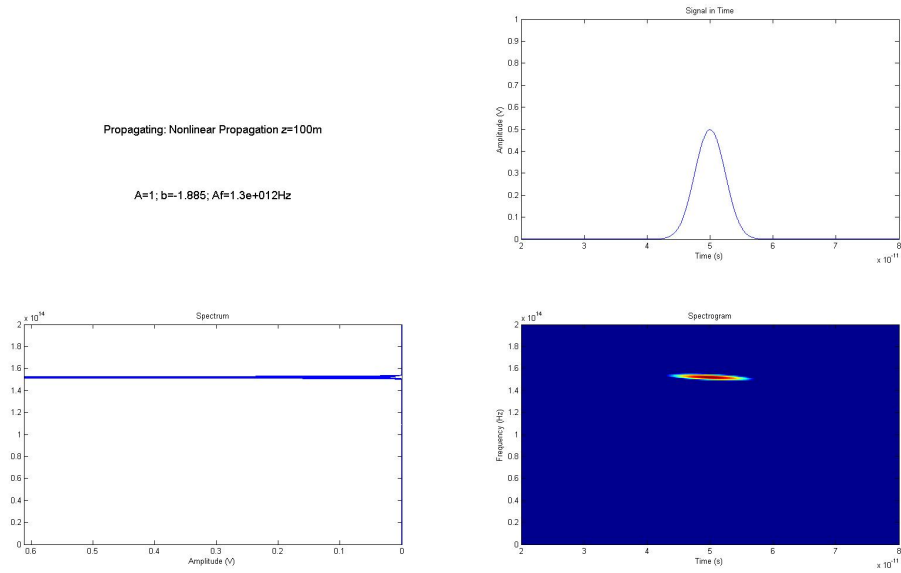


Figure 6.39:  $b = -2\pi \frac{2}{10} \Rightarrow \Delta f = 0,98 \text{ THz}$

Figure 6.40:  $b = -2\pi \frac{3}{10} \Rightarrow \Delta f = 1.76 \text{ THz}$ Figure 6.41:  $b = -2\pi \frac{3}{10} \Rightarrow \Delta f = 1.3 \text{ THz}$

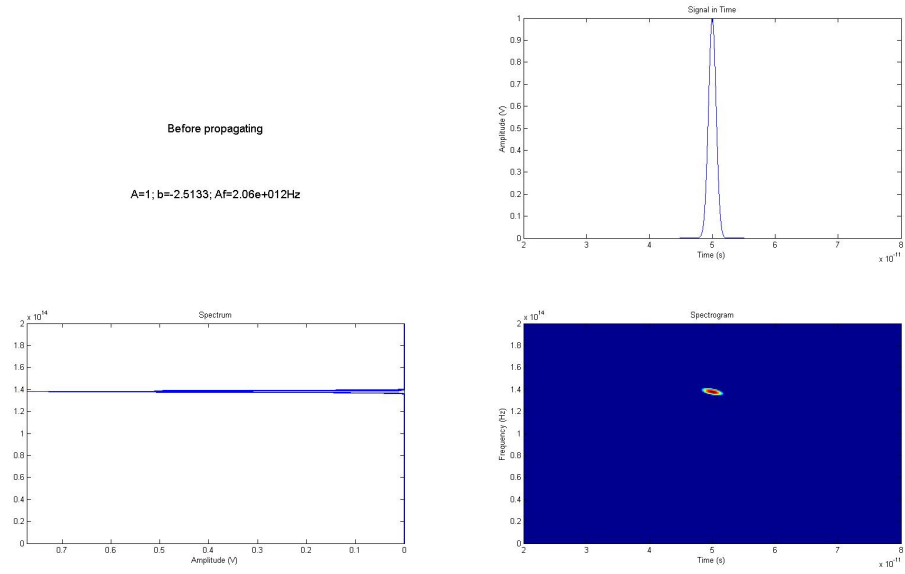


Figure 6.42:  $b = -2\pi \frac{4}{10} \Rightarrow \Delta f = 2,06 \text{ THz}$

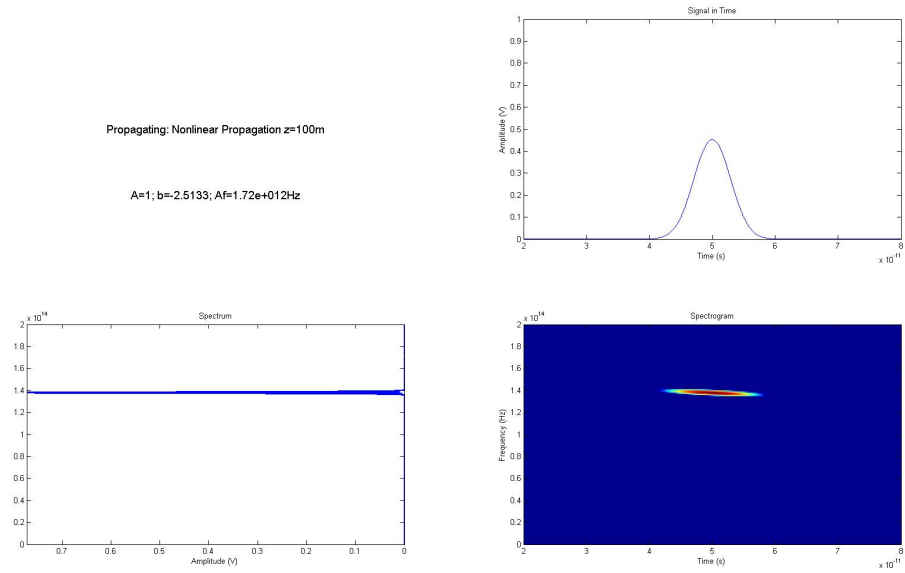
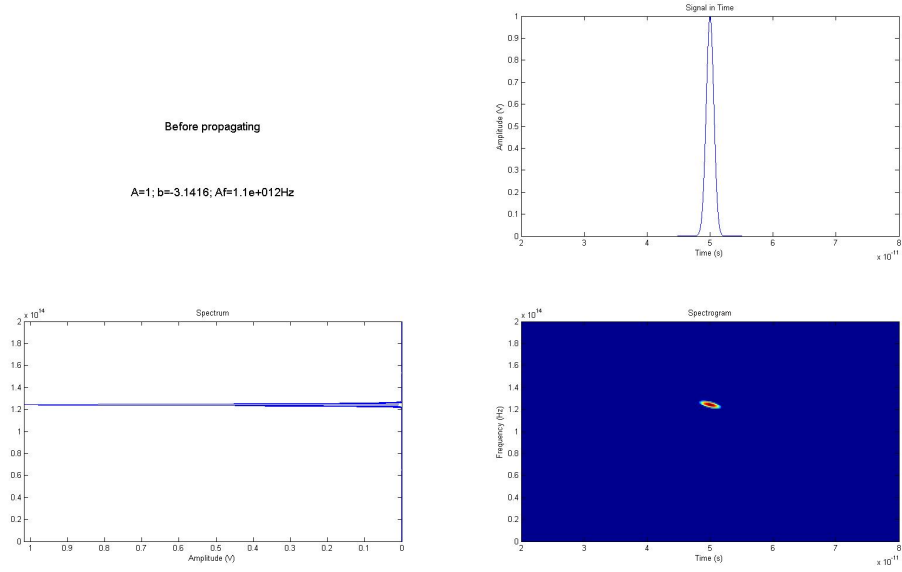
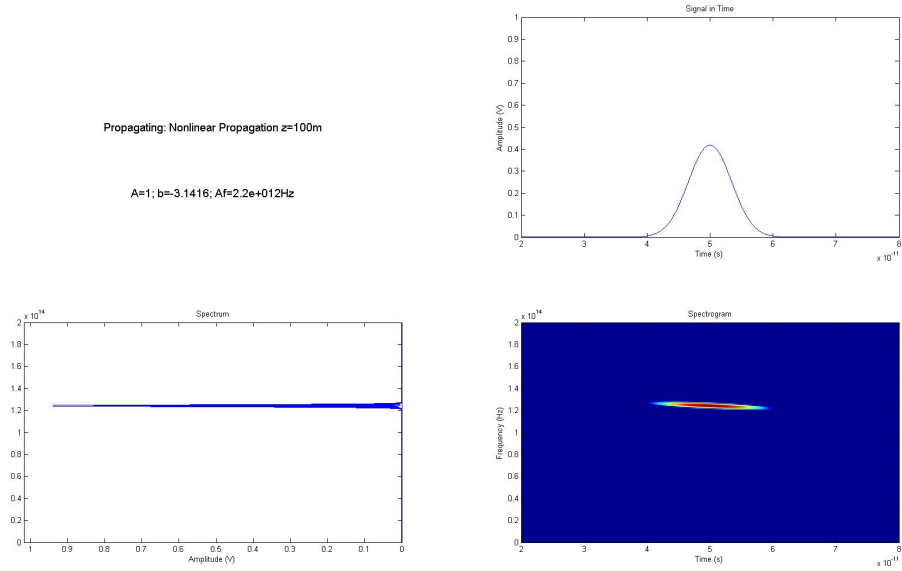


Figure 6.43:  $b = -2\pi \frac{4}{10} \Rightarrow \Delta f = 1,72 \text{ THz}$

Figure 6.44:  $b = -2\pi \frac{5}{10} \Rightarrow \Delta f = 2,51 \text{ THz}$ Figure 6.45:  $b = -2\pi \frac{5}{10} \Rightarrow \Delta f = 2,2 \text{ THz}$



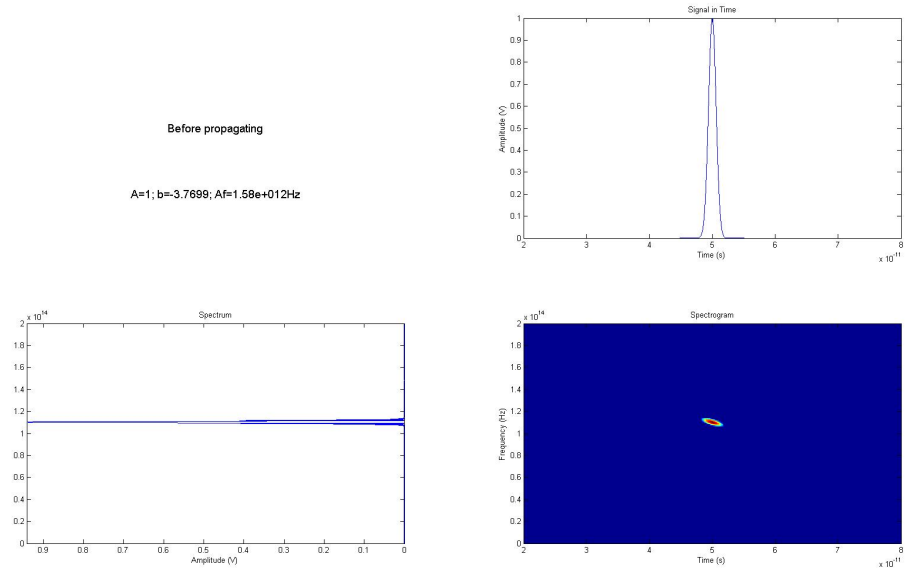


Figure 6.46:  $b = -2\pi \frac{6}{10} \Rightarrow \Delta f = 2,84 \text{ THz}$

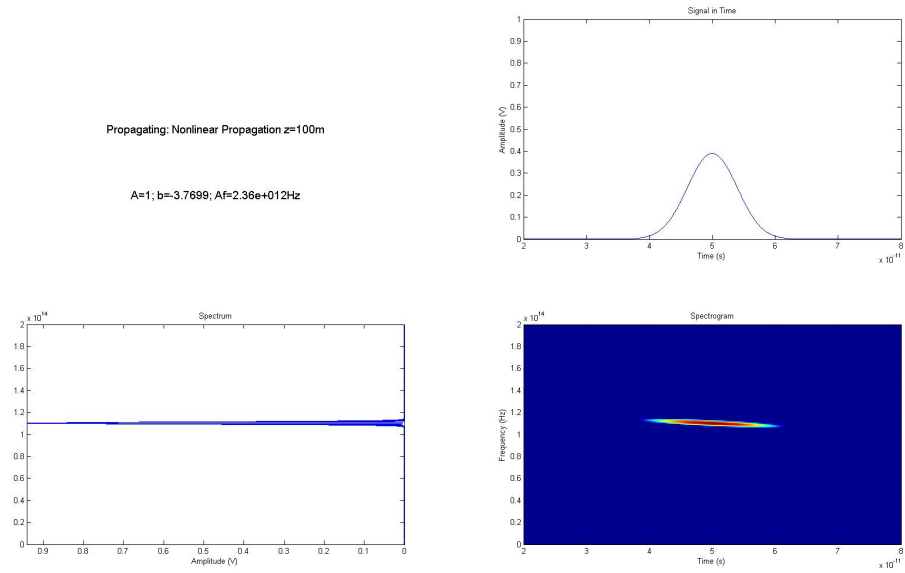
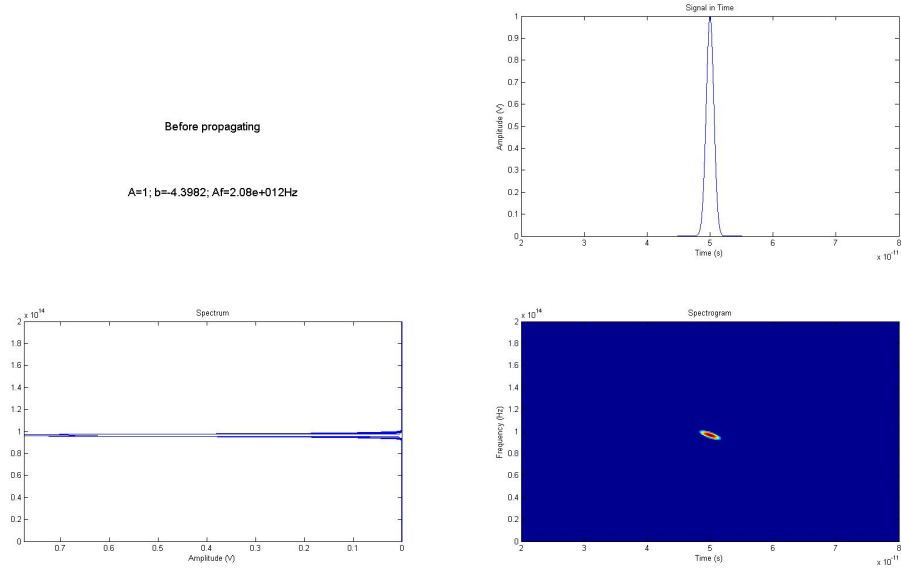
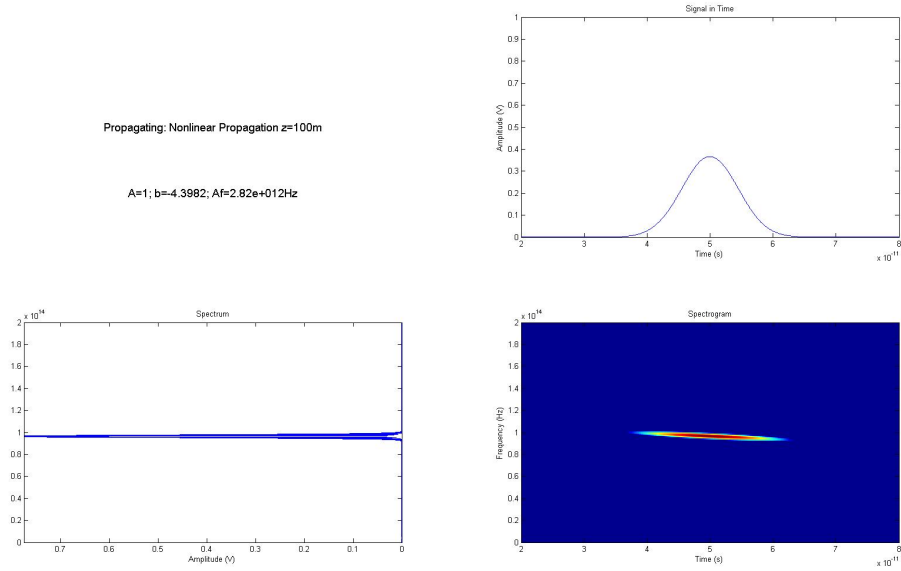


Figure 6.47:  $b = -2\pi \frac{6}{10} \Rightarrow \Delta f = 2,36 \text{ THz}$

Figure 6.48:  $b = -2\pi \frac{7}{10} \Rightarrow \Delta f = 3,27 \text{ THz}$ Figure 6.49:  $b = -2\pi \frac{7}{10} \Rightarrow \Delta f = 2,82 \text{ THz}$

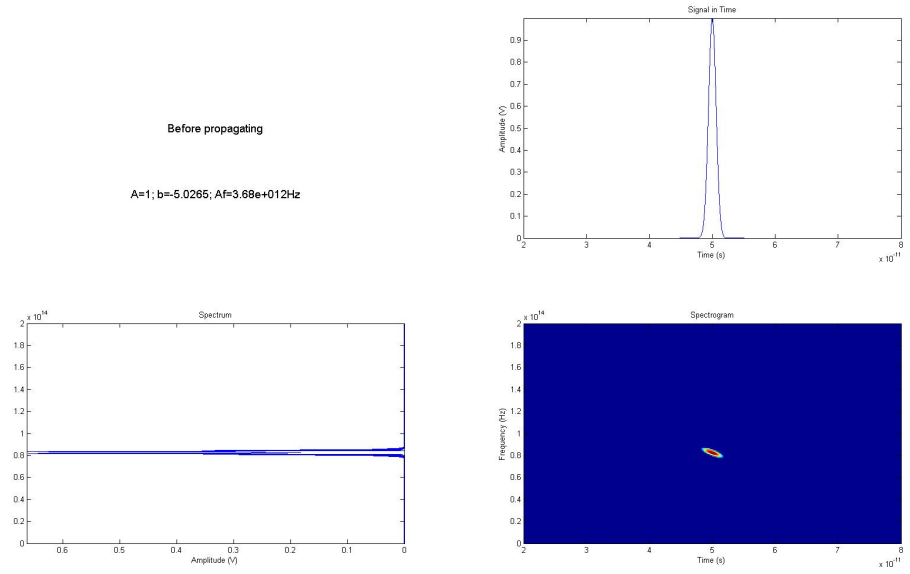


Figure 6.50:  $b = -2\pi \frac{8}{10} \Rightarrow \Delta f = 3,68 \text{ THz}$

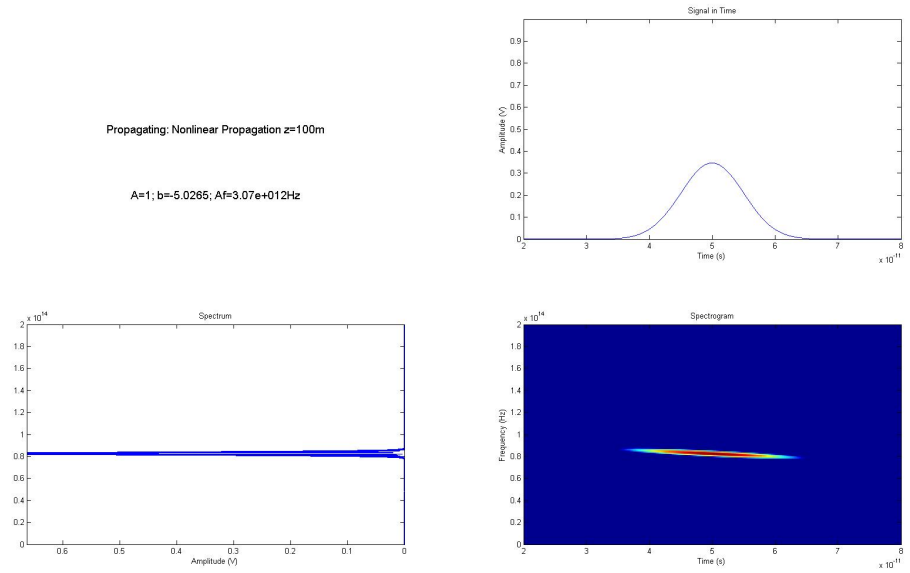
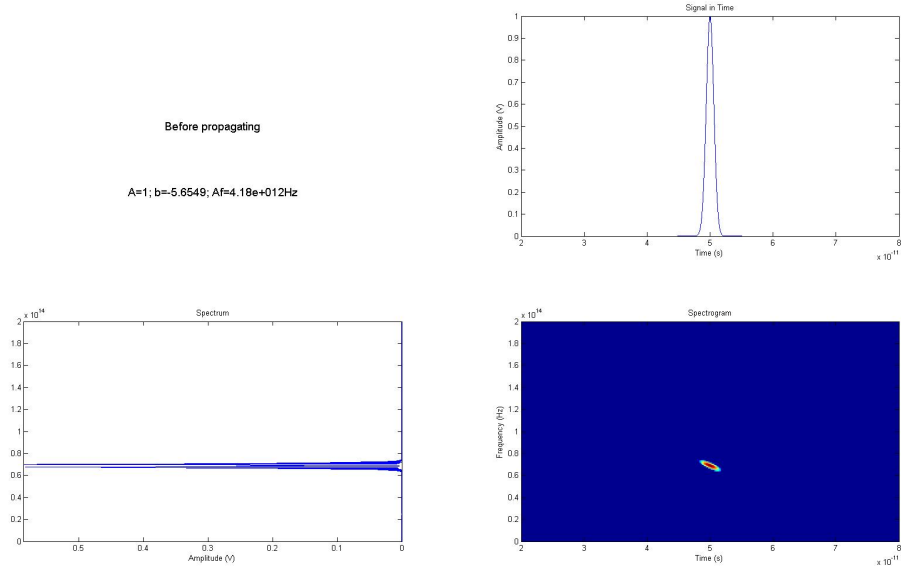
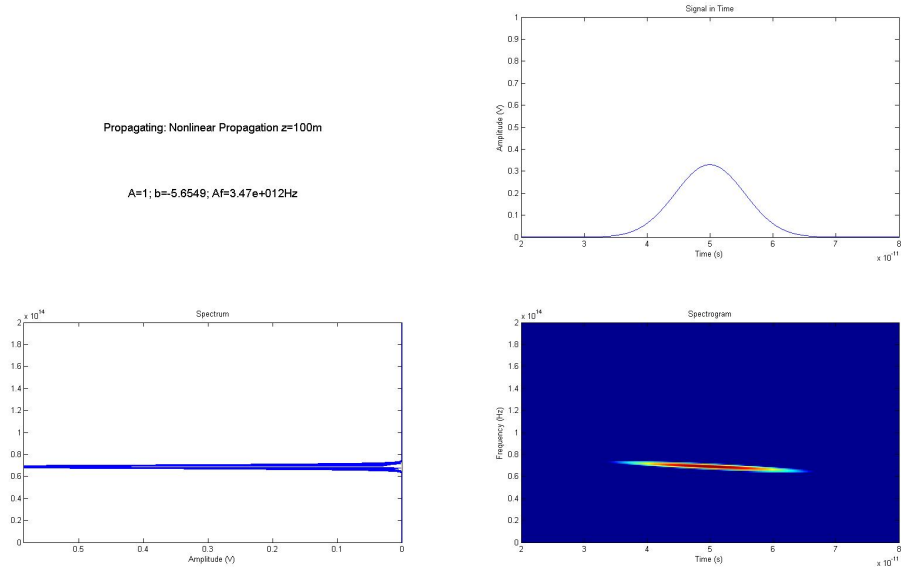


Figure 6.51:  $b = -2\pi \frac{8}{10} \Rightarrow \Delta f = 3,07 \text{ THz}$

Figure 6.52:  $b = -2\pi \frac{9}{10} \Rightarrow \Delta f = 4.18 \text{ THz}$ Figure 6.53:  $b = -2\pi \frac{9}{10} \Rightarrow \Delta f = 3.47 \text{ THz}$

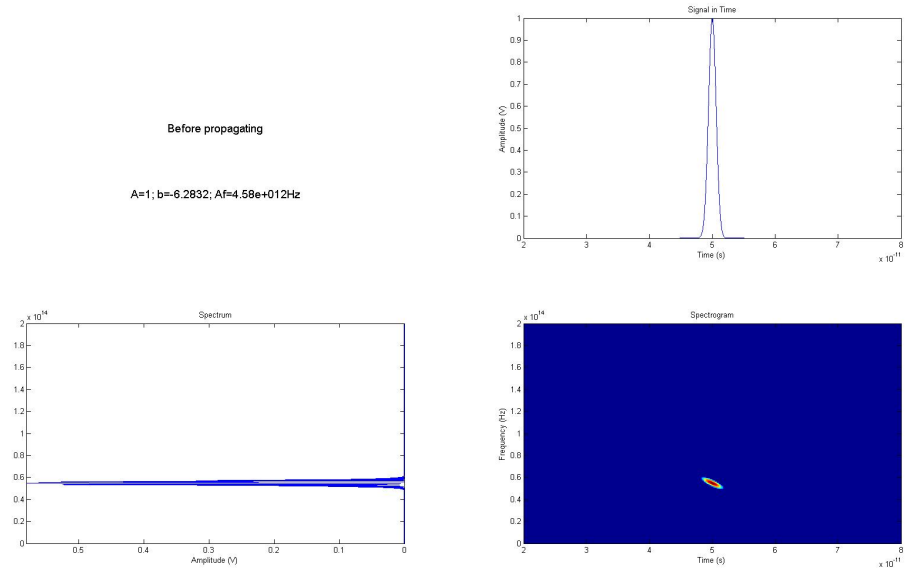


Figure 6.54:  $b = -2\pi \frac{10}{10} \Rightarrow \Delta f = 4,58 \text{ THz}$

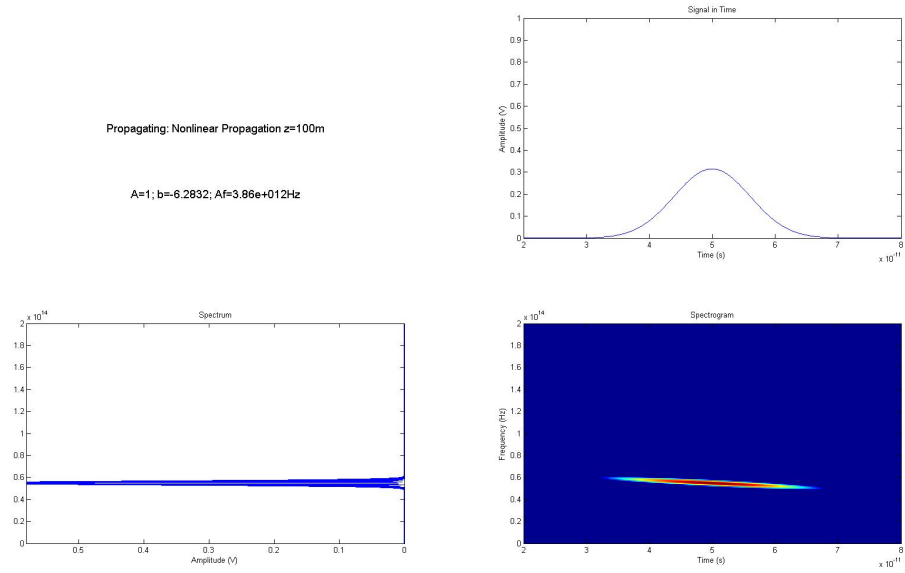


Figure 6.55:  $b = -2\pi \frac{10}{10} \Rightarrow \Delta f = 3,86 \text{ THz}$

Summarizing

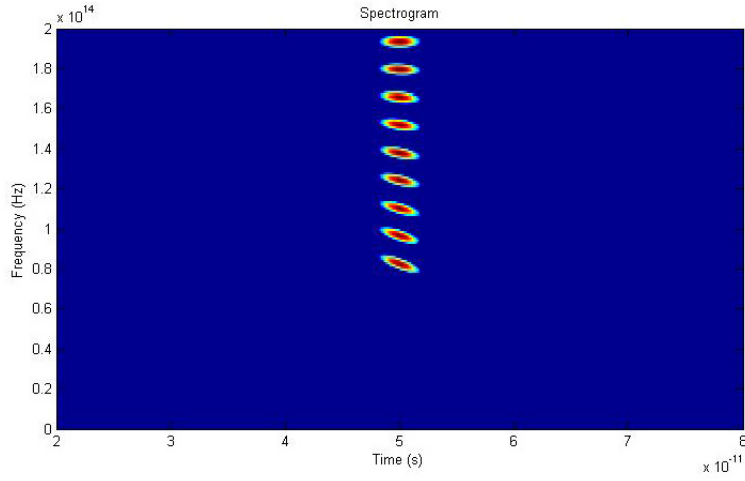


Figure 6.56: before propagating from  $b = 0$  (top) to  $b = -2\pi\frac{10}{10}$  (bottom)

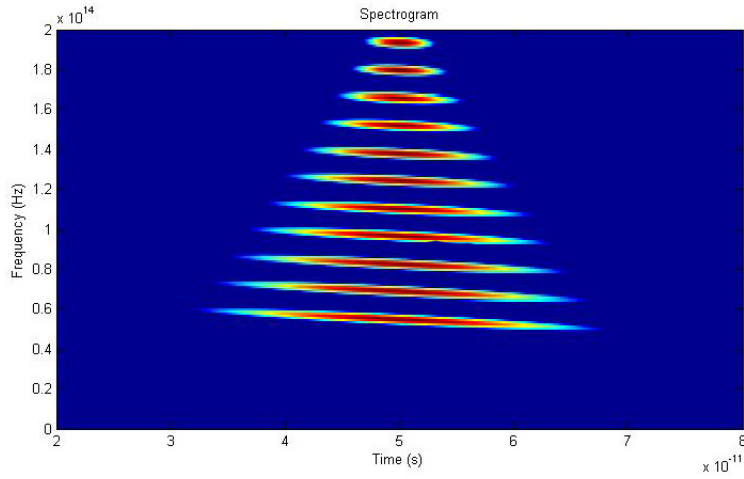


Figure 6.57: after propagating from  $b = 0$  (top) to  $b = -2\pi$  (bottom)

At a glance, can be seen as each measure is experienced a shift in frequency and temporal broadening due to the dispersion.

Effects of varying the phase  $b$

$b$	$\Delta f$ (THz) Before Propagating	$\Delta f$ (THz) After Propagating
0	0,88	0,6
$-2\pi\frac{1}{10}$	0,74	0,44
$-2\pi\frac{2}{10}$	1,28	0,98
$-2\pi\frac{3}{10}$	1,76	1,3
$-2\pi\frac{4}{10}$	2,06	1,72
$-2\pi\frac{5}{10}$	2,51	2,2
$-2\pi\frac{6}{10}$	2,84	2,36
$-2\pi\frac{7}{10}$	3,27	2,82
$-2\pi\frac{8}{10}$	3,68	3,07
$-2\pi\frac{9}{10}$	4,18	3,47
$-2\pi$	4,58	3,86

Table 6.6:  $\Delta f$  for different values of  $b$

Graphically

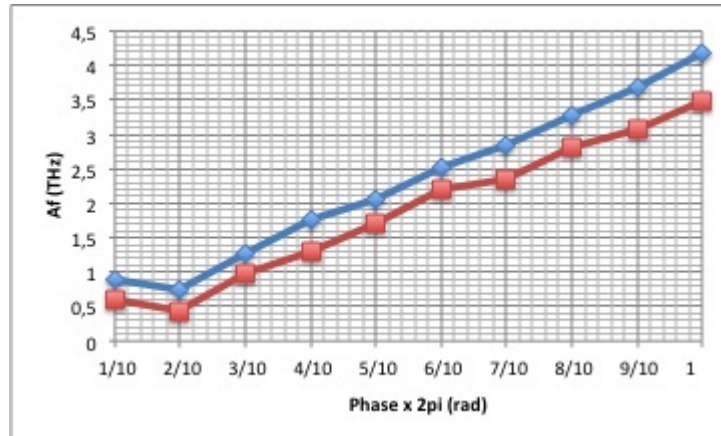


Figure 6.58: Blue  $\Rightarrow$  Before Propagating ; Red  $\Rightarrow$  After Propagating

The pulse width (in frequency) of the propagated signal gets bigger as the phase increases, exactly as happens with the signal before propagating. So it can be said that the phase value affects the signal as an offset, for the whole range from 0 to  $2\pi$ .

### 6.2.3 Propagating 100 meters changing the phase function

This new experiment consists in changing the second term of equation (6.1), the chirp, for other kinds of functions, so the phase of the pulse will be different. Again,  $z$  is fixed at 100 meters,  $A$  is 1 and the pulse FWHM is 2ps.

In previous experiments, the phase of the chirp function varied between 0 and  $\frac{bt_{max}^2}{\sigma^2} \approx 2 \cdot 10^4$ . Therefore the phase of the new function should take values within the same range. Now the signal to propagate is

$$E = Ae^{-\frac{(t-t_0)^2}{\sigma^2}} e^{jp(t)} e^{j\omega_0 t} \quad (6.2)$$

where  $p(t)$  is the phase function, which can vary between several typical functions such as sawtooth, sine, square pulses, etc.

#### Sawtooth function

Taking  $p(t)$  as a sawtooth function of the form:

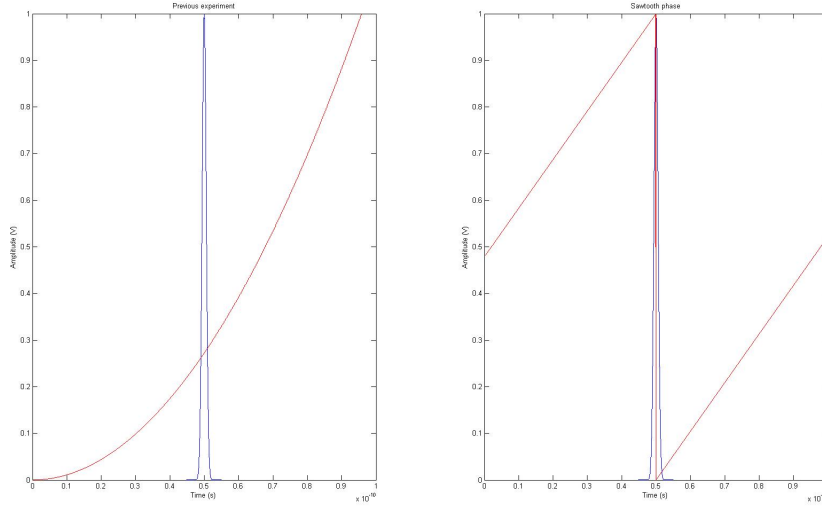
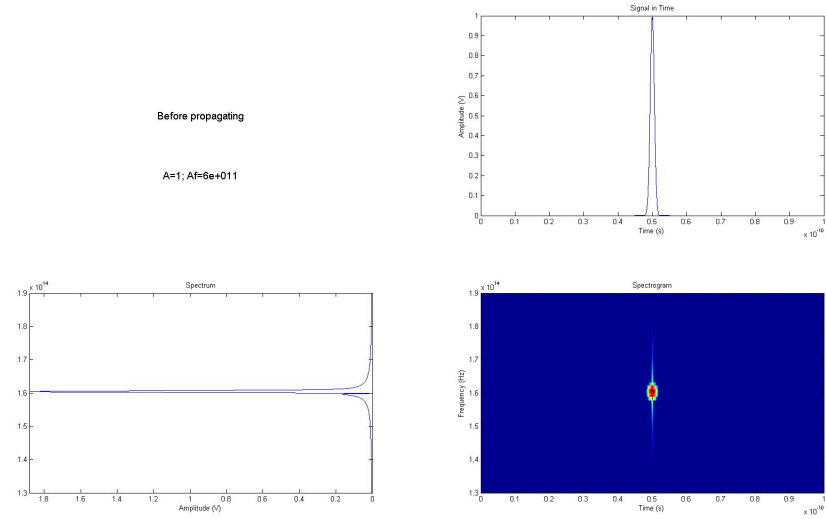


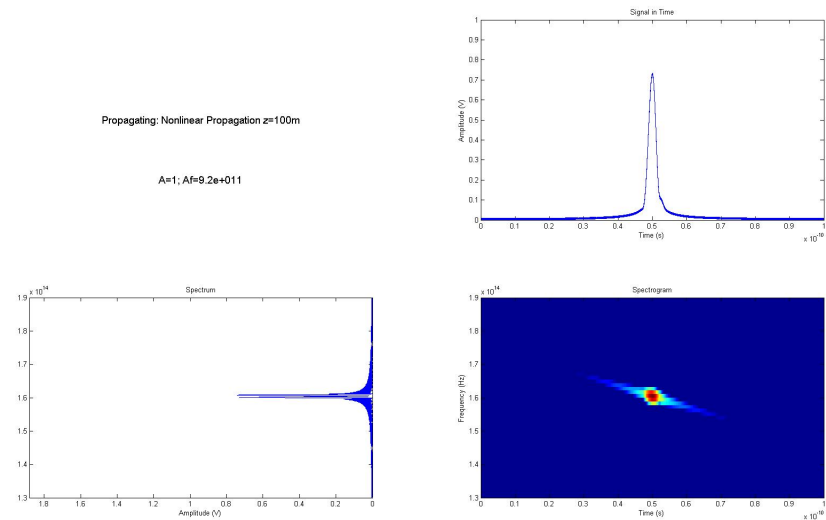
Figure 6.59: Signal in time vs phase



## Before propagating

Figure 6.60:  $A=1 \Rightarrow \Delta f=0,6$  THz; Before propagating

## After Propagating

Figure 6.61:  $A=1 \Rightarrow \Delta f=0,92$  THz

Now, increasing the amplitude  $A$  up to 20. As discussed in Chapter 5, must have a commitment to time-frequency resolution, so that, higher amplitudes need a wider window

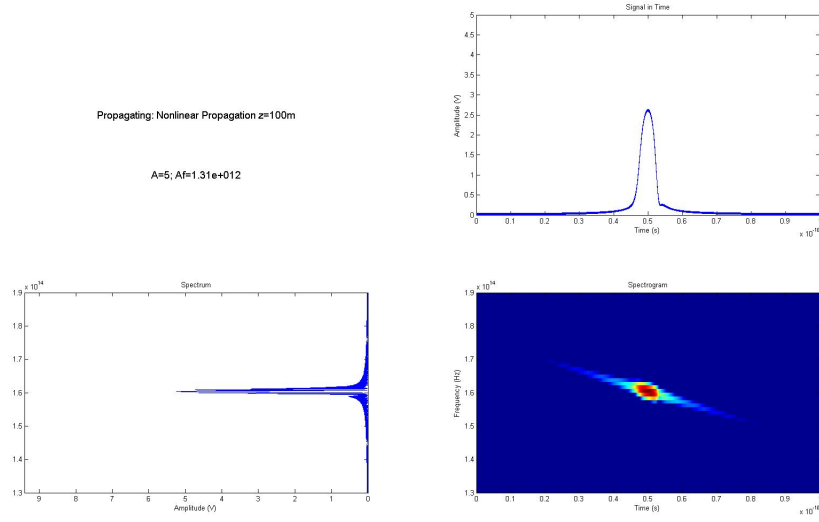


Figure 6.62:  $A=5 \Rightarrow \Delta f=1,31$  THz

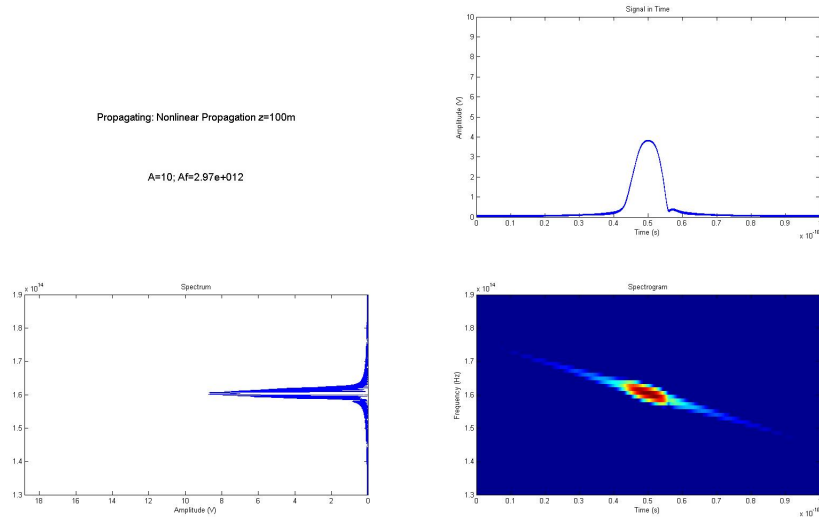
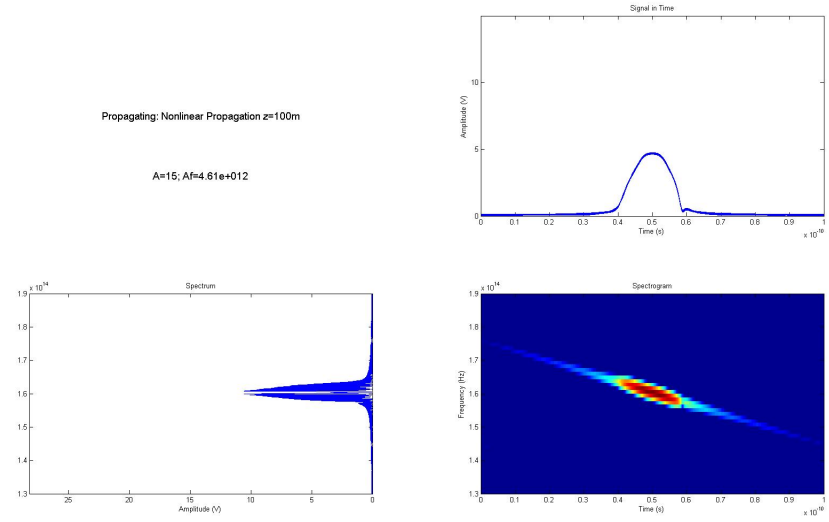
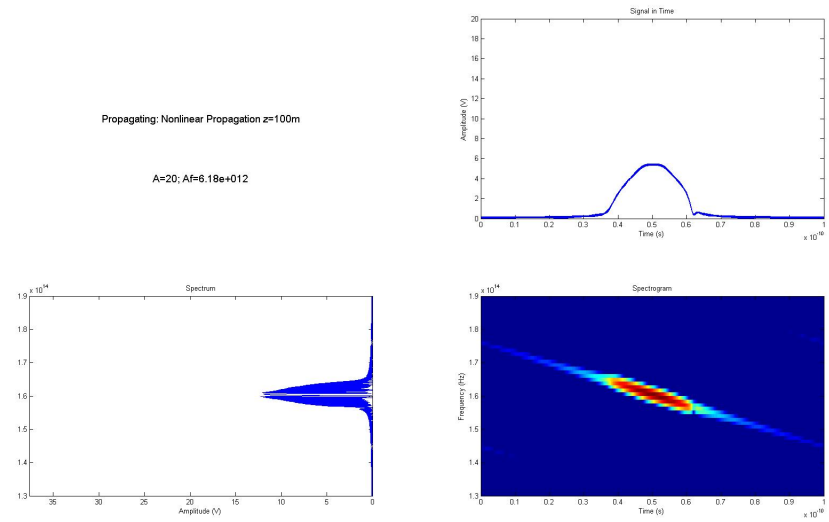


Figure 6.63:  $A=10 \Rightarrow \Delta f=2,97$  THz

Figure 6.64:  $A=15 \Rightarrow \Delta f=4,61 \text{ THz}$ Figure 6.65:  $A=20 \Rightarrow \Delta f=6,18 \text{ THz}$

### Sine function

Same conditions for a sine function of the form:

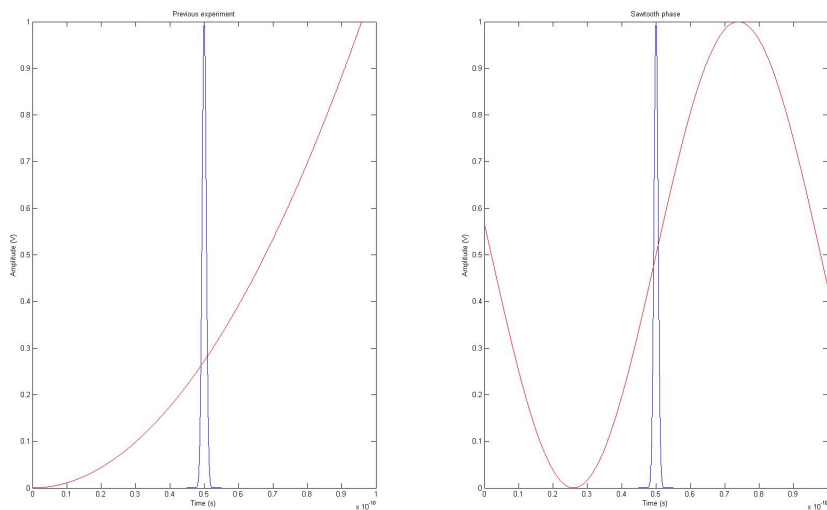


Figure 6.66: Signal in time vs phase

### Before propagating

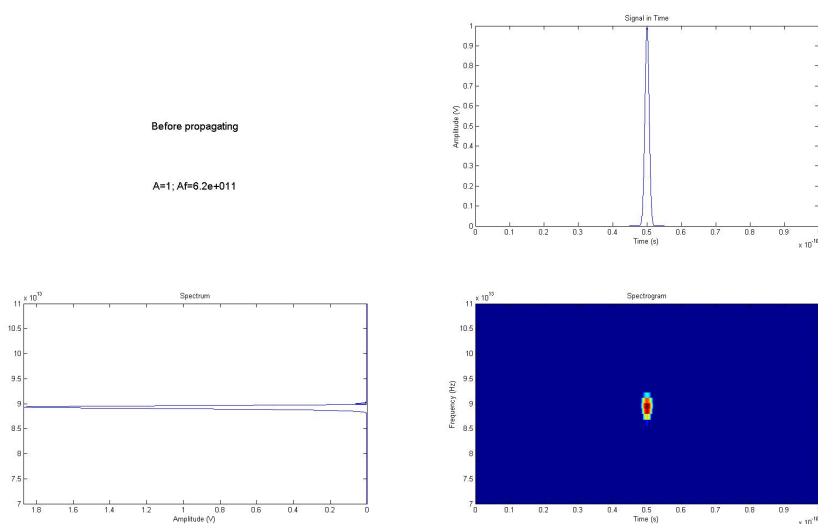


Figure 6.67:  $A=1 \Rightarrow \Delta f=0,62$  THz; Before propagating

## Propagating

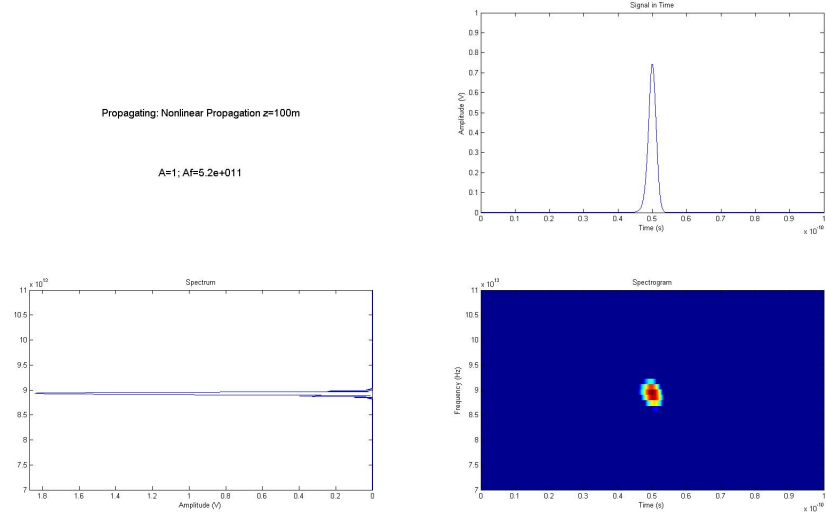


Figure 6.68:  $A=1 \Rightarrow \Delta f=0,52$  THz

Now, increasing the amplitude  $A$  up to 50.

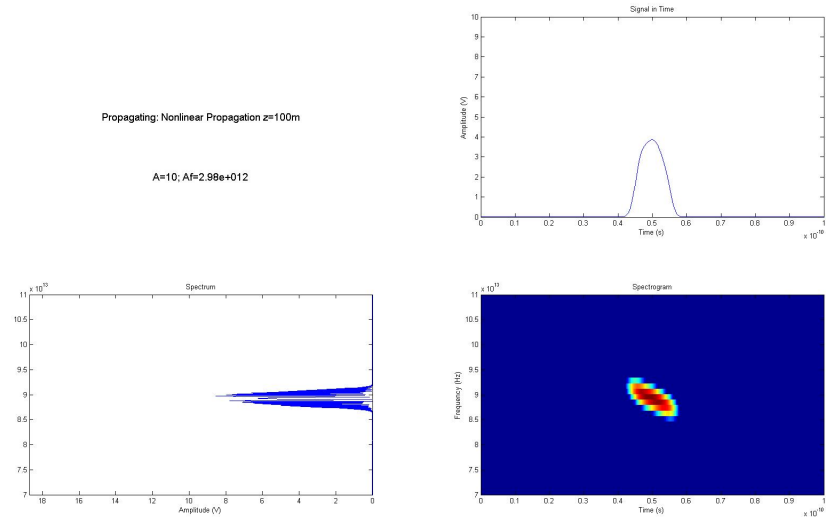
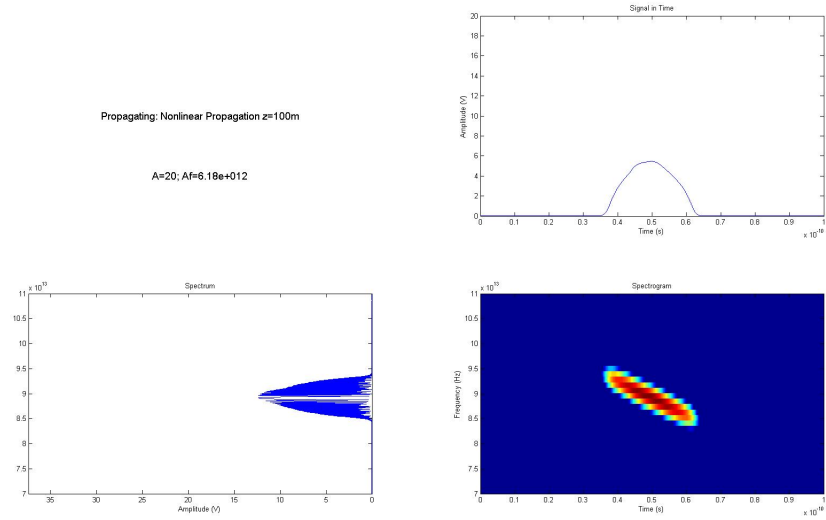
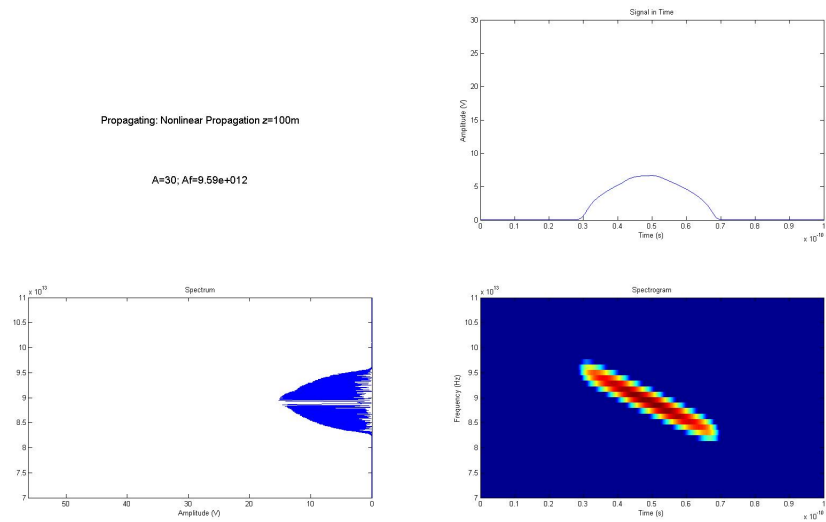
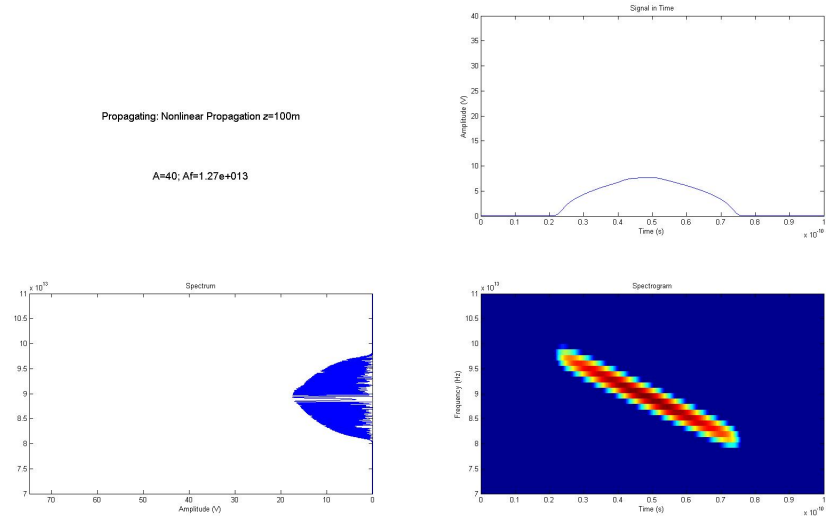
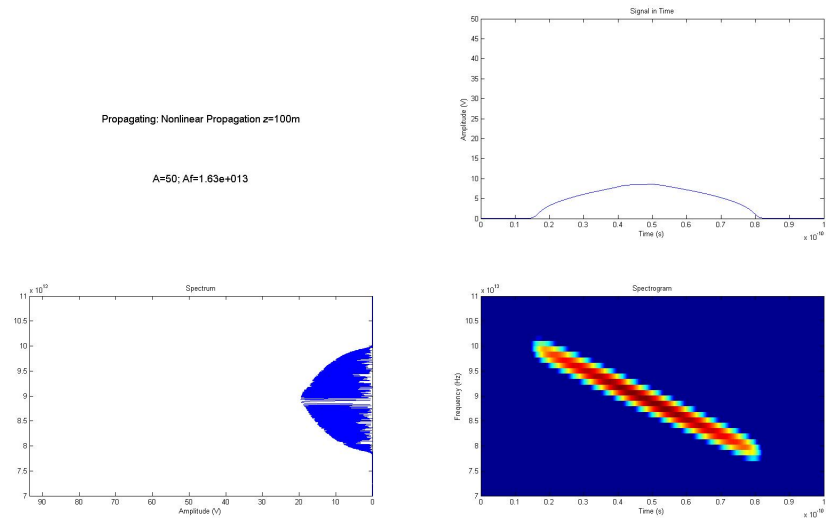


Figure 6.69:  $A=10 \Rightarrow \Delta f=2,98$  THz

Figure 6.70:  $A=20 \Rightarrow \Delta f=6,18 \text{ THz}$ Figure 6.71:  $A=30 \Rightarrow \Delta f=9,59 \text{ THz}$

Figure 6.72:  $A=40 \Rightarrow \Delta f=12,7 \text{ THz}$ Figure 6.73:  $A=50 \Rightarrow \Delta f=16,3 \text{ THz}$

### Square function

Same conditions for a sine function of the form:

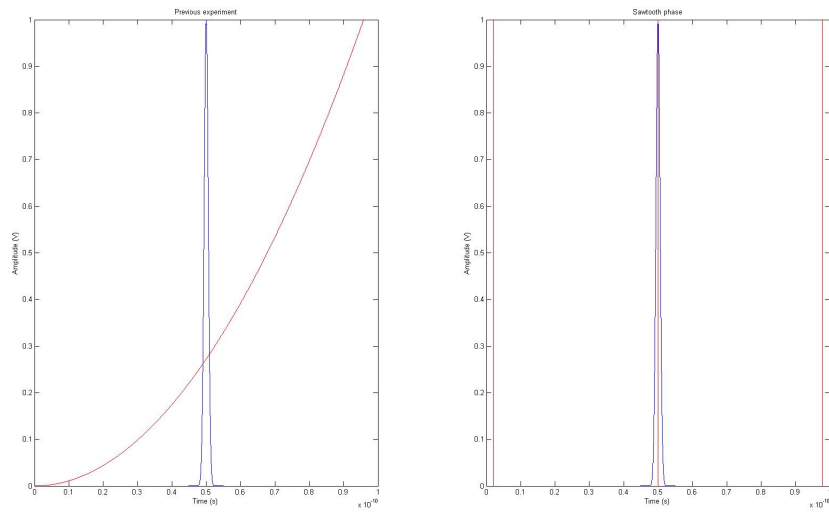


Figure 6.74: Signal in time vs phase

### Before propagating

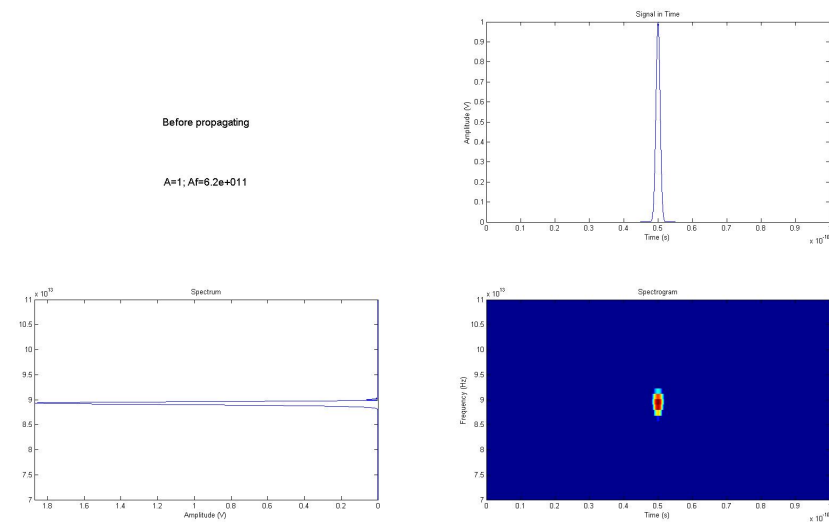
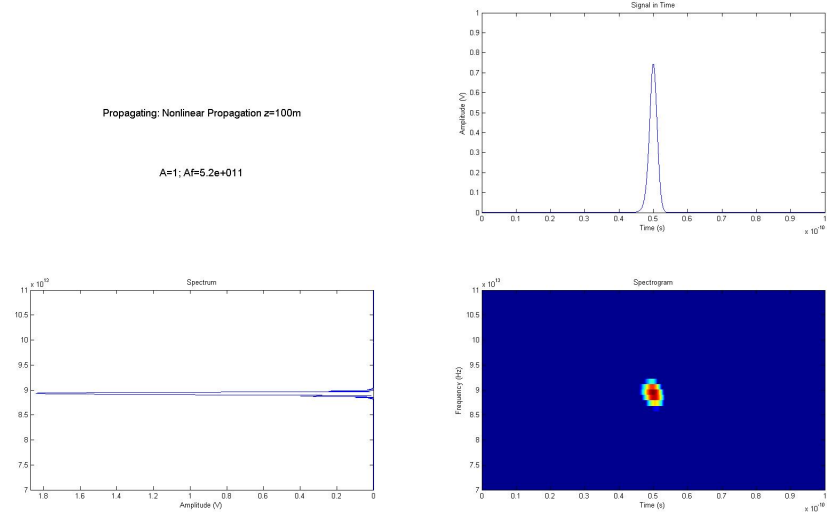


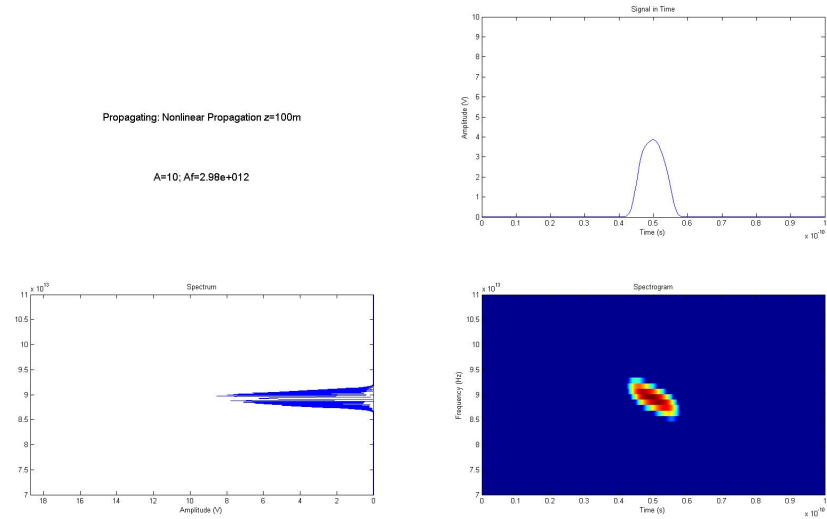
Figure 6.75:  $A=1 \Rightarrow \Delta f=0,62$  THz; Before propagating

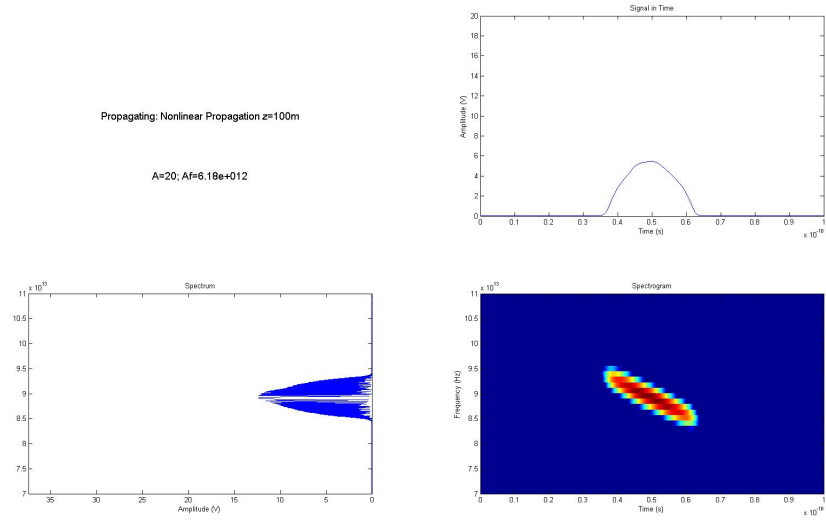
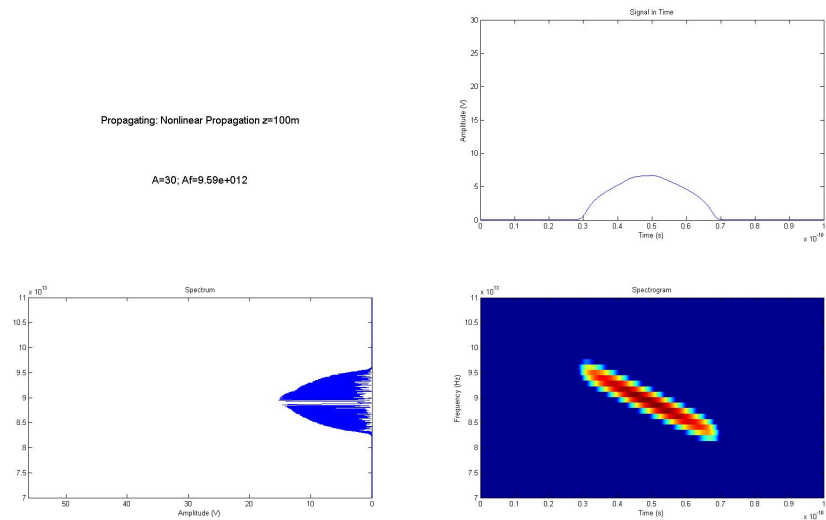


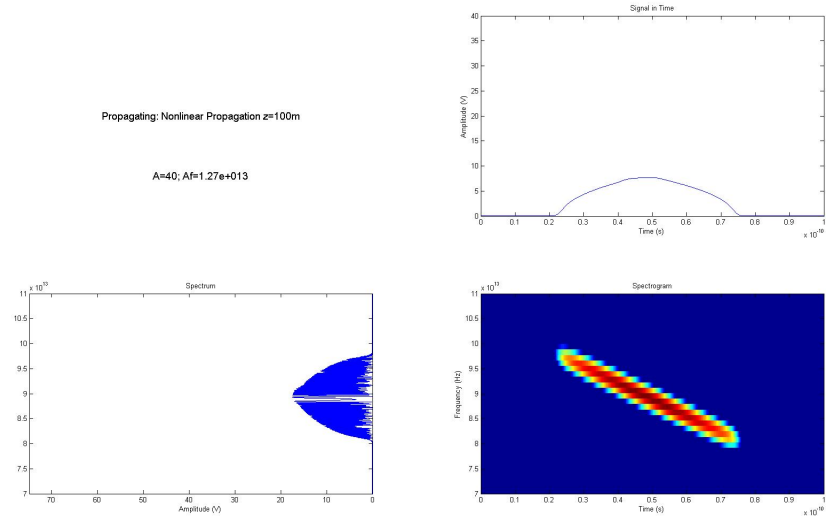
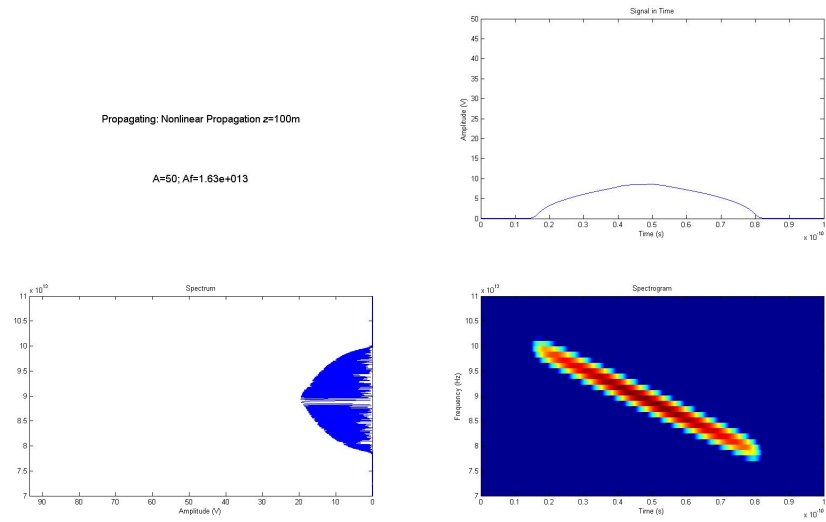
## After Propagating

Figure 6.76:  $A=1 \Rightarrow \Delta f=0,52$  THz

Now, increasing the amplitude  $A$  up to 50.

Figure 6.77:  $A=10 \Rightarrow \Delta f=2,98$  THz

Figure 6.78:  $A=20 \Rightarrow \Delta f=6,18 \text{ THz}$ Figure 6.79:  $A=30 \Rightarrow \Delta f=9,59 \text{ THz}$

Figure 6.80:  $A=40 \Rightarrow \Delta f=12,7$  THzFigure 6.81:  $A=50 \Rightarrow \Delta f=16,3$  THz

Viewing the above results, it looks like the red part of the spectrogram (where more intense is the signal) practically does not change in any of the cases, so is needed a visual comparison to appreciate the difference between the different phases functions and their effects.

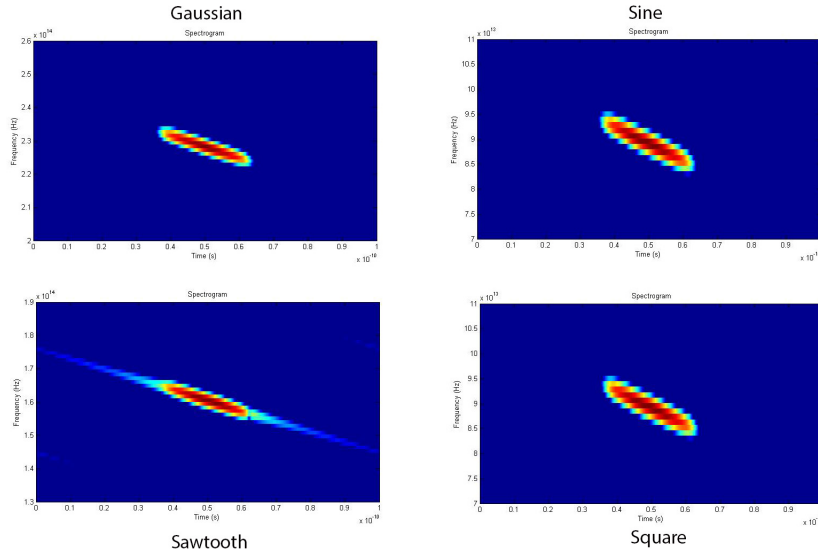


Figure 6.82: Gaussian, Sine, Sawtooth and Square phase functions ( $z=100\text{m}$ ;  $A=20\text{V}$ )

Is seen as sine and square are exactly the same, while the gaussian function is somewhat narrower and sawtooth function covers almost the entire window with replicas of lower amplitude.



# Chapter 7

## Conclusion

On the results were used different wavelengths for the linear (800nm) and nonlinear (1550nm) case so can not make a direct comparison of them. Nevertheless, the behavior in each case is known, so is possible to do a qualitative comparison and check how nonlinearities affect the propagation in optical fibers.

As a first conclusion, one can say that the best fiber of the commercial fibers tested is SF10, with very similar performance to the Lakl21 and better than the most famous, fused silica. While the fiber with the worst performance is BK7.

In the linear case, has been demonstrated that the amplitude does not affect the pulse width (both in time and frequency), it remains constant for any value of amplitude. On the other hand, in the nonlinear case, increasing the amplitude causes an increase in the temporal and spectral width.

However, the phase does not affect the same way to the propagation, as both the function and the phase value has been shown to produce no frequency dispersion (chirp). Although, in the nonlinear case, there is time dispersion due to the terms of third (GVD) and fourth order (TOD) wavelength polynomial (see equation 3.30).

Finally, can be stated that for a linear medium, in which the nonlinearities not interfere, a signal could propagate farther without suffering much dispersion. However in the real world, this situation does not occur and the nonlinearities affect the pulse, in particular the increase of the amplitude, that introduces dispersion and will require the use of other devices to compensate it or use smaller amplitudes and therefore less distance to propagate.



# Chapter 8

## References

- [1] Anonymous, Transverse electromagnetic mode, <http://www.microwaves-101.com/encyclopedia/TEM.cfm>, September 2010
- [2] Govind P. Agrawal, Nonlinear Fiber Optics, USA, July 2006
- [3] Ursula Keller, Ultrafast Laser Physics, Switzerland, 1997
- [4] Newport, The Effect of Dispersion on Ultrashort Pulses
- [5] H. A. Haus and E. P. Ippen, Group velocity of solitons, 2001
- [6] C. J. Hope and d. J. Furlong, Time-Frequency distributions for time morphing: The Wigner distribution versus the stft, Brazil, August 1997
- [7] Tobias Hansson. Time-domain methods for optical propagation in dispersive media, USA, December 2006.
- [8] Kane Yee. Numerical solution of initial boundary value problems involving Maxwell's equations in isotropic media, 1966.
- [9] Adriana Salvia, Metodos numericos para la resolucion de ecuaciones diferenciales.
- [10] T.A.C.M. Claasen and W.F.G Mecklenbrauker, 'The Wigner Distribution - A Tool for Time-Frequency Signal Analysis, part 1: Continuous-Time Signals', Phillips Journal of Research, 1980.
- [11] J. Ville, 'Thorie et applications de la notion de signal analytique', Ca-



bles et Transmission, 1948.

[12] J. Goswami, A. Chan, Fundamentals of Wavelets, Primera edicin, Wiley, Texas, 1999.

[13] Alfredo Rosado Munoz, Desarrollo de tecnicas de Deteccion de Fibrilacion Ventricular basadas en Algoritmos de tiempo-frecuencia, Las transformadas Tiempo-Frecuencia.

[14] L. Cohen, Generalized Phase-Space Distribution Functions, 1966.



# Chapter 9

## Appendices

### 9.1 Material parameters table

Material	$\lambda$ (nm)	$n$ ( $\lambda$ )	$dn/d\lambda$ ( $\mu\text{m}^{-2}$ )	$d^2n/d\lambda^2$ ( $\mu\text{m}^{-2}$ )	$d^3n/d\lambda^3$ ( $\mu\text{m}^{-3}$ )	GVD (fs <sup>2</sup> /mm)	TOD (fs <sup>3</sup> /mm)
<b>Fused Silica</b>							
	400	1.470	-0.109	0.861	-9.600	97.43	30.2
	450	1.466	-0.076	0.512	-4.984	82.43	27.24
	500	1.462	-0.055	0.323	-2.809	71.4	25.53
	550	1.460	-0.042	0.214	-1.686	62.82	24.62
	600	1.458	-0.033	0.146	-1.064	55.85	24.28
	650	1.457	-0.027	0.103	-0.699	49.98	24.42
	700	1.455	-0.023	0.074	-0.476	44.87	24.99
	750	1.454	-0.020	0.054	-0.333	40.3	25.99
	800	1.453	-0.017	0.040	-0.239	36.11	27.44
	850	1.453	-0.016	0.030	-0.175	32.18	29.36
<b>LakL21</b>							
	400	1.659	-0.179	1.463	-16.950	165.6	57.42
	450	1.652	-0.123	0.855	-8.552	137.7	49.42
	500	1.647	-0.089	0.534	-4.731	118	44.78
	550	1.643	-0.067	0.351	-2.804	103.2	42.05
	600	1.640	-0.052	0.239	-1.753	91.4	40.59
	650	1.637	-0.042	0.168	-1.144	81.68	40.06
	700	1.636	-0.035	0.121	-0.774	73.37	40.3
	750	1.634	-0.030	0.089	-0.540	66.06	41.25
	800	1.632	-0.026	0.066	-0.386	59.46	42.89
	850	1.631	-0.023	0.049	-0.282	53.37	45.25
<b>SF10</b>							
	400	1.778	-0.543	5.946	-97.730	672.9	510.5
	450	1.757	-0.335	2.899	-36.740	467.1	301.6
	500	1.743	-0.225	1.632	-17.080	360.8	213.5
	550	1.734	-0.161	1.006	-9.046	295.9	168.1
	600	1.727	-0.120	0.660	-5.237	251.9	141.5
	650	1.721	-0.093	0.453	-3.235	219.8	124.7
	700	1.717	-0.074	0.322	-2.100	195.2	113.6
	750	1.714	-0.060	0.235	-1.418	175.5	106.1
	800	1.711	-0.050	0.176	-0.988	159.2	101.1
	850	1.709	-0.042	0.134	-0.708	145.5	97.97
<b>BK7</b>							
	400	1.529	-0.130	1.082	-12.300	122.4	40.2
	450	1.524	-0.089	0.638	-6.262	102.9	34.72
	500	1.520	-0.063	0.403	-3.485	89.07	31.31
	550	1.517	-0.047	0.268	-2.074	78.74	29.02
	600	1.515	-0.035	0.185	-1.301	70.69	27.39
	650	1.514	-0.028	0.132	-0.851	64.22	26.19
	700	1.513	-0.022	0.097	-0.576	58.89	25.28
	750	1.512	-0.018	0.073	-0.402	54.42	24.57
	800	1.511	-0.015	0.056	-0.288	50.6	24.01
	850	1.510	-0.012	0.044	-0.210	47.31	23.55

Figure 9.1: Material parameters for Fused Silica, LakL21, SF10 and BK7

## 9.2 Linear Propagation code

```

clear all; clc; close all;

% PARAMETERS
A=1000; % gaussian amplitude
b=pi/2; % chirp
N=2^14;
z=10000; % distance in m
FWHM=2e-13;
lambda0=0.8; % in um (800nm)
t=linspace(0,1e-11,N);

dt=(t(2)-t(1));
df=1/dt;
f=[-N/2:(N-1)/2]*df/N;
w=2*pi*f;
f0=3e8/800e-9; % f=3.75e14 Hz
w0=2*pi*f0;
c=3e14; %in um/s

% Signal before propagation
sigma=FWHM/(2*sqrt(2*log(2)));
gaussian=A*exp(-((t-t(N/2)).^2)/sigma^2);
Et=gaussian.*exp(j*w0*t).*exp(j*b/sigma^2*t.^2);

% Spectrum before propagation
Ef=real(fft(Et))/sqrt(N)/2;

% Code to get the pulse width
med=max(Ef)/2;
width=find(Ef>med);
Af=f(max(width))-f(min(width));

%Ploting the spectrogram, signal and spectrum
figure, subplot(2,2,1)
text(0.5,0.5,'Before propagating','FontSize',14,'HorizontalAlignment','center')
text(0.5,0.2,['A=',num2str(A),'; b=',num2str(b),'; Af=',num2str(Af,3)],'FontSize',14)
subplot(2,2,2), plot(t,abs(Et))
axis([0.44e-11 0.56e-11 min(abs(Et)) max(abs(Et))])

```

```

title('Signal in Time'), xlabel('Time (s)'), ylabel('Amplitude (V)')
subplot(2,2,4), sgram(Et, 2*max(f), 40), colorbar('hide')
title('Spectrogram'), axis([0.44e-11 0.56e-11 0 max(f)])
subplot(2,2,3), plot(f, abs(fftshift(Ef)))
axis([0 max(f) 0 max(real(Ef))]), view(-90,90)
title('Spectrum'), ylabel('Amplitude (V)')

% Linear Propagation
% fused silica fiber
a='fused silica fiber';
n=1.453;
dn=-0.017; % um^-2
dn2=0.040; % um^-2
dn3=-0.239; % um^-3
% % LakL21
% a='LakL21';
% n=1.632;
% dn=-0.026; % um^-2
% dn2=0.066; % um^-2
% dn3=-0.386; % um^-3
% % SF10
% a='SF10';
% n=1.711;
% dn=-0.050; % um^-2
% dn2=0.176; % um^-2
% dn3=-0.988; % um^-3
% % BK7
% a='BK7';
% n=1.511;
% dn=-0.015; % um^-2
% dn2=0.056; % um^-2
% dn3=-0.288; % um^-3

k0=2*pi/lambda0; %um^-1
dk=(n-(lambda0*dn))/c; % 1/vg (s/um)
dk2=(lambda0^3)*dn2/(2*pi*(c^2)); % GVD (s^2/um)
dk3=-(1/(4*(pi^2)*(c^3)))*((3*(lambda0^4)*dn2)+(lambda0^5)*dn3); % T
k=k0+dk*(w-w0)+0.5*dk2*(w-w0).^2+1/6*dk3*(w-w0).^3; % in um^-1

Efz=fft(Et,N).*exp(-j*k*z)/sqrt(N)/2;
Etz=ifft(Efz,N)*sqrt(N)*2;

```

```

% code to center the gaussian in 0
aux=Etz;
center=find(Etz==max(Etz));
num=N-center;
if center>N/2
    Etz(N/2:num+N/2)=aux(center:N);
    Etz(num+N/2+1:N)=aux(1:N/2-num);
    Etz(1:N/2-1)=aux(N/2-num+1:center-1);
elseif center<N/2
    Etz(N/2:N)=aux(center:N/2+center);
    Etz(1:num-N/2)=aux(N/2+center+1:N);
    Etz(num-N/2+1:N/2-1)=aux(1:center-1);
end
Efz=real(fft(Etz))/sqrt(N)/2;

% Code to get the pulse width
medz=max(Efz)/2;
widthz=find(Efz>medz);
Afz=f(max(widthz))-f(min(widthz));

%Ploting the spectrogram, signal and spectrum
figure,subplot(2,2,1)
text(0.5,0.5,['Propagating: ',a,' z=',num2str(z),'m'],'FontSize',14,'Hori
text(0.5,0.2,['A=',num2str(A),''; b=',num2str(b),''; Af=',num2str(Afz,3)],'
subplot(2,2,2),plot(t,abs(Etz))
axis([0.44e-11 0.56e-11 min(abs(Et)) max(abs(Et))])
title('Signal in Time'),xlabel('Time (s)'),ylabel('Amplitude (V)')
subplot(2,2,4),sgram(Etz,2*max(f),40),colorbar('hide')
title('Spectrogram'),axis([0.44e-11 0.56e-11 0 max(f)])
subplot(2,2,3),plot(f,abs(fftshift(Efz))),axis([0 max(f) 0 max(real(Ef))
view(-90,90),title('Spectrum'),ylabel('Amplitude (V)')

```

## 9.3 Nonlinear Propagation code

```
clear all; clc; close all;
```

```

% PARAMETERS
A=2; % gaussian amplitude
b=pi/2; % chirp
% p=1e4;

```

```

FWHM=2e-12;
N=2^16;
z=100; % distance in m
lambda0=1.55; % in um (1550nm)
t=linspace(0,1e-10,N);

dt=(t(2)-t(1));
df=1/dt;
% f=((0:N-1)-N/2)/df;
f=[-N/2:(N-1)/2]*df/N;
w=2*pi*f;
f0=3e8/1.55e-6; % f=1.935e14 Hz
w0=2*pi*f0;
c=3e14; %in um/s

% Signal before propagation
sigma=FWHM/(2*sqrt(2*log(2)));
gaussian=A*exp(-((t-t(N/2)).^2)/sigma^2);
Et=gaussian.*exp(j*w0*t).*exp(j*b/sigma^2*t.^2);
% Et=gaussian.*exp(-j*w0*t).*exp(-j*p*sawtooth(f/100));

% Spectrum before propagation
Ef=real(fft(Et))/sqrt(N)/2;

% Code to get the pulse width
med=max(Ef)/2;
width=find(Ef>med);
Af=f(max(width))-f(min(width));

% Plotting the spectrogram, signal and spectrum
figure,subplot(2,2,1)
text(0.5,0.5,'Before propagating','FontSize',14,'HorizontalAlignment','center')
text(0.5,0.2,['A=',num2str(A),'; b=',num2str(b),'; Af=',num2str(Af),''])
subplot(2,2,2),plot(t,abs(Et))
axis([min(t) max(t) min(abs(Et)) max(abs(Et))])
title('Signal in Time'),xlabel('Time (s)'),ylabel('Amplitude (V)')
subplot(2,2,4),sgram(Et,2*max(f),40),colorbar('hide')
title('Spectrogram'),axis([0 max(t) 0 max(f)])
subplot(2,2,3),plot(f,abs(fftshift(Ef))),axis([0 max(f) 0 max(real(Ef))])
view(-90,90),title('Spectrum'),ylabel('Amplitude (V)')

```

```

% Nonlinear Propagation
a='Nonlinear Propagation';
delta_z = 1e-2;
n = ceil(z/delta_z);
dz = z/n;
T = N*(t(2)-t(1)); % T(time period = N * dt
omega = 2*pi/T*[(0:N/2-1) (-N/2:-1)]; % angular freq. axis

beta_2 = 5.1*1e-27; % s^2/km
gamma = 2.2e-3; % 1/W km
alpha = 0.051e-3; % 1/km

D = 1/2*(sqrt(-1)*beta_2*omega.^2 - alpha)*delta_z;
exp_D = exp(D);

Etz = ifft(exp(0.5*D).*fft(Et)); % The first half step
for i = 1:n
    Etz = ifft(exp_D.*fft(Etz.*exp(delta_z*sqrt(-1)*gamma*abs(Etz).^2)));
end
Etz = ifft(exp(-0.5*D).*fft(Etz)); % The last half step backwards

% code to center the gaussian in 0
aux=Etz;
center=find(Etz==max(Etz));
num=N-center;
if center>N/2
    Etz(N/2:num+N/2)=aux(center:N);
    Etz(num+N/2+1:N)=aux(1:N/2-num);
    Etz(1:N/2-1)=aux(N/2-num+1:center-1);
elseif center<N/2
    Etz(N/2:N)=aux(center:N/2+center);
    Etz(1:num-N/2)=aux(N/2+center+1:N);
    Etz(num-N/2+1:N/2-1)=aux(1:center-1);
end

Efz=real(fft(Etz))/sqrt(N)/2;

% Code to get the pulse width
medz=max(Efz)/2;
widthz=find(Efz>medz);
Afz=f(max(widthz))-f(min(widthz));

```



```
%Plotting the spectrogram, signal and spectrum
figure,subplot(2,2,1)
text(0.5,0.5,['Propagating: ',a,' z=',num2str(z),'m'],'FontSize',14)
text(0.5,0.2,['A=',num2str(A),'; b=',num2str(b),'; Af=',num2str(Afz)])
subplot(2,2,2),plot(t,abs(Etz))
axis([min(t) max(t) min(abs(Et)) max(abs(Et))])
title('Signal in Time'),xlabel('Time (s)'),ylabel('Amplitude (V)')
subplot(2,2,4),sgram(Etz,2*max(f),40)
colorbar('hide'),title('Spectrogram'),axis([0 max(t) 0 max(f)])
subplot(2,2,3),plot(f,abs(fftshift(Efz)))
axis([0 max(f) 0 max(real(Ef))]),view(-90,90)
title('Spectrum'),ylabel('Amplitude (V)')
```

## 9.4 Others

Linear Time/Frequency Toolbox (LTFAT) <http://ltfat.sourceforge.net/>